

CONTRACTOR REPORT

SAND82—7126/2
Unlimited Release
UC—63a

Reliability-Economics Analysis Models for Photovoltaic Power Systems

Volume 2

Lawrence H. Stember, William R. Huss, Michael S. Bridgman
Battelle Columbus Laboratories
505 King Avenue
Columbus, OH 43201

Prepared by Sandia National Laboratories Albuquerque, New Mexico 87185
and Livermore, California 94550 for the United States Department of Energy
under Contract DE-AC04-76DP00789

Printed November 1982

**When printing a copy of any digitized SAND
Report, you are required to update the
markings to current standards.**

Issued by Sandia National Laboratories, operated for the United States Department of Energy by Sandia Corporation.

NOTICE: This report was prepared as an account of work sponsored by an agency of the United States Government. Neither the United States Government nor any agency thereof, nor any of their employees, nor any of their contractors, subcontractors, or their employees, makes any warranty, express or implied, or assumes any legal liability or responsibility for the accuracy, completeness, or usefulness of any information, apparatus, product, or process disclosed, or represents that its use would not infringe privately owned rights. Reference herein to any specific commercial product, process, or service by trade name, trademark, manufacturer, or otherwise, does not necessarily constitute or imply its endorsement, recommendation, or favoring by the United States Government, any agency thereof or any of their contractors or subcontractors. The views and opinions expressed herein do not necessarily state or reflect those of the United States Government, any agency thereof or any of their contractors or subcontractors.

Printed in the United States of America
Available from
National Technical Information Service
U.S. Department of Commerce
5285 Port Royal Road
Springfield, VA 22161

NTIS price codes
Printed copy: A08
Microfiche copy: A01

Reliability-Economics Analysis Models for Photovoltaic Power Systems

Volume 2

Lawrence H. Stember
William R. Huss
Michael S. Bridgman
Battelle Columbus Laboratories
505 King Avenue
Columbus, OH 43201

Abstract

This report describes the development of modeling techniques to characterize the reliability, availability, and maintenance costs of photovoltaic power systems. The developed models can be used by designers of PV systems in making design decisions and trade-offs to minimize life-cycle energy costs. Three actual intermediate PV system designs were modeled as examples. The input data estimates used and the results of the analyses are presented.

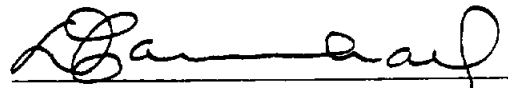
Prepared for Sandia National Laboratories Under Subcontract No. 62-8278.

ACKNOWLEDGMENT

The authors acknowledge and express their appreciation for the significant technical contributions to this study made by C. Badger, J. P. Ehounou, G. T. Noel, and G. H. Stickford of Battelle's Columbus Laboratories. The cooperative efforts of the three PRDA project managers--J. McGuirk of Arizona Public Service, W. R. Kauffman of Braddock, Dunn & MacDonald, and P. Felfe of Lea County Electric were invaluable in obtaining the latest functional block diagrams and other needed design information.

Miguel Rios of Sandia National Laboratories was the Technical Monitor for this study. His interest, guidance, and strong encouragement are gratefully acknowledged.

REPORT APPROVAL:



Donald C. Carmichael, Manager
Solar Photovoltaic Programs
Battelle, Columbus Laboratories

VOLUME I

TABLE OF CONTENTS

	<u>Page</u>
INTRODUCTION	1
SUMMARY	5
PHOTOVOLTAIC SYSTEM CATEGORIZATION AND DATA.	9
Flat-Panel Photovoltaic System	9
Photovoltaic Concentrator Systems	12
PV System Reliability and Maintenance Data.	17
Data Needed for Reliability Models	17
Reliability Data	20
Reliability Versus Cost	22
Maintenance Data	28
SYSTEM RELIABILITY ANALYSIS DEVELOPMENT.	31
Considerations in Selecting the Methodology	31
Discussion of Reliability/Availability Methodologies.	31
Fault Tree Model.	35
Array Field Design Analysis Methodology--Output Power Degradation Due to Solar Cell Failures.	38
General.	38
Analysis Procedure	40
State Space Methodology	41
State Space Model.	44
Combining Subsystem Results.	56
System Degradation Effects	58
Energy Production Computations	59
Maintenance Costs.	60
Corrective Maintenance Costs.	60
Preventive Maintenance Costs.	62
Example System for Analysis--PV Concentrator (Passively Cooled)--Generic Design	63
Example Application of the State Space Approach.	67
Failure Rates and Repair Rates.	67
State Space Model	69
Energy Production Computations.	77
Maintenance Costs	80

VOLUME I

TABLE OF CONTENTS
(Continued)

	<u>Page</u>
The Simulation Methodology - The SOLREL Model.	84
General	84
The Simulation Model.	84
The Initial Event File: Scheduling Failures	85
Component Failure.	86
Power Output Calculation Including the Effect of Degradation.	86
Maintenance	87
Scheduling Repair.	87
Maintenance Costs.	88
Preventive Maintenance and Array Cleaning.	88
Tables and Plots	89
Changes to Model	90
SOLREL Analysis of Example System	90
Variability in Results	96
The Computer Program for SOLREL	96
Comparison of Results from the State Space Approach and the SOLREL Simulation Model of the Generic PV System	96
LIFE-CYCLE COST ANALYSIS.	105
Defining the Procedure	105
Life-Cycle Costs (LCC).	105
Life-Cycle Energy Cost (LEC).	108
Applying the Procedure to a Specific System.	111
SENSITIVITY ANALYSIS.	115
SOLREL	115
Summary of SOLREL Analysis.	115
Reduction of Variation in Results	117
Flat-Panel--Test for More Reliable Inverter	122
Flat-Panel--Test for Cleaning Intervals	133
Passively Cooled Concentrator--Test for Cleaning Intervals.	133
Sensitivity Analysis Using the State Space Methodology	133
General Discussion--Sensitivity Analyses	142
CONCLUSIONS AND RECOMMENDATIONS	145
REFERENCES	147

VOLUME I

LIST OF TABLES

	<u>Page</u>
Table 1. Range of Component Failure Rates For Evaluating Solar DHW Systems ⁽⁵⁾	22
Table 2. Reliability Versus Cost	25
Table 3. Reliability Analysis Techniques Examined.	32
Table 4. Dual Subsystem Cases.	52
Table 5. Steady-State Solutions For the Dual Subsystem Cases . .	54
Table 6. Estimated Reliability and Maintenance Data Inputs For Task 2 Analysis of Generic PV Concentrator, Passively Cooled Power System (General Functional Design Phoenix Airport, Phase I PRDA)	65 & 66
Table 7. Failure Rate and Time to Repair of Major System Components.	70
Table 8. Array Field Subsystem Results	73
Table 9. Power Conditioning Subsystem Results.	73
Table 10. Serial Element Subsystem Results.	76
Table 11. System States	76
Table 12. Output Duration Curve For Generic PV Concentrator (Passively Cooled).	78
Table 13. Monthly Array Power Data.	79
Table 14. Permanent Degradation Factors	79
Table 15. Dirt Accumulation Degradation Factors	81
Table 16. Estimated Annual Generic PV System Output Using the State Space Approach.	82
Table 17. Computer Program-Related Changes Necessary For Adjustments to Model.	91
Table 18. Description of Input Parameters Generic Concentrator System (Cleaning at 3-Month Intervals and Repair After 5 Array Failures-Case).	93
Table 19. Monthly Output Duration Curves For Generic Concentrator System (Input Data).	94
Table 20. SOLREL Results: Levelized Cost, ¢/kWh.	95
Table 21. SOLREL Results: Lifetime Cost, 1981 Dollars x 10 ³ . . .	95
Table 22. SOLREL Results: Lifetime Output, kWh x 10 ⁶	95

VOLUME I

LIST OF TABLES
(Continued)

	<u>Page</u>
Table 23. Log of System Performance, Maintenance Costs and Events	97
Table 24. Sample Printout of Annual Costs and Output Energy from Generic Concentrator System.	98
Table 25. Generic Concentrator System Availability	99
Table 26. Generic Passively Cooled Concentrator System Component Failures	100
Table 27. Estimate of Variance Among SOLREL Runs--6 Cases, Repair on First Array Failure, Clean Every 3 Months	103 & 104
Table 28. Description of Scenarios Tested.	114
Table 29. Comparison of Life-Cycle Energy Costs in Cents per kWh.	114
Table 30. Levelized Life-Cycle Energy Cost as a Function of Cleaning Intervals Assuming 13 Percent Discount Rate.	115
Table 31. Levelized Life-Cycle Energy Cost as a Function of Inverter Reliability and Cost	116
Table 32. Flat Panel, Summary of Tests For More Reliable Inverter (1/2 System).	123
Table 33. Flat Panel - Test For More Reliable Inverter, MTBF = 12 Months, Discount Rate = 13 Percent.	125
Table 34. Flat Panel - Test For More Reliable Inverter, MTBF = 32.4 Months, Discount Rate = 20 Percent.	126
Table 35. Flat Panel - Test For More Reliable Inverter, MTBF = 64.8 Months, Discount Rate = 20 Percent.	128
Table 36. Flat Panel - Test For More Reliable Inverter, MTBF = 24 Months, Discount Rate - 20 Percent	130
Table 37. Comparison of System Levelized Life-Cycle Energy Cost (¢/kWh) for Alternative Inverters	131
Table 38. Flat Panel - Simulation Runs to Test For Cleaning Interval Effect on Life-Cycle Energy Costs, Discount Rate = 13 Percent	134
Table 39. Flat Panel - Simulation Runs to Test For Cleaning Interval Effect on Life-Cycle Energy Costs, Discount Rate = 13 Percent	135
Table 40. Passively Cooled Concentrator-Simulation Runs to Test For Cleaning Interval Effect on Life-Cycle Energy Costs, Discount Rate = 13 Percent.	137

VOLUME I

LIST OF TABLES
(Continued)

	<u>Page</u>
Table 41. Passively Cooled Concentrator-Simulation Runs to Test For Cleaning Intervals Effect on Life-Cycle Energy Costs, Discount Rate = 13 Percent.	138
Table 42. Potential Changes in System's Input Data and Their Effects on State Space Model	140
Table 43. Results of Changes in Inverter Logical Configuration on All Three Systems	141
Table 44. Tests Run Using SOLREL to Investigate Random Errors. . .	143 & 144

LIST OF FIGURES

Figure 1. Relationships Between the Availability and Life-Cycle Energy Cost Models.	3
Figure 2. System Life-Cycle Cost As a Function of Reliability . .	3
Figure 3. Block Diagram of General PV System (Without Storage), Interactive With Utility.	10
Figure 4. Functional Block Diagram-Typical Flat Panel PV Power System, Interactive With Utility, No Storage.	11
Figure 5. Simplified Functional Block Diagram For Generic Flat-Panel PV Power System, Interactive With Utility, No Storage.	13
Figure 6. Functional Block Diagram-Typical Concentrator PV Power System, Passively Cooled, Interactive With Utility, No Storage	14
Figure 7. Simplified Functional Block Diagram-Generic Concentrator PV Power System, Passively Cooled, Interactive With Utility, No Storage.	15
Figure 8. Functional Block Diagram-Typical Concentrator PV Power System, Actively Cooled With Thermal Load, No Electrical Storage, Interactive With Utility	16
Figure 9. Simplified Functional Block Diagram-Generic Concentrator PV Power System, Actively Cooled, Interactive With Utility, No Storage.	18
Figure 10. Power Output Duration Curve--For 1 of 12 Months of Typical Year	24
Figure 11. MTBF Versus Cost--General Relationship For Electronics	26

VOLUME I

LIST OF FIGURES
(Continued)

	<u>Page</u>
Figure 12. PV System Maintenance Time Estimates.	29
Figure 13. Overview of Interactions of Availability Method- ology With The System Design Process.	34
Figure 14. Example Solar PV System And Fault Tree Model Showing Functional/Probability Relationships to Focus Designer Attention on Subsystem Requiring Reliability Emphasis.	36
Figure 15. Percent Degradation in Peak Output Capability Versus Period of Continuous Operation With No Module Replacement--Flat Panel System.	42
Figure 16. Overview of State Space Approach.	43
Figure 17. Overview of State Space Model	47
Figure 18. State Space Model For a Serial Subsystem.	49
Figure 19. State Transition Diagrams For The Dual Sub- system Cases.	52
Figure 20. Simplified Functional Block Diagram--Generic Concen- trator PV Power System, Passively Cooled, Interactive With Utility, No Storage.	64
Figure 21. Reliability Logic Diagram For The Generic PV System . .	68
Figure 22. Markov Model For The Array Field.	70
Figure 23. Reduction of Redundant Controls to a Single Element . .	75
Figure 24. Flowchart For Simulation Program - SOLREL	85
Figure 25. Output Calculation For Each Month	87
Figure 26. Output of Maintenance Costs and Energy For APS/Motorola PV System.	101
Figure 27. Output of Maintenance Costs And Levelized Maintenance Cost Per Unit Energy For APS/Motorola PV System	102
Figure 28. Cash Flow of Hypothetical Investment With 10-Year Life, Initial Year Dollars.	106
Figure 29. Cash Flow of Hypothetical Investment With 10-Year Life, Current Dollars	106
Figure 30. Cash Flow of Hypothetical Investment With 10-Year Life, Present Value Initial Year Dollars.	107
Figure 31. Cost Escalation of Purchased Energy	108
Figure 32. Hypothetical Output From Photovoltaic System.	109
Figure 33. Output in Current Dollars Equivalent.	110
Figure 34. Output in Present Value Dollars	110

VOLUME I

LIST OF FIGURES
(Continued)

	<u>Page</u>
Figure 35. Flow Chart For Three-Phase Approach to Reduce SOLREL Output Variability.	118
Figure 36. Maintenance Cost Frequency Distributions For Components, General Maintenance Activities and The System	119
Figure 37. Maintenance Cost Frequency Distribution, Showing Effect of Multiple Runs on Variability of Costs and The Mean	121
Figure 38. Test for Optimum Inverter Reliability, Flat-Panel System, Discount Rate = 20 Percent	132
Figure 39. Test For Cleaning Intervals Flat-Panel System, Discount Rate = 13 Percent	136
Figure 40. Test For Cleaning Intervals Passively Cooled Concentrator System, Discount Rate = 13 Percent.	136

**INTRODUCTION, REPORT
ORGANIZATION AND SUMMARY**

FINAL REPORT

RELIABILITY-ECONOMICS ANALYSIS
MODELS FOR PHOTOVOLTAIC
POWER SYSTEMS

VOLUME I

LAWRENCE H. STEMBER, WILLIAM R. HUSS,
AND MICHAEL S. BRIDGMANINTRODUCTION

The objective of this study is to review the characteristics of current and future photovoltaic power systems and develop alternative system reliability/availability models which incorporate design, reliability, cost, and maintenance information to predict both annual maintenance cost and energy production over the system life. Thus, combined with initial cost and operating cost information, the model would predict levelized cost per kWh; and PV system designers would have a method to use in design tradeoffs to minimize life-cycle energy cost.

The operation of large terrestrial photovoltaic (PV) power systems (over 50 kWp) is a fairly recent event. Thus, failure rate, repair time and cost data for many PV subsystems and components are lacking. In spite of this, reliability/availability models can still significantly affect today's system design decisions by enabling the designer to estimate the change in life-cycle energy costs as alternative subsystems and configurations are represented. As accurate test and field data become more generally available at lower systems levels, the models can represent the systems at a greater level of detail and with better accuracy. At present, their principal value is to emphasize reliability and maintainability early in the system design process, with resulting improvements in component part application and subsystem design.

The purpose of this study is to provide an integrated reliability/maintainability model (an availability model) which represents failure, lost production, scheduled and unscheduled maintenance. (See Figure 1.)

The optimal system is the one with relatively low initial cost which assures a reliable, easily maintained system where the total life-cycle cost per unit of energy delivered is minimized. The life-cycle cost portion of this optimization is shown as a function of MTBF (mean time between failure) in Figure 2. The minimum of the familiar U-shaped life-cycle cost curve locates the MTBF goal. This would assume that energy delivered over system life is independent of MTBF. From a life-cycle energy cost minimization view, if energy delivered over system life increases slightly, as is likely with increasing MTBF, the optimum MTBF would be slightly higher.

The content of this report is covered in the summary; however, for general orientation, the report's overall organization is described in the following: It is divided into two volumes. The first volume contains the development of an example application of the methodologies. This is followed by the use of the outputs of the example in life-cycle energy cost and sensitivity analysis for systems optimization. The second volume includes the application of the techniques to three PV system designs. Also included are other details of the methodologies' developments.

Photovoltaic power systems are the primary systems considered, so the three basic PV system types are described in the beginning of Volume I. After this, the kinds of reliability and maintenance data needed for analysis are outlined. Then, alternative analysis approaches are described, and the two methodologies chosen for use in the program are demonstrated in some detail using a generic passively cooled photovoltaic concentrator system for the analysis.

The methodologies chosen are: an analytical approach, namely, the state space methodology which uses Markov chain techniques; and a simulation methodology, which employs available computer simulation programs that can incorporate a wide variety of statistical distributions through Monte Carlo techniques.

After the two methodologies are demonstrated by using the same PV system design and data, the utility of life-cycle energy cost calculations and their compatibility with the previously described methodologies are covered. Examples of variations in system design or maintenance philosophies are then used to demonstrate the methodologies' application to sensitivity studies and to compare designs and choose one with the lower life-cycle energy cost.

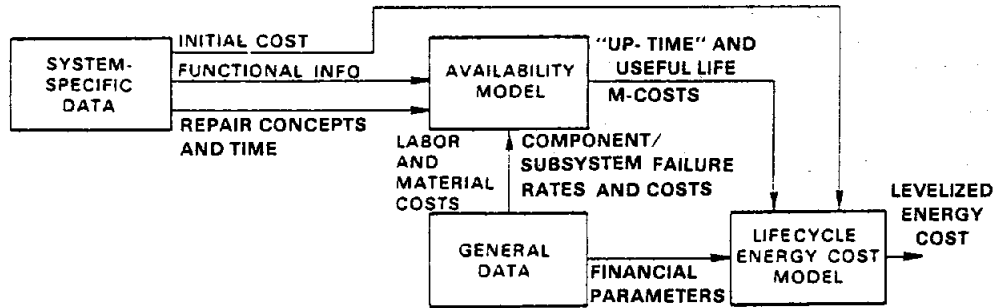


FIGURE 1. RELATIONSHIPS BETWEEN THE AVAILABILITY AND LIFE-CYCLE ENERGY COST MODELS

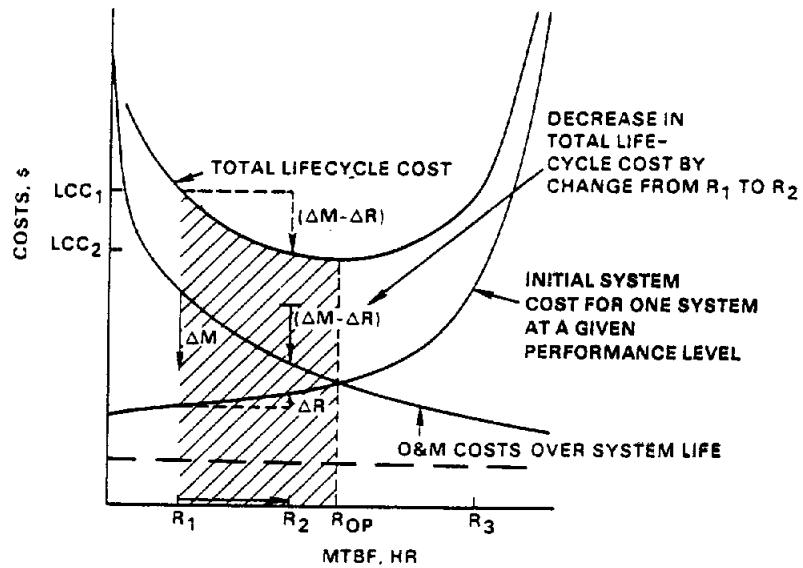


FIGURE 2. SYSTEM LIFE-CYCLE COST AS A FUNCTION OF RELIABILITY

Volume II contains an analysis of three present-day solar projects. These are intermediate-size photovoltaic systems built under DOE sponsorship, which are either now on-line or scheduled to be producing energy in the near future. Three separate sections in this second volume contain the application of each of the two methodologies to each system. In the latter part of the third section, the results of the application of the two techniques are compared. The volume also contains appendixes which provide mathematical developments and programming details for the two techniques.

SUMMARY

Many factors in PV system design, development, reliability, maintenance, and economics are considered in this report. The models developed pull all of these aspects together to join preliminary design activities with life-cycle cost equations. The main missing link that the developed methodologies provide is a direct way to calculate annual maintenance cost and annual energy produced, recognizing failures, preventive maintenance, degradation, and other conditions which incur cost or reduce energy output by the systems.

In order to orient the reader to photovoltaic system designs, three typical classes of photovoltaic systems are described in detail. These are: the flat-panel system, the passively cooled concentrator system, and the actively cooled concentrator system. Briefly, the first of the three is a passive system which is usually built at a fixed angle, facing south, using large solar-cell module areas to intercept the sunlight and transform its energy to electrical output. The second and third systems use lenses or mirrors to concentrate the sunlight onto much smaller solar cell areas. This concentration results in a magnification of cell energy density on the order of 20 to 200 times. However, these systems must focus directly on the sun, tracking it throughout the day, in order to accomplish this increase in energy intercepted per unit cell area. The main difference between these two concentrator systems is that the first type is cooled by fins to maintain the solar cells below their maximum operational temperature, whereas the actively cooled type has a working fluid which transfers the heat away from the cells, sometimes to a useful load. Block diagrams and general characteristics of these systems are discussed, and examples are given of the transformation of detailed functional block diagrams into simpler function block diagrams usable in reliability analysis.

The general type of reliability data needed for these analyses are described, and reliability analysis approaches are explained to fit the data into the context of the problem. The kinds and availability of maintenance-time and cost data are also discussed. One overriding factor in both areas is that, because of the newness of many of the system designs, dependable data are not yet available. However, some information can be extrapolated from

similar equipment in other fields such as uninterruptable power supplies, which make use of batteries and inverters.

After a wide-ranging discussion of reliability/availability methodologies, an example of a fault tree model is presented in some detail. Following this, the methodology developed by the Jet Propulsion Laboratory (JPL) to analyze the degradation caused in array fields by individual cell failure is explained.

Two methodologies were selected and developed. These were the state space and the SOLREL techniques. The development of the state space methodology and its application to photovoltaic systems is extensively explained and demonstrated using the generic PV concentrator system. A simulation methodology called SOLREL was developed using the GASP IV computer program. It is described in detail and the same generic concentrator system is analyzed to show the approaches and capabilities of the simulation method as contrasted with the state space methodology. Extensive details of the input data required are given and references are made to the Volume II appendixes which contain mathematical details and sections of the computer program. A wide variety of output tables, charts, and graphs are used in Volume I to provide concrete examples of the output of these two techniques.

As in most analytical modeling techniques, the state space method has the disadvantage of requiring more assumptions to be accepted than the more extensive computer simulation method, but it can be accomplished with less manpower and computer resources. The simulation approach has the disadvantage of producing a result which has a wide confidence band, but its capabilities are such as to present a more detailed representation of the real world. Repeated runs of the computer model can reduce the size of the confidence interval. Its other disadvantage is that a large computer is usually required and a programmer or someone familiar with the algorithm used must be employed to make changes in the model. The analytical approach, using a hand-held calculator, would thus be more useful early in the system design, while the simulation approach should be valuable later in the process as more detailed knowledge becomes available.

Life-cycle energy cost calculation methods and their computer implementations are described to show how the output of the methodologies developed are used as inputs for the life-cycle energy costs computations.

The primary output that has been unavailable for life-cycle energy computations to date is that of annual system maintenance costs. Since failures, repair, preventive maintenance, and other costs are simulated with the methodologies, a reasonable and practical estimate of annual power output by year over a long-term period may be provided. This includes the degradation due to lost time caused by failures of subsystems; degradation in array output due to dirt, yellowing, cell failures, and the like; and interruptions in system operation due to high winds or other extreme weather conditions. Of course, all of these outputs are no better than the input data and, for the purposes of this report, many of these data are only general extrapolations or approximations. Extensive operational experience with actual systems and components is needed to provide data which are truly representative of long-term photovoltaic system operation.

The second volume of the report contains the application of each of the two methodologies to three separate photovoltaic systems in the intermediate size class. The first is the Lea County Electric flat-panel system in Lovington, New Mexico; the second is the Arizona Public Service installation at the Sky Harbor airport in Phoenix, Arizona, with a passively cooled concentrator system array; and the third is the Braddock, Dunn & MacDonald (BDM) actively cooled concentrator system installed on the roof of their facility near the airport in Albuquerque, New Mexico. Input data estimates, the process of modeling the systems, and the outputs resulting from each methodology are presented in that volume.

A brief section then presents a comparison of the results calculated using the two different methodologies.

The program has resulted in the development of two reliability-economic analysis models that, combined with proper collection of field data on photovoltaic components and subsystems, can develop predictions of system maintenance cost and annual power output over time. The models need to be applied to future system designs as well as to additional contemporary systems to accommodate data in order to further evolve the techniques and increase their usefulness. It is also recommended that these techniques be applied to other PV systems of both larger and smaller size and to remote systems with energy storage to further expand their usefulness.

PV SYSTEMS AND DATA

PHOTOVOLTAIC SYSTEM CATEGORIZATION AND DATA

Photovoltaic systems providing energy compatible with the 60 Hz power grid and those remote stand-alone PV power systems independent of the grid are the two major categories of PV power. The present study deals with the grid-connected systems, which are composed of three size classes: Residential, Intermediate, and Central Station. The Intermediate-size systems(1), which are emphasized in this project (for businesses, schools, hospitals, etc.), are characterized by the ranges from 20 kWp to 500 kWp. Figure 3 shows a general block diagram of the kind of systems involved. Failure of the PV power does not interrupt the power to the load because it is backed up by the utility grid.

Flat-Panel Photovoltaic System

Figure 4 expands the general diagram of Figure 3 and illustrates the functional details of a generic flat panel power system. This generic array type is designed to face south in rows with panels fixed at an angle with the horizontal approximately equal to that of the latitude (without seasonal adjustment). Essentially, it is a passive system with no moving parts. The solar cells are wired as a large network of series-parallel connections with bypass diodes in parallel with the cells. This arrangement minimizes the effect of failure of individual cells on the system power output. The power conditioning subsystem contains large silicon-controlled rectifiers and power transistors to convert the d-c power from the array to 3-phase a-c. It also includes a control module and a large, special transformer to step up the voltage. These components interface and synchronize the inverter output with the 3-phase voltage of the local distribution system. Load shedding typically is not a control function, because the interconnection is such that the utility will make up for whatever load the PV system does not carry. The logic functions typically provided in the control module will allow for start-up and turn-off, as well as sense fault or "utility down" conditions in the system. The PV systems are normally designed to operate unattended.

(1) Refer to REFERENCES at the end of Volume I.

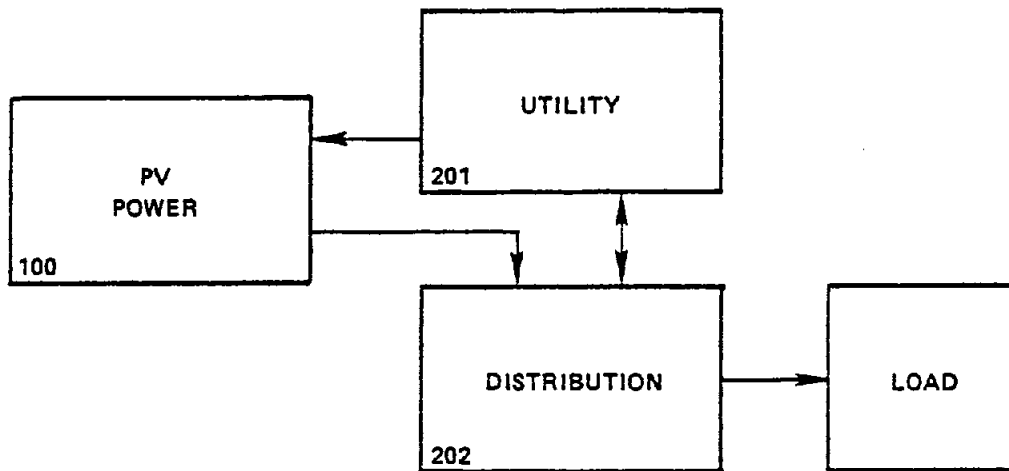
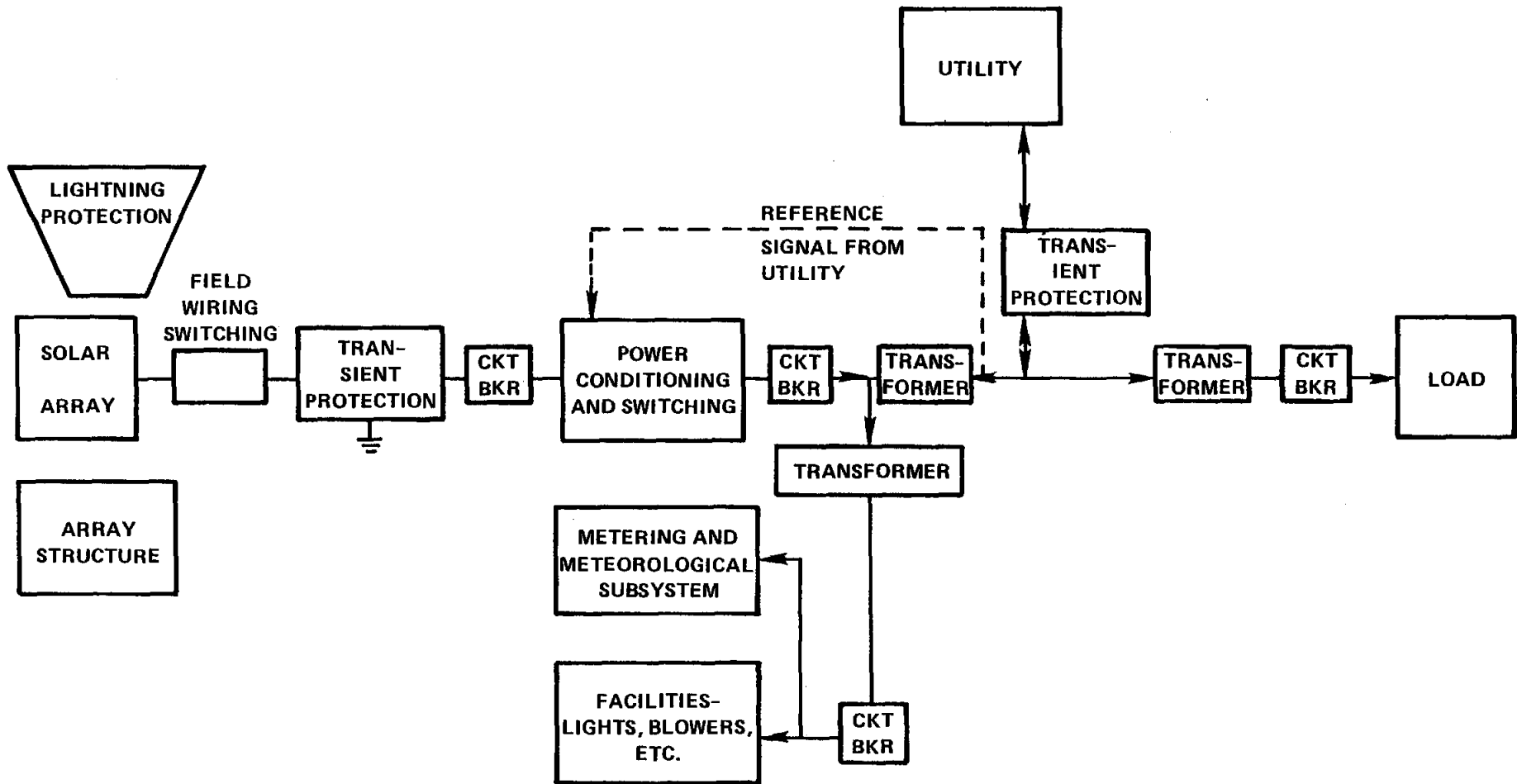


FIGURE 3. BLOCK DIAGRAM OF GENERAL PV SYSTEM (WITHOUT STORAGE), INTERACTIVE WITH UTILITY



17

FIGURE 4. FUNCTIONAL BLOCK DIAGRAM-TYPICAL FLAT PANEL PV POWER SYSTEM, INTERACTIVE WITH UTILITY, NO STORAGE

Figure 5 is a simplified functional block diagram of a flat panel PV system. The diagram incorporates the major subsystems which can cause loss of power output from the PV subsystem or from other subsystems to the load.

Photovoltaic Concentrator Systems

The drawing of Figure 6 presents a detailed functional block diagram of a passively cooled PV concentrator system. This is a power system that has a group of arrays, each with some means to track the sun. Each contains a lens or a reflector which focuses the sun onto a single solar cell (point focus collector) or a row of cells (linear focus collector), so that the sun's intensity on the cells is typically from 25 to 200 times the intensity seen by the flat panel's cells. These arrays track the sun across the sky during the day and only provide significant output when they are receiving direct sunlight. This tracking may be one- or two-axis. Because of the resulting intensity of the sunlight, the cells need to be cooled. In some cases, this is done by passing a liquid through a heat exchanger attached to the cells. Often the thermal output of such subsystems is used by a thermal load. In the particular system shown in Figure 6, the cells are cooled passively with heat sinks. A simplified block diagram of the concentrator system is given in Figure 7. This system has more subsystems than the flat panel and these must be considered in the reliability model. The sun-sensor, control computer, and tracking mechanism comprise the control subsystem which guides each array to lock onto the sun's position in the sky. The reliability model must deal with the failure of these subsystems in addition to the failures which occur in the d-c power subsystem which is electrically similar to the flat-panel system. Thus, in order for the life-cycle energy cost to equal that of the flat-panel system, the higher efficiency of the concentrator system must compensate for its potentially lower reliability due to greater complexity.

Figure 8 is a functional block diagram that gives a general overview of a concentrator system with an active thermal subsystem. It provides a thermal as well as electrical output to a load, has no electrical storage and is interactive with the utility. This system is more complex than the one shown in Figure 7 because of the required connections and control for the

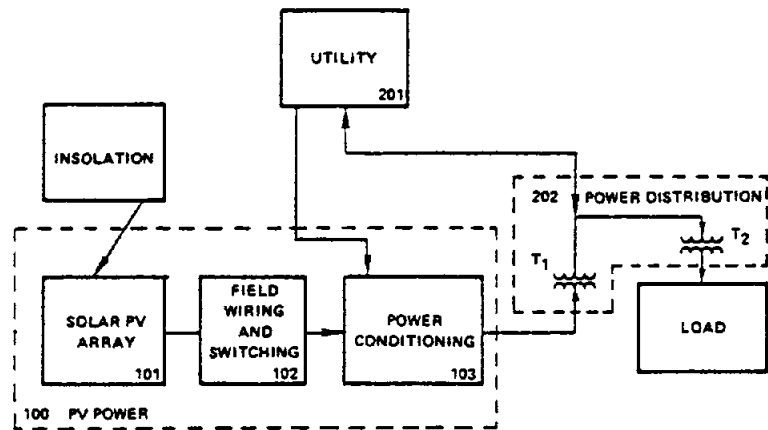


FIGURE 5. SIMPLIFIED FUNCTIONAL BLOCK DIAGRAM FOR GENERIC FLAT-PANEL PV POWER SYSTEM, INTERACTIVE WITH UTILITY, NO STORAGE

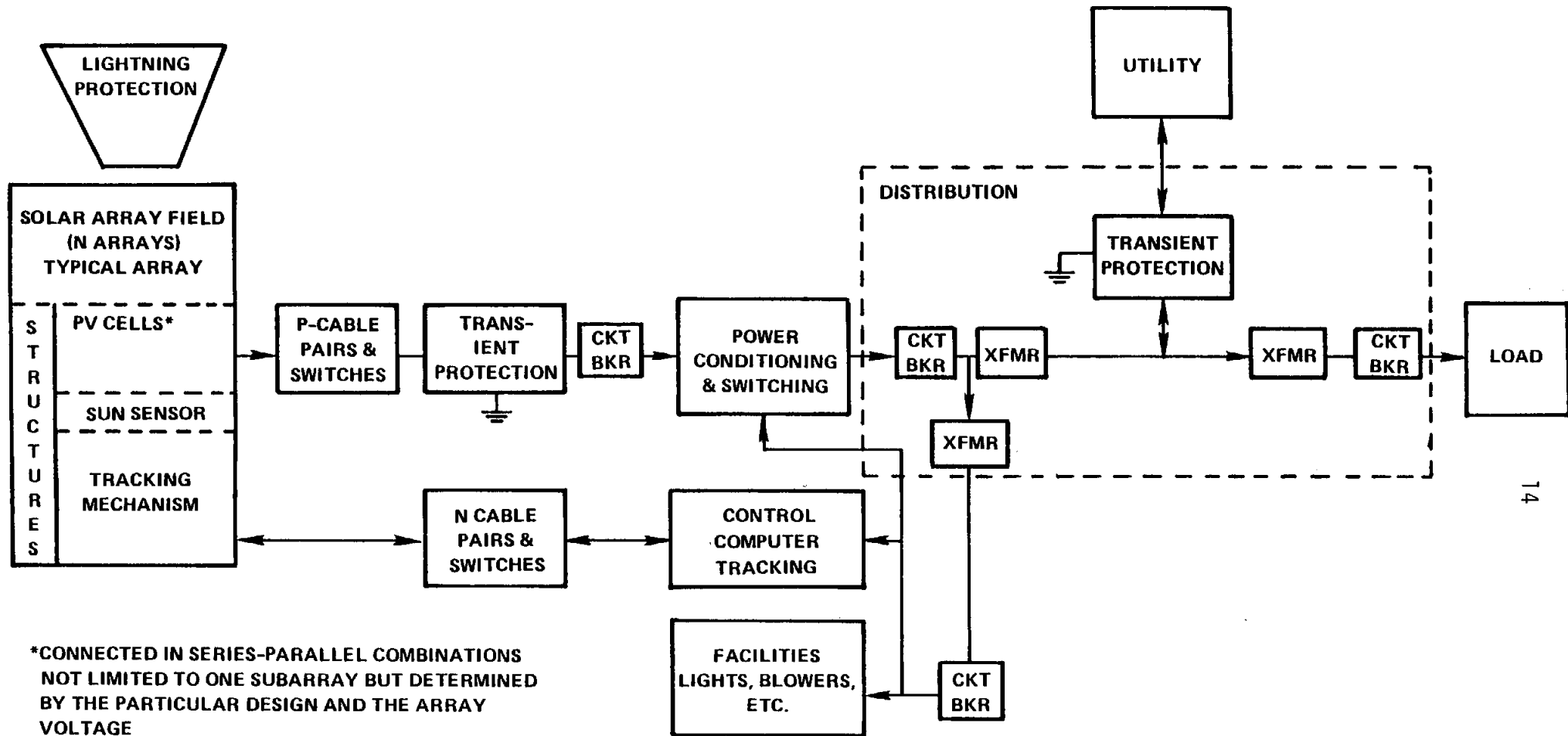
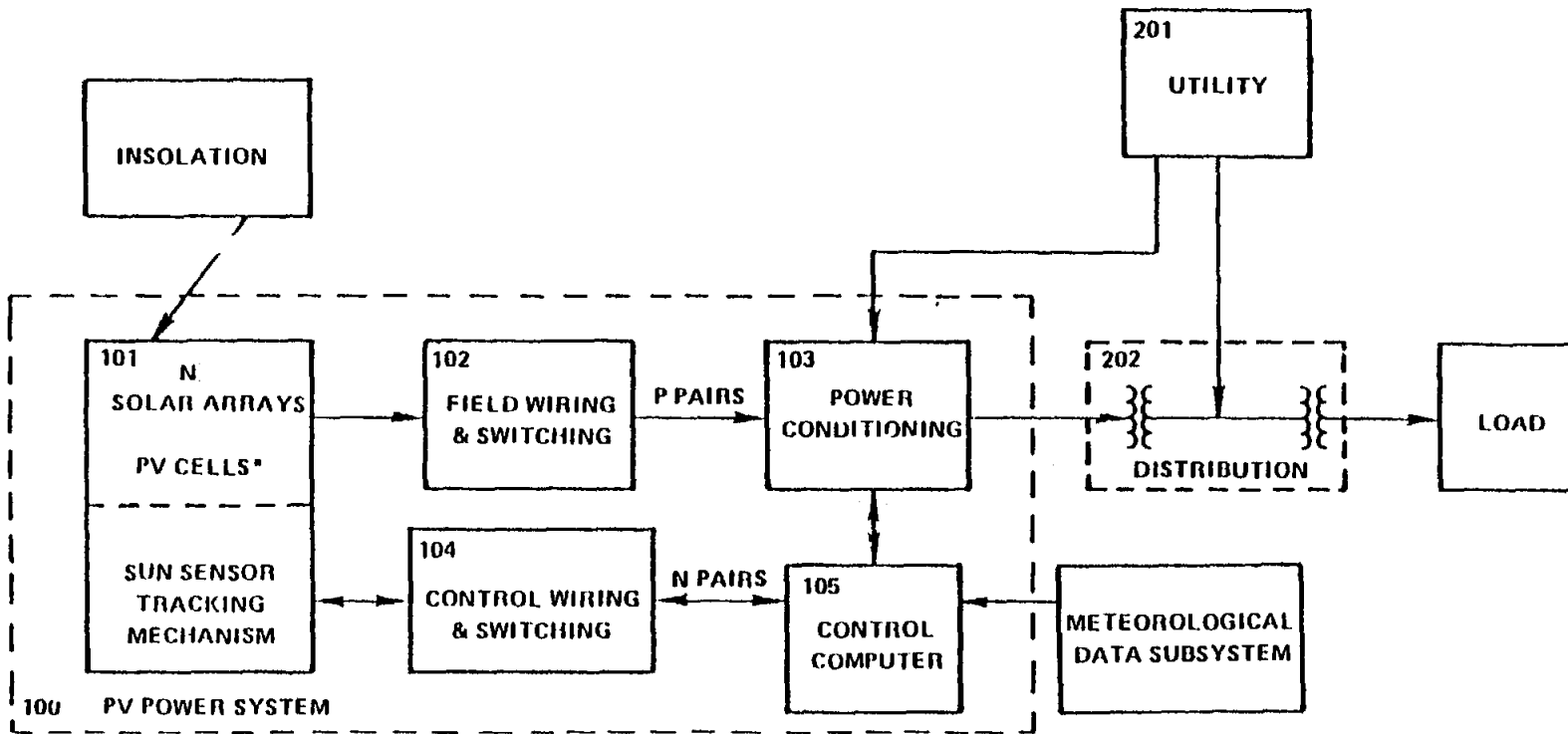
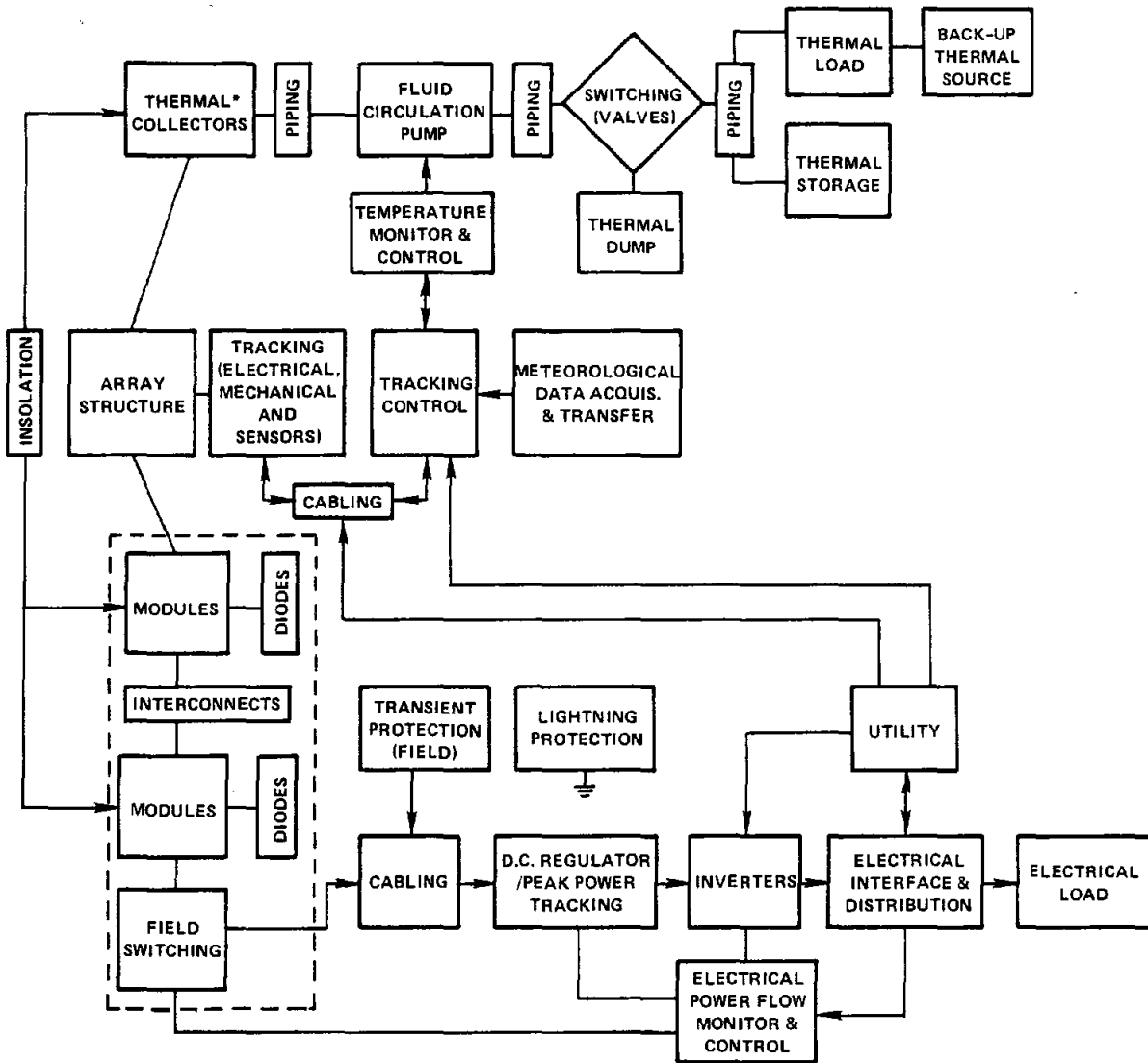


FIGURE 6. FUNCTIONAL BLOCK DIAGRAM-TYPICAL CONCENTRATOR PV POWER SYSTEM, PASSIVELY COOLED, INTERACTIVE WITH UTILITY, NO STORAGE



*CONNECTED IN SERIES-PARALLEL COMBINATIONS
 NOT LIMITED TO ONE ARRAY BUT DETERMINED
 BY THE PARTICULAR DESIGN AND THE ARRAY
 VOLTAGE

FIGURE 7. SIMPLIFIED FUNCTIONAL BLOCK DIAGRAM-GENERIC CONCENTRATOR PV POWER SYSTEM, PASSIVELY COOLED, INTERACTIVE WITH UTILITY, NO STORAGE



* Note: The thermal collectors and PV modules are mounted together. They are shown here separately for functional purposes only.

FIGURE 8. FUNCTIONAL BLOCK DIAGRAM-TYPICAL CONCENTRATOR PV POWER SYSTEM, ACTIVELY COOLED WITH THERMAL LOAD, NO ELECTRICAL STORAGE, INTERACTIVE WITH UTILITY

thermal subsystem. Figure 9 describes this system in a simplified block diagram form, emphasizing those portions which can cause system failure. Consequently, there exists a major subsystem which provides thermal and electrical outputs and which has back-up sources of power for each load. The system is usually designed to shut down upon failure of the utility, making the solar subsystem incapable of providing redundancy during utility outage because of safety considerations.

PV System Reliability and Maintenance Data

Data Needed for Reliability Models

System reliability is the probability of successful system performance at a given time, given that the system has operated according to specified operational and environmental conditions. The simplest reliability model results when three basic assumptions are made. The first assumption is that all parts in the system are series-connected such that a failure of any one of them results in system failure. The second assumption is that all components are independent of one another; that is, the failure of one part does not cause the failure of another. These two assumptions allow the system's probability of success to be computed by multiplying together the probability of success of each of the parts. Thus,

$$P_S \text{ system} = \prod_{\text{all } i} P_S \text{ part } i \cdot$$

The third simplifying assumption is that the failure events are randomly distributed in time so that the probability of success over time can be represented with the exponential distribution as follows:

$$P_S = \prod_{\text{all } i} \exp(-\lambda_i t) = \exp(-t \sum_{\text{all } i} \lambda_i)$$

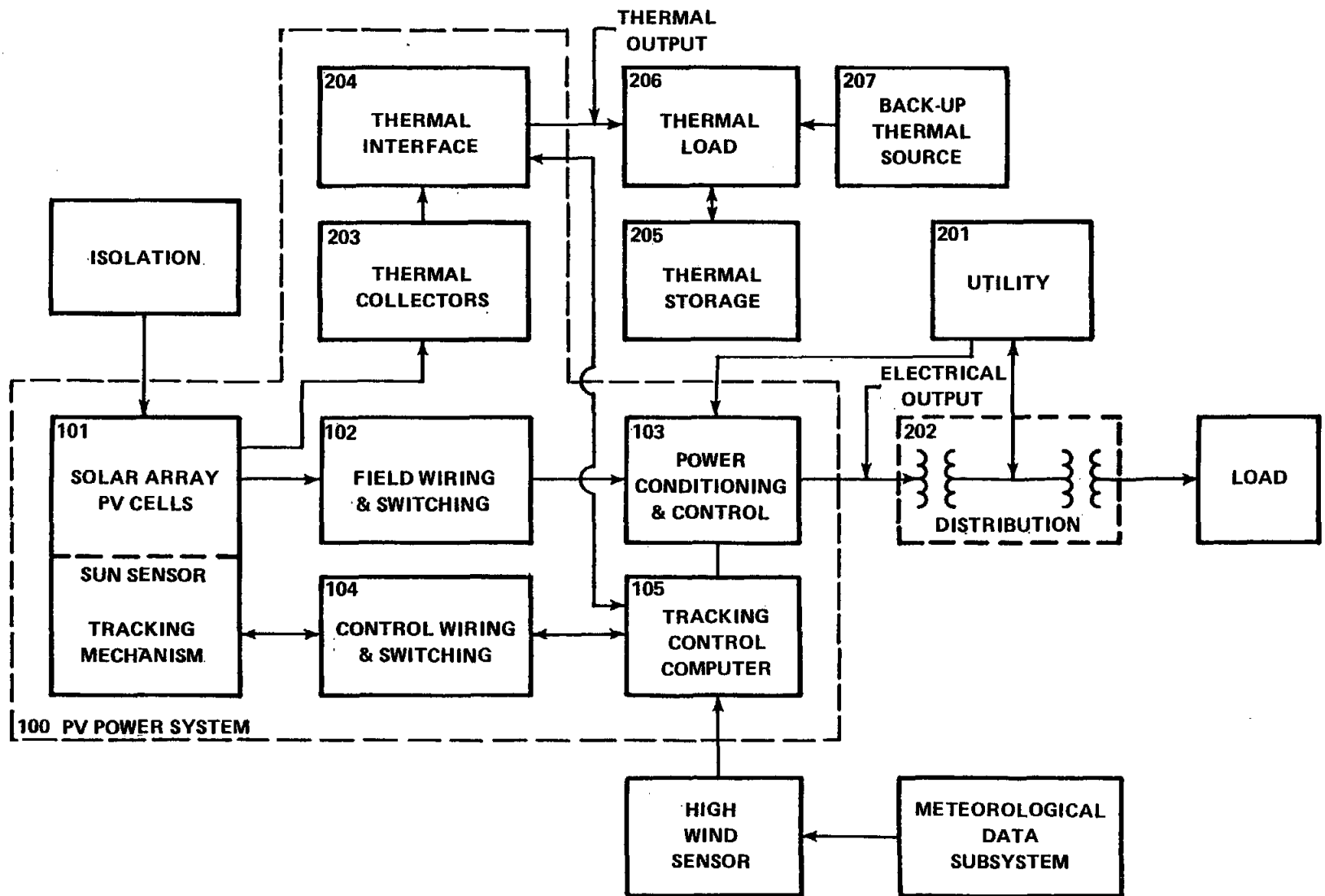


FIGURE 9. SIMPLIFIED FUNCTIONAL BLOCK DIAGRAM-GENERIC CONCENTRATOR PV POWER SYSTEM, ACTIVELY COOLED, INTERACTIVE WITH UTILITY, NO STORAGE

where λ_i is the failure rate of the i th part and t is time. This simple approach allows for the addition of the failure rates of the parts to produce the reliability or failure rate of the entire assembly. This assembly could be either a component or an item of equipment and, if these simplifying assumptions are maintained up through the subsystem and system level, adding of the failure rates of the parts will produce the system failure rate. Additionally, in these cases, the mean time to failure (MTBF) is the reciprocal of the failure rate, i.e., $MTBF = 1/\lambda$. These assumptions are often very useful in early subsystem design stages when functional details and precise parts information are not yet available. Thus, failure rate data are the primary data needed by simple reliability models. Reliability of the subsystem can be estimated roughly by an estimate of the parts count. Time is usually measured as operating time. In PV power systems, time is best measured as lapsed time on a 24-hour-a-day basis (operating or nonoperating), since, in some cases such as with battery storage, part of the system operates continuously and the rest intermittently. The related failure-rate data used would have to be adjusted accordingly for each subsystem. In any given year, depending on location, there is approximately a 2.5 to 1 ratio between lapsed-time and the hours which a no storage PV system would operate.

Since failure rates for individual parts can be extremely small, on the order of 10^{-6} to 10^{-9} failures per hour, it is difficult and expensive to conduct tests of sufficient length, with large enough sample sizes to establish reliable estimates of their failure distribution shape and parameters. Thus, a body of data is accumulated only over a long period of time after new devices, components, equipment, and systems are designed, fabricated, tested, and used in the field in large numbers.

Distributions encountered in reliability models are those representing the part's probability of success over time. These include the exponential, the Weibull, and the normal distributions. The exponential is in greatest use in representing the "middle-life" period of electronic systems--after the infant mortality stage is passed and before wear-out. The Weibull can be used to represent early life, the exponential middle life, as well as increasing failure rate behavior. The normal distribution is sometimes applied to model mechanical and other parts with a wear-out failure mode that is important to the system.

In the modeling of the PV array subsystem of PV power systems, the technique developed by JPL will be used(2,3). This "Flat-Plate Photovoltaic Module and Array Circuit Design Optimization Methodology" establishes the resulting degradation over the lifetime of the modules connected in "n"-parallel strings and "m" series blocks, with bypass diodes at alternative locations. Using the binomial distribution, these optimizations often show that with no maintenance during the 20-year life of the system, a well-designed large array field will exhibit successful operation with only 5 to 10 percent degradation in power output due to cell failure. In addition to the circuit design, the other data needed for this analysis include an estimated cell failure-rate value. In such cases, the array may be represented by this degradation and the failure probability of the flat-panel array field subsystem (or the cell portion of concentrator arrays) can be assumed to be zero in the overall system reliability model. In these cases the designer may attend to other subsystems to optimize system reliability. This technique will be discussed later in more detail, as will more functionally accurate reliability models than the series model discussed above. These include fault tree, state variable, and simulation approaches used in combination with a system functional diagram. The simulation approach allows use of normal, Weibull, lognormal, and other distributions. Thus, data to enumerate the characteristic parameters of these distributions are needed for these analysis.

Reliability Data

Few field reliability data are available at this time for PV subsystems and components. Approximations and estimates must be used based on subsystems and components of similar types. The models will use estimated data that attempt to represent the reliability of mature production systems. The reliability data from DOE's and other operating PV systems will be useful after they have been functioning for about a year when the system debugging is completed and the "infant mortality" period has passed.

The inverter is a primary subsystem of each of the three PV power systems which were studied. Several inverter manufacturers were interviewed and it was decided to represent all inverters in all the systems modeled in

this program with one mature production reliability figure--that being a one-year (lapsed time) mean time between failure (8,760 hours). In addition, preventive maintenance would be defined as replacement of main contactors every three years and a minor annual cleanup and air-filter replacement. The time for this annual preventive maintenance is included in the general PV power system annual maintenance data.

The cells will not be directly represented by failure rates in the system reliability model, but by using the JPL technique as discussed above. An estimated failure rate of 0.0001 failures per year which is 114×10^{-6} failures per hour (lapsed time) will be assumed for the flat-panel cells. A failure rate of 0.0005 failures per year will be used for the more highly stressed concentrator cells. This is a failure rate of 570×10^{-6} failures per hour. Cell failures do not result in array field failure. The output from the JPL program is represented as a gradual power degradation from a large array since individual cell failures are masked by the series-parallel arrangement and the bypass diode placement.

The control systems will be modeled with one number--a mean time between failure which is typical of electronics of this complexity.

Utility data to represent distribution systems, transformers, switches, and the reliability of the grid are all drawn from the Appendices of IEEE Standard 493-1980(4).

The data for the thermal subsystems for the actively cooled concentrators were obtained from an Argonne Laboratory paper(5). Table 1 is extracted from this paper. It shows the wide range of failure rate data for each part or component. Reasonable estimates were made from these.

The actual data used are given in tables later in the report, together with the discussion of the systems being analyzed. It must be made clear that the data used at this time are best estimates. The actual field behavior of PV power system components, parts and subsystems cannot be based on factual data until more years of experience have been obtained.

Also, data were needed for degradation effects such as yellowing of plastics and the accumulation of dirt on flat panels and concentrating units. No single set of data will apply for a wide variety of locations so, in these cases, estimates were used based on general information available(6,7,8).

TABLE 1. RANGE OF COMPONENT FAILURE RATES FOR
EVALUATING SOLAR DHW SYSTEMS⁽⁵⁾

Component	Failure Rate Range (/10 ⁶ hr)
Collector panel	11.4-114
Storage or expansion tank	7.6-23
Storage tank with heat exchanger	11.4-23
Hose	23-38
Soldered joints/pipe	0.02-5
Powered valve	5.7-57
Pump	3-350
Check valve	5.7-11.4
Pressure relief valve	5.7-11.4
Air vent or air separator	14-200
Control system	5-30
Heat exchanger	2.3-14.3
Damper	11.4-38
Fan	2.8-11.4

As a starting point in all the analyses, a monthly power output duration curve was used. This is a plot frequently used in the utility industry. It represents the power output of the system versus the number of hours in a given month that power is equal to or greater than a given value (see Figure 10). These curves were obtained from earlier computer simulations of the PV system's array design, assuming a certain location and no failures or degradation. They were used as a base of reference for each month of the 12-month year. Annual power output was then computed from these monthly curves in conjunction with the effects of degradation, failures, and shutdowns for repair, which reduced the output in appropriate amounts.

Reliability Versus Cost. If it becomes desirable to evaluate the sensitivity of the effect of the reliability of subsystems on the life-cycle energy cost of the PV system, it would be necessary to estimate initial subsystem cost for various reliability levels. There are few data available showing these relationships. Table 2 provides some general relationships among electronic equipment reliability, complexity, and cost values selected from a wide variety of space, military, and commercial programs. These are shown in graphic form in Figure 11 which is a plot of the relationship between MTBF per 1000 component parts and cost per 1000 parts.

To make use of this relationship, consider an inverter which is estimated⁽⁹⁾ to cost \$0.31 per Wp for a system whose total cost is \$6.00 per Wp. A 50,000-watt inverter would thus cost \$15,500. Its MTBF has been estimated at 8760 clock hours for this program. However, the data in Table 2 and Figure 11 are in operating hours. Approximately 3700 of the 8760 hours would be operating hours for a PV system in the southwest without storage. Using the curve of Figure 11, a 3700-hour inverter made up of about 600 component parts is equivalent to a 6167 hour/1000 part system. A transfer of the cost of this \$15,500 inverter into a "per-1000-part" basis results in \$25,833. If we raise the MTBF from 3700 hours to 10,000 hours, a line parallel to the one given in Figure 11 could be used to estimate the change in cost as a function of reliability. A point on this line is a reasonable estimate of cost for the more reliable inverter. This point would be calculated as follows.

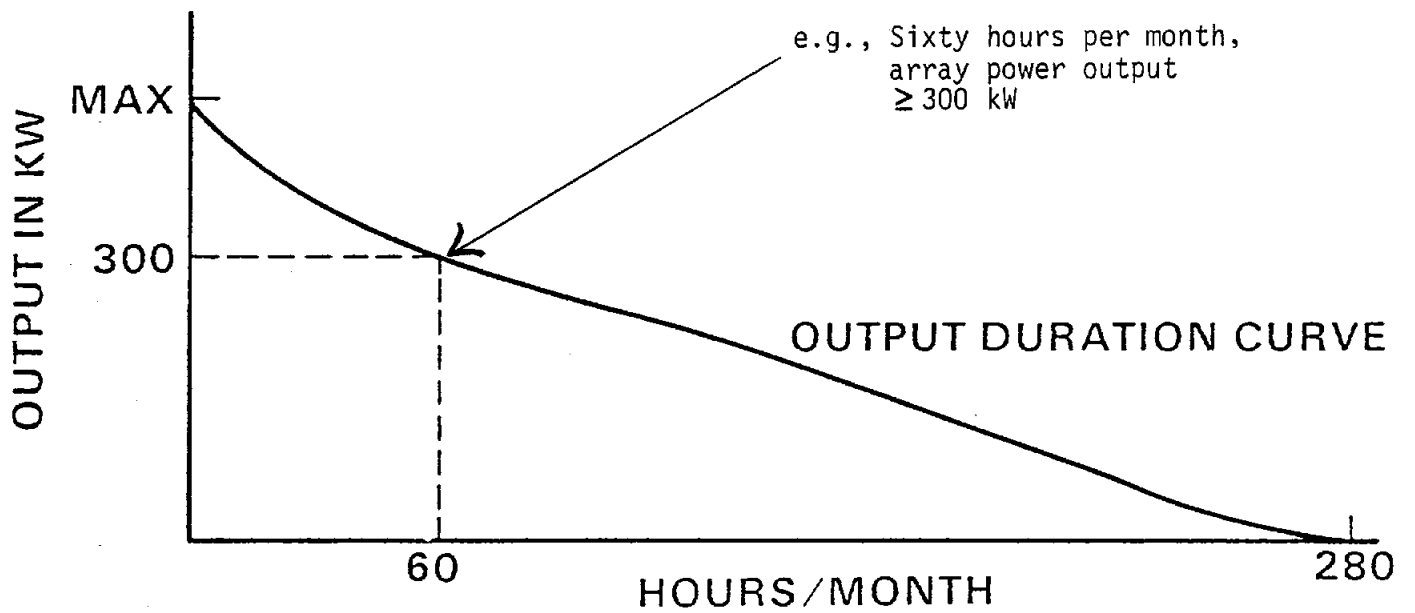


FIGURE 10. POWER OUTPUT DURATION CURVE -- FOR 1 OF 12 MONTHS OF TYPICAL YEAR

TABLE 2. RELIABILITY VERSUS COST

	MTBF, hr	Parts Count	MTBF per 1000 Parts	Cost Dollars	Cost per 1000 Parts
Color TV (~1975)	450	300	135	480	1,600
Altimeter, Missile	1,880	486	914	2,525	5.195
TV Monitor (B&W)	1,250	800	1,000	1,250	1,560
Computer, Minuteman G&C	8,611	6,698	57,676	200,000	29,860
Programmer, Lunar Orbiter	18,504	4,400	81,417	240,000	54,550

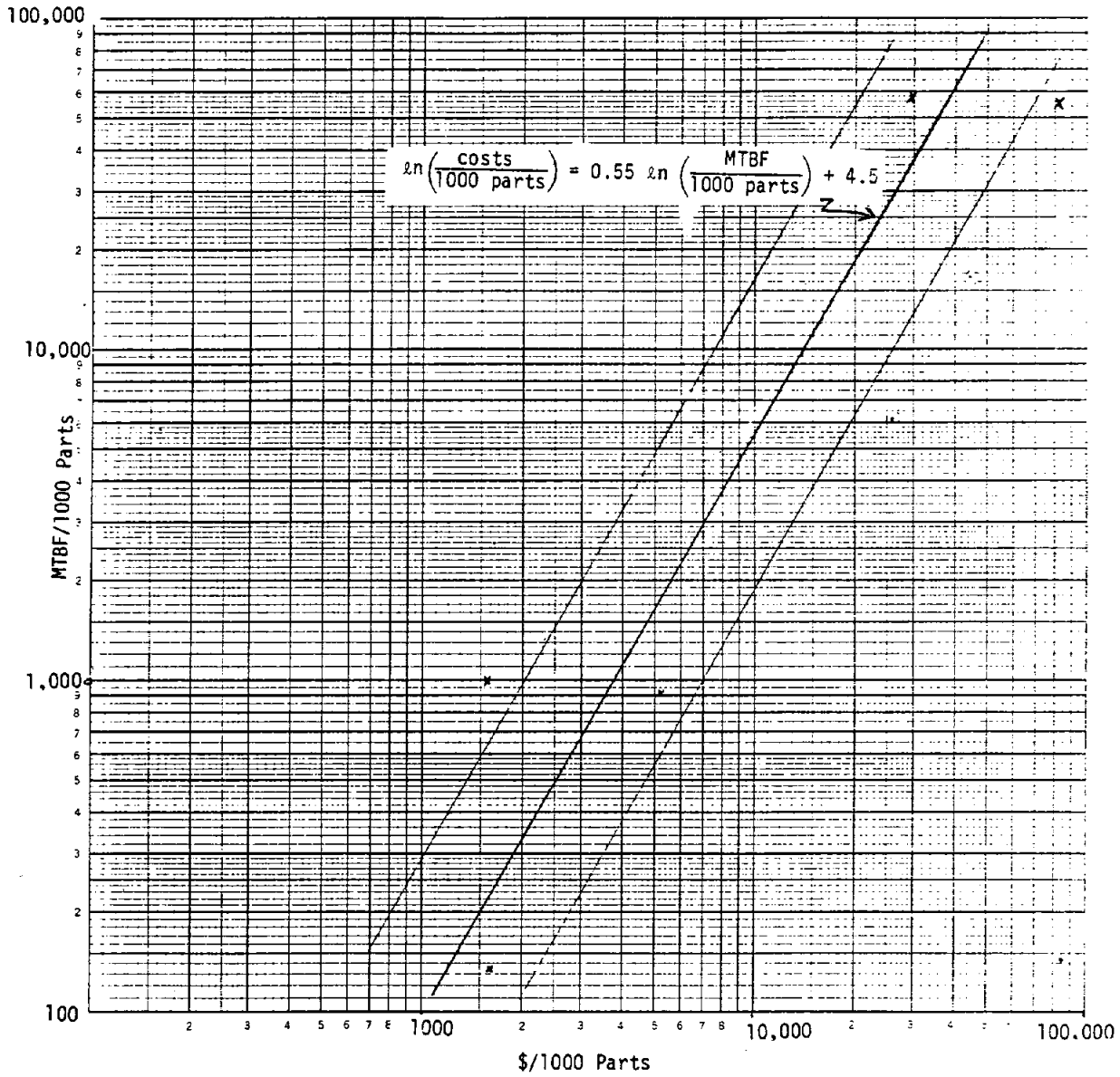


FIGURE 11. MTBF VERSUS COST -- GENERAL RELATIONSHIP FOR ELECTRONICS

The original equation is:

$$\ln (\text{cost}/1000 \text{ parts}) = 0.55 (\text{MTBF}/1000 \text{ parts}) + 4.5$$

To compute a line parallel to it, we calculate a new intercept in place of 4.5.

$$\ln (25,833) = 0.55 \ln (6167) + N$$

$$N = 10.159 - 0.55 (8.727) = 5.36.$$

and, given the desired MTBF increase:

$$\frac{10,000}{3,700} = 2.7 \text{ (factor increase of MTBF)}$$

and substituting this factor and the new intercept into the original equation and solving for cost per 1000 parts, we have:

$$\begin{aligned} \ln C_2 &= 0.55 \ln (2.702 \times 6167) + 5.36 \\ &= 0.55 (9.721) \\ &= 5.34 + 5.36 \\ &= 10.70 \end{aligned}$$

$C_2 = \$44,578$ for a 1000 part system, which is the point needed.

For a 600 part system

$$C_2 = \$26,747.$$

Thus, the increase in cost to obtain the higher MTBF is a $\frac{26,747}{15,500} = 1.73$ ratio. This is an increase of 73 percent in cost to get a 2.7 ratio or 170 percent increase in MTBF.

Similar calculations may be used to obtain costs for inverters of other complexities and MTBF.

Maintenance Data

A paper describing operational experience at the Natural Bridges PV System provided some information on the kinds of maintenance skills, times and costs involved in photovoltaic system operation(10). These data are plotted in Figure 12 on a lognormal scale. Lognormal distributions of time-to-repair have been found to be appropriate to represent actual repair activities(11,12). The estimates used were related to each particular system and are shown later in the report with the reliability data. They are considered to be reasonable estimates for the specific systems involved.

Although, the methodologies developed on this program will result in values of levelized life-cycle energy cost, they should not be taken as accurate predictions of system effectiveness until more factual input data can be obtained.

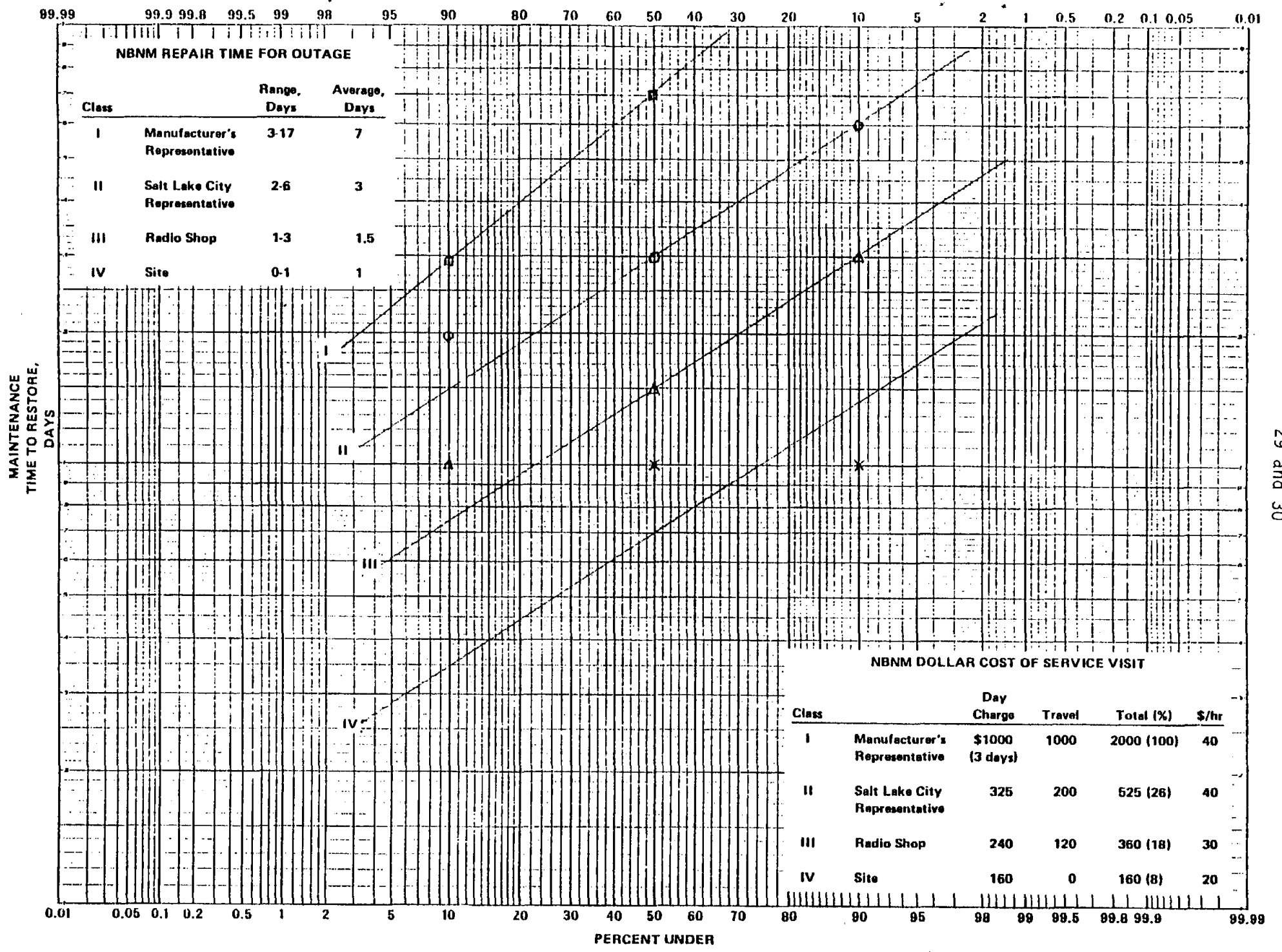


FIGURE 12. PV SYSTEM MAINTENANCE TIME ESTIMATES⁽¹⁰⁾

RELIABILITY ANALYSIS DEVELOPMENT

SYSTEM RELIABILITY ANALYSIS DEVELOPMENT

Considerations in Selecting the Methodology

Arriving at a methodology for analyzing PV systems is a matter of selecting among models previously developed and proven by the reliability community. Many factors must be considered in selecting and integrating the techniques that will be used to model the reliability, maintainability, and cost of the PV systems. A model is inappropriate if it requires data at a level of detail which are unavailable. The design stage of the system (conceptual, verification, full-scale development, or production stage) as well as the system's complexity must be considered, as must consistent definitions of failure and the planned interaction with the life cycle cost model. Table 3 presents a list of reliability/availability models which were considered during this study. The simpler models are listed toward the top of the table. These are more useful for conceptual designs and PV systems of little complexity, whereas those at the bottom of the table are more practical in representing complex systems at later design stages.

The selection of a reliability methodology to satisfy all conditions is not likely to result in a practical approach if it is limited to one analysis technique to cover all systems and design stages. Two or three techniques will be needed.

Discussion of Reliability/Availability Methodologies

In considering a system-level approach to analyze photovoltaic system reliability, it must be recognized that the methodology should accept reliability model outputs of a varied nature. Each subsystem can be characterized using an MTBF, a probability of success at one point in time, or a probability distribution with parameters representing the expected value and variance.

For most of the subsystems shown previously, these interfaces among subsystems are fairly straightforward. For example, the utility and the distribution system can readily be represented by an MTBF or failure rate. The utility, of course, needs to be included to represent power available to the

TABLE 3. RELIABILITY ANALYSIS TECHNIQUES EXAMINED

Class: Model's Output:	<u>Reliability Models</u> Time to First Failure	<u>Availability Models</u> Time Between Failures (Includes Repair)
	<ul style="list-style-type: none"> ● Series Exponential Model ● Fault Trees/Functional Model ● Failure Mode and Effects Analysis (FMEA)--a Design Review Technique ● Series/Parallel Probability Model ● State Variables--Markov Chain Solution (involving exponential rates of failure only) ● Simulation with Functional Model--Nonexponential Distributions can be Included 	<ul style="list-style-type: none"> ● Fault Trees--Minimal Cut Set Approach*, Including Repair ● Network Reduction* ● State Variables--Markov Solution (both rates of failure and repair assumed exponential) ● Simulation with Functional Model--Including Effects of Degradation Failures, Repair, and Array Washing

*As in IEEE Std. 493-1980, "Recommended Practice for Design of Reliable Industrial and Commercial Power Systems".(4)

load. The power conditioning and the field wiring and switching subsystems can be represented by a series-exponential model whose characteristic parameter is an MTBF or failure rate.

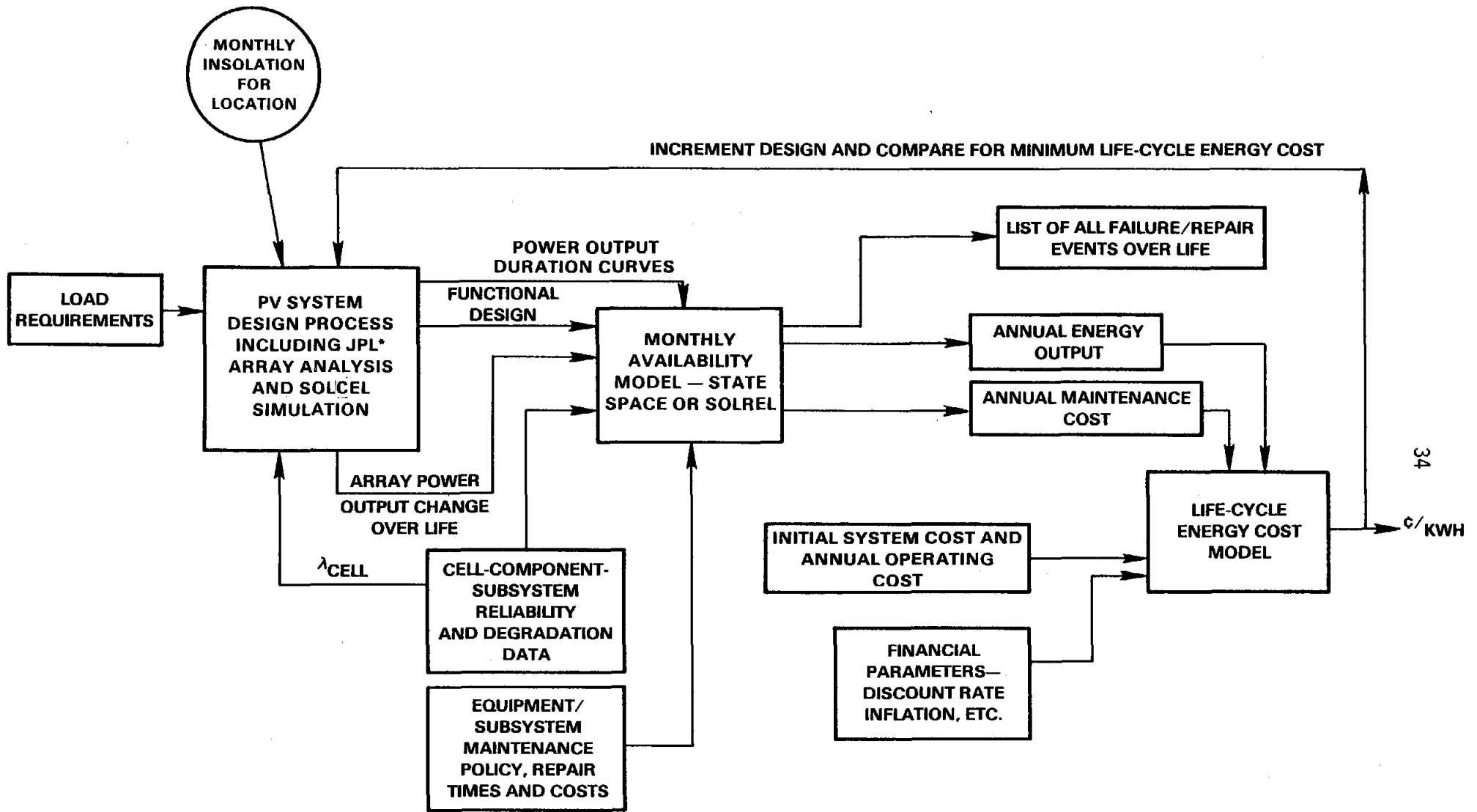
The models which provide the interface with the solar PV array subsystems are the most complex, and are also in an embryonic stage. For the flat-panel array, JPL has developed an Array Design Methodology(3), as described earlier. It results in an array subsystem design that is tolerant to cell or module failure. That is, the interconnections are made such that

cell failures have little impact on the system power output. The technique contains a binomial model to represent the effect of cell failures as well as a network model to represent the electrical interactions of the series-connections of cells and parallel-connections of cells and bypass diodes. For analysis purposes, it provides an output curve representing power generated versus time for a selected cell failure rate and replacement policy.

The PV array for concentrator systems has further levels of complexity. First, the series-parallel cell connection, bypass diode arrangement must be analyzed. The JPL technique described above may be used for this portion of the analysis. The tracking subsystem also needs to be modeled. Since these subarrays are usually series-connected in pairs or triples, the failure of one tracking subassembly will cause the failure of two or three out of 50 or 60 arrays in a typical large array field. Should the concentrator system also contain active cooling--that is, a pumped fluid running through the heat sinks of the solar cells to maintain them at an efficient operating temperature and to provide heat to a thermal load--the complexity of the modeling of this subsystem would increase.

These considerations have been included in the choice of models for PV power systems which are discussed later. First, an overview of the methodologies will be given.

The flow chart of Figure 13 presents the basic approach of the analysis methodologies selected--the state space and the simulation models. These were chosen for their ability to represent both failure and repair in one model. The two boxes at the left of the figure, the load requirements, and the PV system design and simulation, including the JPL methodology, deal with the iterations which result in the initial array field and system design. The outputs of this process provide the baseline inputs of a monthly power output duration curve (related to insolation) and degradation of the PV array field over time (related to cell failure). This information, together with the functional design of the rest of the system and the maintenance and reliability data are used as inputs to the availability (reliability/ maintenance) methodology. As Figure 13 shows, the outputs are then fed to the life-cycle energy cost model to reflect the costs and energy losses due to failures, repairs and preventive maintenance. The feedback loop at the top shows the



**"FLAT PLATE PV MODULE AND ARRAY CIRCUIT DESIGN OPTIMIZATION", JPL HANDBOOK

FIGURE 13. OVERVIEW OF INTERACTIONS OF AVAILABILITY METHODOLOGY WITH THE SYSTEM DESIGN PROCESS

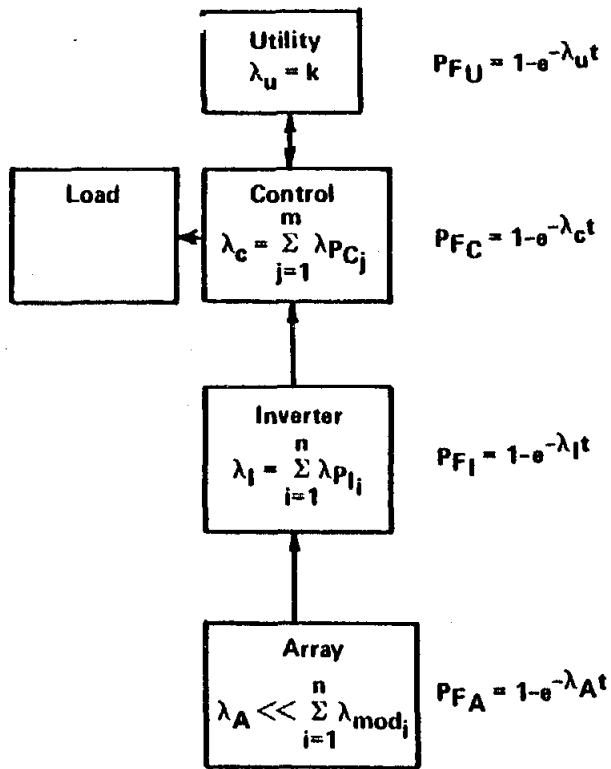
optimization process--to increment the design by establishing the sensitivity of various hardware, reliability, and maintenance factors to life-cycle energy costs.

Fault Tree Model

Early design decisions regarding relative system configuration can be aided by simple reliability analysis techniques such as fault trees. Simple techniques can be used to compare alternate designs in light of reliability/availability specifications for the system.

Figure 14 shows the example flat-panel PV system shown earlier in Figure 5. It is functionally diagrammed in the top left-hand side of the figure. The array feeds a d-c to a-c inverter under the management of a control subsystem to provide for normal operations of supplying the load, backfeeding the utility, feeding the load in conjunction with the utility, or permitting the utility to carry the load should the photovoltaic system not be providing power. The combination of the inverter and control subsystem is often referred to as a power conditioning unit (PCU). The fault tree diagram which logically models the impact of each respective subsystem's failure on system failure is shown below the functional block diagram. At the top level, system failure can be caused by the control subsystem alone, since it is in series with all paths from the sources to the load. The symbol next to the letter "c" is that of an "OR" gate which indicates that failure of any of the inputs from the bottom will cause system failure. The symbol next to the letter "b" is an "AND" gate which means all inputs from the bottom of the symbol must fail before its output is a failure; thus, either the array and the utility, or the inverter and the utility must fail before a system failure occurs. The probability-of-failure relationships are written as exponential distributions on the functional diagram. This is a convenient distribution but not the only one that can be used. The balance of the model deals with probabilities, not failure rates (λ). This functional logic can be represented by probability relationships as shown. These flow from the bottom of the fault tree diagram upward, and show the relationships between the probability of failure at the output of each logic gate and the inputs from below.

SOLAR PV SYSTEM



PROBABILITY RELATIONSHIP FROM FAULT TREE

Note: P_S = Prob. of Success
 P_F = Prob. of Failure

$$P_{F(a)} = P_{FA} + P_{FI} - P_{FA} P_{FI}$$

$$P_{F(b)} = P_{FU} (P_{FA} + P_{FI} - P_{FA} P_{FI})$$

$$P_{F(c)} = P_{Fsystem} = P_{FU} (P_{FA} + P_{FI} - P_{FA} P_{FI}) + P_{FC} - P_{FC} P_{FU} (P_{FA} + P_{FI} - P_{FA} P_{FI})$$

Assuming $\lambda_A \approx 0$; $P_{FA} \approx 0$

$$P_{Fsystem} = P_{FU} (P_{FI}) + P_{FC} - P_{FC} P_{FU} P_{FI}$$

$$= (1 - P_{FC}) P_{FU} P_{FI} + P_{FC}$$

Since $(1 - P_{FC}) = P_{SC} \approx 1$

$$P_{Fsystem} = P_{FC} + P_{FU} P_{FI}$$

Thus the failure rate or reliability of the control system has the biggest impact on system reliability while the failure of the inverter is tempered by the redundancy of the Utility connection. The inverter and Utility must both fail for system failure to occur.

FAULT TREE – (Functional Model)

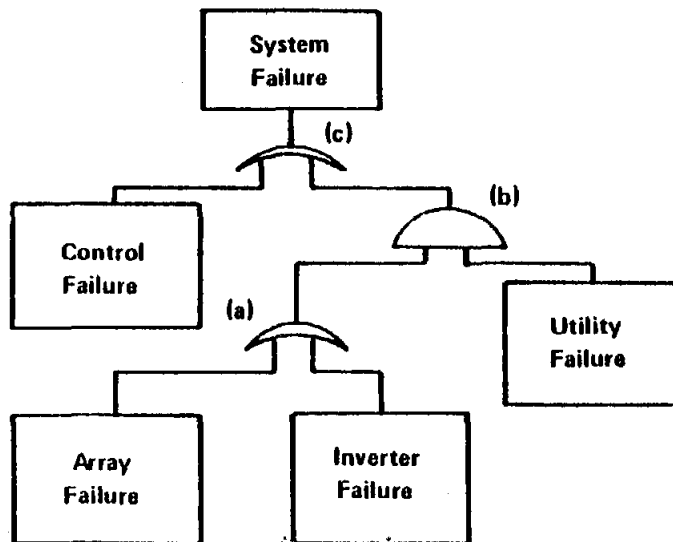


FIGURE 14. EXAMPLE SOLAR PV SYSTEM AND FAULT TREE MODEL SHOWING FUNCTIONAL/PROBABILITY RELATIONSHIPS TO FOCUS DESIGNER ATTENTION ON SUBSYSTEM REQUIRING RELIABILITY EMPHASIS

They are developed upward to the probability of failure at Point "c", which is the system probability of failure. If the array is designed to be very redundant with bypass diodes used generously, and array field failure is defined as a 5 or 10 percent decrease in output, we can assume that its probability of failure is zero, and this term drops from the equation. The last equation in Figure 14 is for the probability of system failure which is represented by (only) those subsystems which contribute to a system failure. It is noted that it is equal to the probability of the control subsystem failure added to the product of the probability of failure of the utility times the probability of failure of the inverter. Since the last term is the product of two probabilities much less than one, it will be much smaller than the first term (the control-subsystem failure probability) if all three subsystem failure probabilities were the same order of magnitude. Thus, the control subsystem is the major contributor to system failure in this example. So it is up to the designer to see that the probability of failure of the control subsystem is made small relative to the utility and inverter probabilities of failure so that its impact on the system failure is minimized. Of course, costs must be involved in the decision as to just how small to attempt to make this subsystem's probability of failure. That is where the maintenance cost and life cycle cost models come into use, since it is initial cost and maintenance cost changes that relate reliability to life-cycle cost.

Most PV power systems have a relatively small number of subsystems, usually from three to five as the previous example illustrated. The fault tree model works well for these simple systems and will accept inputs from other, possibly more complex, models at lower system levels to provide the probabilities needed to represent the reliability of the various subsystems. But it does have certain limitations--it does not dynamically represent maintenance and return-to-operation. The example uses a negative exponential distribution for time between failures which is applicable to many electronic devices but not to mechanical and thermal devices. The inputs at the bottom of the fault tree must be independent and must exhaustively include all possible failure causes for the element up one level. And, as the model becomes more complex, it is difficult to develop the trees with a 100 percent accuracy. More sophisticated state space techniques using state variables and

Markov chains have been developed and applied. These are more appropriate for PV system modeling when the goal is to minimize life-cycle energy cost. They have the advantage of being analytical models which can be solved manually or with a programmable calculator.

As the systems become more complex, as degradation needs to be represented and as various distributions need to be used for different components or subsystems--especially when accurate data are available--computer simulation techniques are useful. These make use of logic flow diagrams and the mathematical representation of the important cause and effect relationships. Random number generation is used to simulate the behavior of components and subsystems over time and to predict failure occurrences, repair times, and other characteristics of interest. A wide variety of computer simulation languages such as GASP IV and SLAM are available to simplify the use of simulation.

These state space and simulation models become more effective as a new system evolves, as data become more complete, as the relationships between subsystems become better understood, and as the system's complexity increases. Discussions of these methodologies follow in this report.

Array Field Design Analysis Methodology-- Output Power Degradation Due to Solar Cell Failures

General

Analyses of array field power loss over time can make use of the JPL Array Design Methodology(3). It assumes a maintenance philosophy in which modules with failed cells are not replaced, but allowed to remain in the field. The analysis is based on a knowledge of the cell series-parallel interconnection scheme of each array, the by-pass diode density (actually, the number of series cells per by-pass diode), and an assumed cell failure rate.

Cell failure rates (λ_{cell}) for specific cell and module designs, and particularly for current designs, have not been established. Estimates of λ_{cell} based on limited field experience with a number of disparate array field and module designs have been published by JPL, MIT Lincoln Laboratories, and others.

Cell "allocations" have also been developed based on speculative projections of module technology. A commonly used λ_{cell} allocation for flat plate technology is 0.0001 failures per year. This failure rate includes both open and short-circuit cell failure modes. In order to produce a conservative prediction, the JPL methodology makes the assumption that any cell failure causes a substring failure, even though this is only assured for the open-circuit mode.

In the analysis of flat-panel systems, failure rate values of 0.001, 0.0001, and 0.00001 failures per year are used, and three separate array power degradation curves generated. The largest (0.001) represents the high end of the field data experience. The 0.0001 value is taken as typical for a mature production line with good quality assurance.

No meaningful data on cell failure rates for concentrator-type photovoltaic arrays exist, primarily because of the limited field experience with these arrays. In developing a number for use in the present analyses, it was projected that cells operating in concentrator arrays are subjected to higher stresses than those in flat-panel modules due to potentially higher temperatures and/or thermal gradients. On this basis, a λ_{cell} of 0.0005 failures per year was allocated to the concentrator cells.

The key factors in determining the ability of a given array to maintain the achieve power output levels near its rated value despite individual cell failures, are the density of parallel interconnections of cells and the density of by-pass diodes. Therefore, the first step in the analysis of array power loss behavior is an assessment of the electrical design of the array. Detailed data about the series block, branch circuit, and by-pass diode connections are required for each system to be analyzed. These are presented with each system description in Volume II. This technique was not used for the example PV system analyzed in Volume I.

Analysis Procedure

The first step in the JPL methodology's calculation of the array power loss as a function of time is to determine the substring* failure density. The methodology uses the binomial equation

$$P_k = \frac{n!}{k! (n-k)!} p^k (1-p)^{n-k}$$

where n is the number of cells per substring, p is the cumulative cell failure density at time T , and k is the expected number of failed cells per substring. Additional assumptions relevant to the analyses are:

- One failed cell results in a failed substring.
- More than one failed cell in a given substring has no additional effect.

With these assumptions, it can be seen that the substring failure density (D) is given by

$$D = 1 - P_0$$

where P_0 denotes P_k with $k = 0$.

Once the substring failure density as a function of time has been determined, the array power loss as a function of time can be determined using computer-generated data developed by the JPL group as part of their Flat Plate Photovoltaic Module and Array Circuit Design Optimization methodology(2,3). The computer program uses the failure density data and, providing for random distribution of the failures, adds in the appropriate manner, the I-V characteristics of the individual devices to assess the net impact on the array performance. The computer analyses include the effects of series-parallel

*The terms substring and series block are synonymous in the case of the two concentrator systems. In the case of the flat-panel system, a series block contained five (parallel) substrings.

interconnections and diodes. JPL has published the computer-generated data in the form of plots for a range of cases (e.g., 1, 4, 8, and 16 parallel sub-strings per series block; 0, 1, 4, 8, and 12 series blocks per by-pass diode; etc.) which permit interpolation to a wide range of existing designs. An extensive set of these curves appears in the handbook from the JPL Workshop on Flat Plate Photovoltaic Module and Array Circuit Design Optimization.⁽³⁾ Appropriate interpolations from the JPL-generated plots of substring failure density versus array power loss fraction will be used in the present analyses to arrive at an array power loss versus time curve. The results of the methodology's application to a typical flat panel system are shown in Figure 15. One of these curves may be used as an input to the availability models to represent array degradation over time due to cell failures.

While the JPL computer analyses were performed with flat-plate systems in mind, the methodology is clearly applicable to cell failures in concentrator systems also.

State Space Methodology

The state space methodology for analyzing PV system life-cycle energy costs is oriented primarily to the early design and development phase. The name of this approach is derived from the fact that a PV system is always in one state (e.g., 100 percent operational, 90 percent operational) of many possible states. States are defined by the operational status of the elements of the system. The "space" is the set of possible states. Transitions from one state to another correspond to changes in the status of the system components, such as failure of a PV cell string or repair of failed tracking motor. Although the only equipment required is a desk calculator, a programmable calculator is useful to reduce the time to perform some mechanics of the analysis.

Figure 16 is an adaptation of Figure 13 to give a specific overview of the state space approach to estimating PV system life-cycle energy costs. Power production and maintenance costs are computed using separate models. They are combined with appropriate discount rates and inflation factors to determine the life-cycle energy cost. Both models require reliability and maintenance data; the maintenance cost model also requires cost factors for labor, parts, and materials. The use of separate models allows flexibility in the

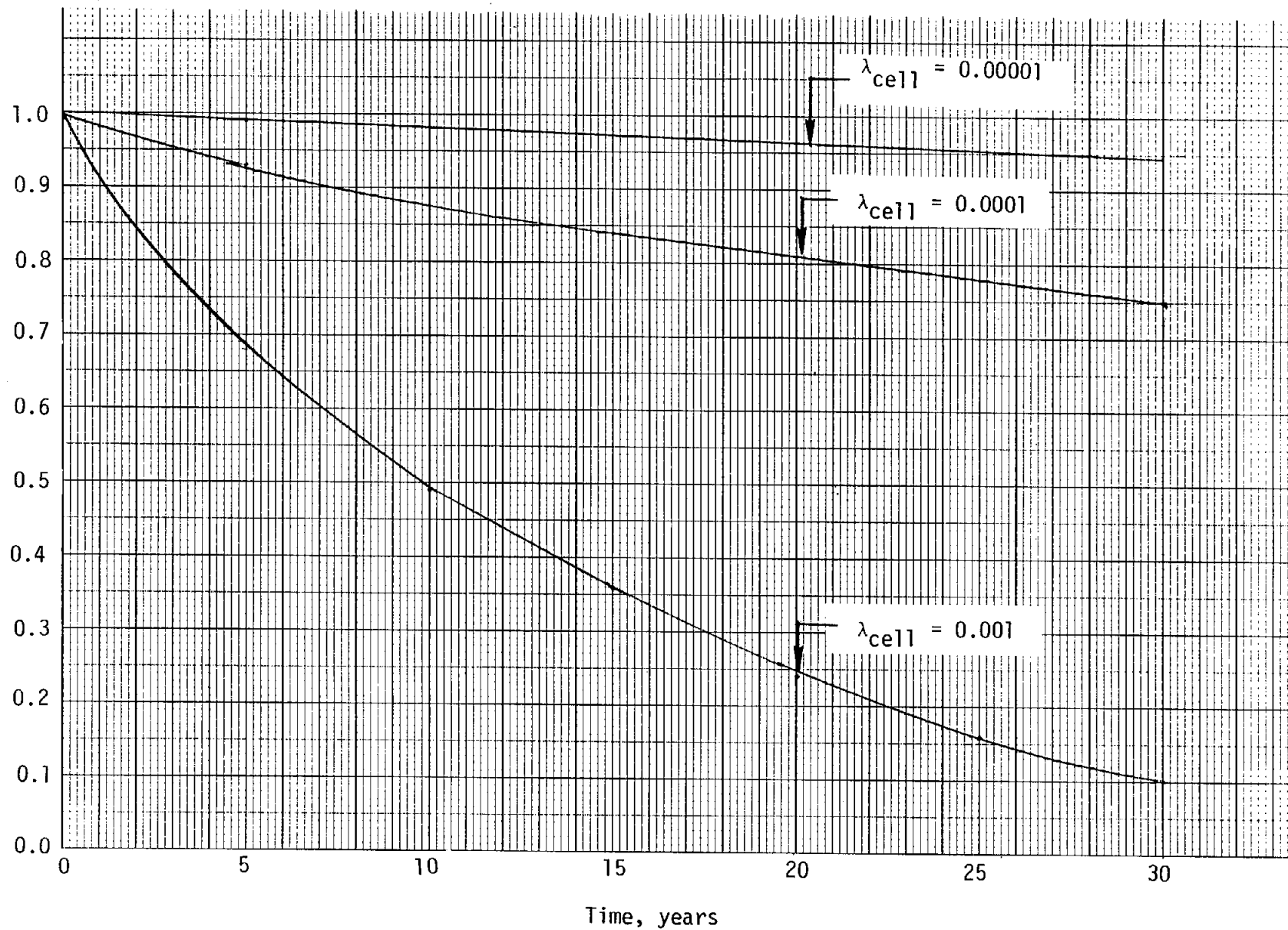


FIGURE 15. PERCENT DEGRADATION IN PEAK OUTPUT CAPABILITY VERSUS PERIOD OF CONTINUOUS OPERATION WITH NO MODULE REPLACEMENT--FLAT PANEL SYSTEM

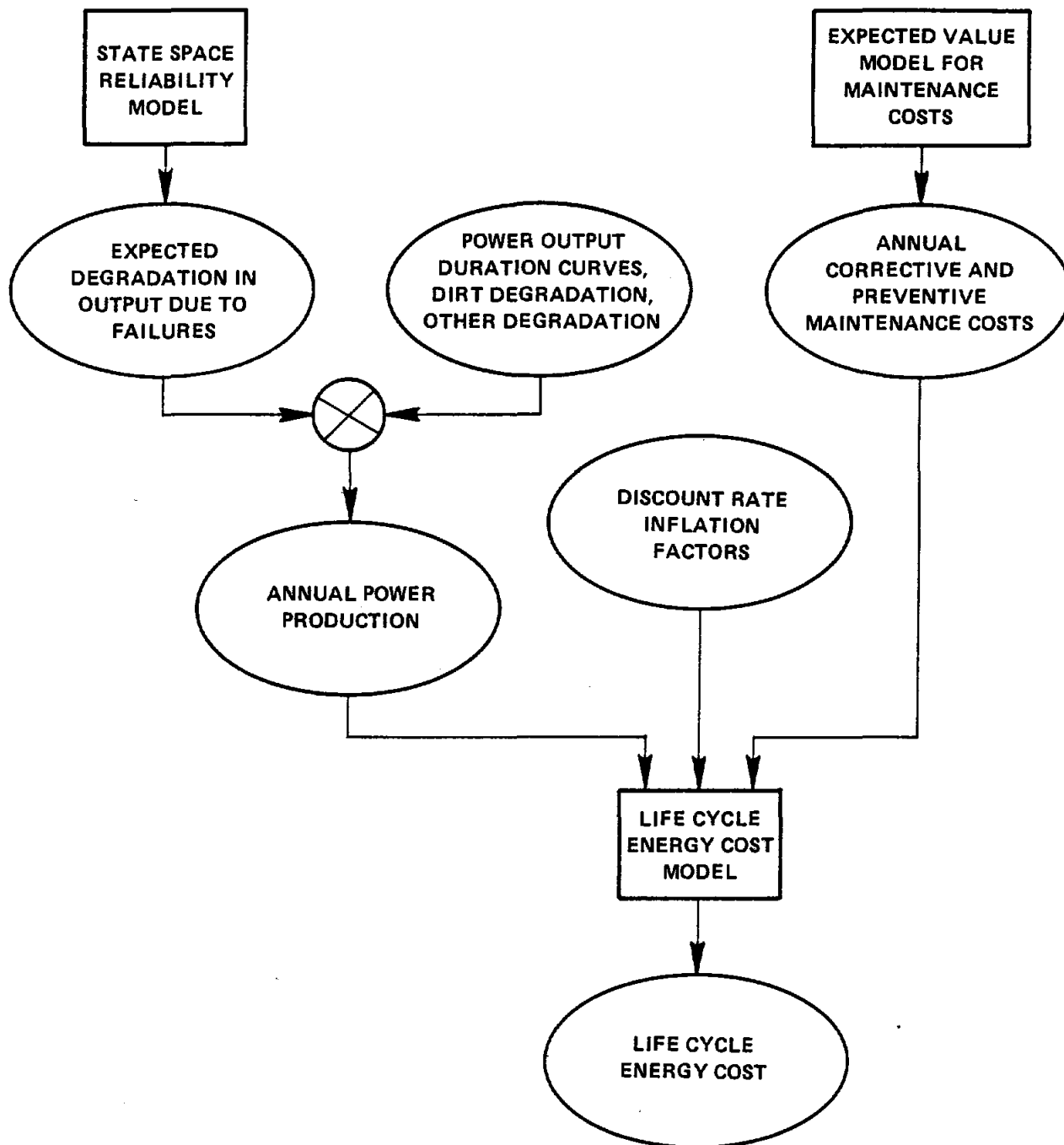


FIGURE 16. OVERVIEW OF STATE SPACE APPROACH

application of the approach. For example, many design or operation changes can be investigated for their impact on system reliability using only the reliability model. The most promising changes can then be evaluated using the entire state space approach to determine the lowest life-cycle energy costs.

This approach assumes that the effects of failures, insolation, and degradation are independent. In reality, some dependencies exist among these effects. For instance, the impact of a failure which results in an hour of system downtime is greater if it occurs during full insolation than during partial insolation. However, for systems with reasonable reliability and only moderate amounts of degradation, the dependencies among the various effects will be negligible.

The following portions of this section discuss details of the energy production, maintenance cost, and life-cycle energy cost models.

Energy production is a function of PV system designs, availability, degradation, and insolation. In this approach, a system state space model is used to compute system production as a function of reliability, maintainability, and system structure. An input to the model is a monthly system power output duration data set which assumes normal insolation for the location and no degradation in any system components. The output of the state space model is the fraction of nominal system capacity which would be realized if the only problems were failures. These are combined with the degradation effects of dirt accumulation on PV cell covers or lenses, and material degradation to compute expected power production for each year.

State Space Model

The state space model is based on the use of system states. Each state is defined in terms of the status of each of the various elements of the system. For each state, the probability of occurrence (a function of failure rate and repair rate data) and the associated fraction of monthly nominal power production are computed. The average fraction of nominal power production is found by combining these quantities for all system states.

The following subsections describe the basic assumptions used in the state space model, specific techniques used for different types of subsystems, and the procedure for combining subsystem results.

Four basic assumptions are made in the state space model. They are:

1. Failures are statistically independent.
2. The time between failures for each element is represented by the negative exponential distribution.
3. The repair times for each element are represented by the negative exponential distribution.
4. Subsystems are independent.

The first assumption is widely used in reliability analysis. Many failures are indeed statistically independent. In addition, a minor amount of correlation between failures has little impact on system reliability.

Use of the negative exponential distribution to represent the time between failures for each element is equivalent to assuming a constant hazard rate (i.e., number of failures per hour). This is a sound and a frequently used assumption for electronic components.

Mechanical component reliability may be represented by a hazard rate which increases as a function of time. The increase corresponds to wear-out of the part. The Weibull and normal distributions are frequently used to model the reliability of mechanical components. However, those distributions are less mathematically tractable than the exponential distribution. Since this model is to be used in the early design phase, it is important to capture the major effects without requiring too much computational effort or resources. The exponential distribution, which is the distribution used in Markov chains, meets these requirements.

A similar argument holds for using the negative exponential distribution to represent the time to repair. Other distributions may be more appropriate, particularly for the variance and higher moments, but the first moments (the means) can be made identical. Since the mean-time-to-repair values are much smaller than the mean-time-to-failure values, the error in the state probabilities associated with using the exponential distribution for repair times will be small.

The assumption of independent subsystems is used to decompose the system into manageable pieces. Breaking the system into independent subsystems allows a separate, single Markov model for each subsystem.

Subsystems may not actually be independent. Failure of one subsystem will often cause the entire PV system to shut down until the failed subsystem is returned to operational status. Failure rates for the other subsystems may be different during the period of shutdown than during normal system operation. Such subsystem interactions are ignored in this state space approach. As long as the annual downtimes are reasonably small (i.e., less than 5 percent), such interactions will have negligible effects on system reliability and life-cycle energy costs.

Using the fourth basic assumption, the PV system to be modeled may be decomposed into several subsystems. A separate state space model is used for each subsystem. Markov model techniques are used to compute the steady state occupancy probabilities for each subsystem state. Associated with each subsystem state is a fraction representing the portion of subsystem capacity available in that subsystem state. The subsystem probabilities are combined with the associated capacity fractions to obtain the expected system capacity. Figure 17 provides an overview of this procedure.

A typical decomposition of a PV system would be as follows:

- (S1) Array field
- (S2) Power conditioning
- (S3) Serial elements.

Array fields can vary significantly in terms of design and reliability logic. Power conditioning subsystems may be significant contributors to system failures and may involve component redundancies (if not, they may be included with the serial elements). Serial element consists of all elements and functions not accounted for in the first two subsystems. Some functions may utilize redundant components. Network reduction formulas are used to express each such function as a single conceptual element.

The following paragraphs describe state space models for the various subsystems.

The states of a given subsystem are defined to represent changes in subsystem capacity due to component failures. In most cases, subsystem states can be readily identified. Consider, for instance, a PV system with dual inverters, each of which can supply a maximum of 50 percent of system capacity. Failure of one inverter will cause the inverter subsystem to degrade from 100 percent capacity to 50 percent capacity. Failure of the second inverter causes output to go to zero. Three inverter subsystem states are defined.

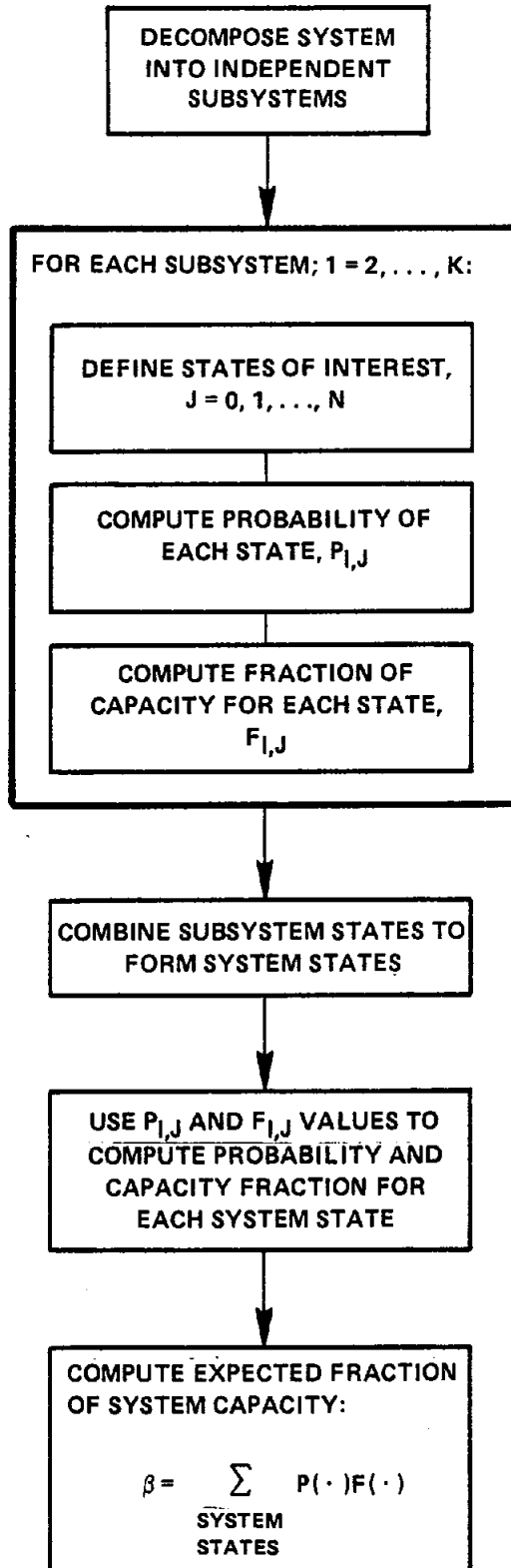


FIGURE 17. OVERVIEW OF STATE SPACE MODEL

Array field subsystems may not always have their states so clearly defined. Failure of a single PV cell in a large collector array may have negligible impact on subsystem capacity, while the cumulative effect of numerous cell failures may cause significant degradation. The analyst can identify the number of cell failures which, as a group, cause enough degradation to warrant definition of a subsystem state. Alternatively, the analyst can use the JPL technique (3) to determine a curve which describes the gradual degradation of system output resulting from cell failures. In the latter case, array field subsystem failure would be defined in terms of wiring, tracking equipment, cooling equipment, and support structures.

A subsystem of elements is in series when the failure of any one element results in failure of the subsystem. Each element in the subsystem is assumed to have two states: Operating, and failed. When one element is failed, the remaining components are not stressed, and therefore not subject to failure, until the failed component is returned to service.

Figure 18 is the state space model for a serial subsystem. The exponential distribution parameters for failure and repair are:

λ_i = Failure rate of element i (failures/hour)

μ_i = Repair rate of element i (repairs/hour).

Note that $1/\lambda$ equals the mean time between failure (MTBF) and $1/\mu$ equals the mean time to repair (MTTR). Each node of the graph represents one state of the subsystem. State 0 is the state of successful subsystem operation. States 1,2,...,n correspond to the subsystem being failed because the component indicated by the associated number is failed.

The steady-state probabilities of subsystem operation and failure are computed using standard Markov techniques. These techniques are appropriate when the probability of each state transition is represented by an exponential distribution. Let

$P_i(t)$ = Probability the subsystem is in state i at time t ,
 $i = 0,1,\dots,n$

P_i = Steady-state probability the system is in state i

P_F = Steady-state probability the system is failed

$\dot{P}_i(t)$ = First derivative of P_i with respect to time.

For each state, the first derivative $\dot{P}_i(t)$ is equal to rate of transition into the state minus the rate of transition out of the state. The differential equations are:

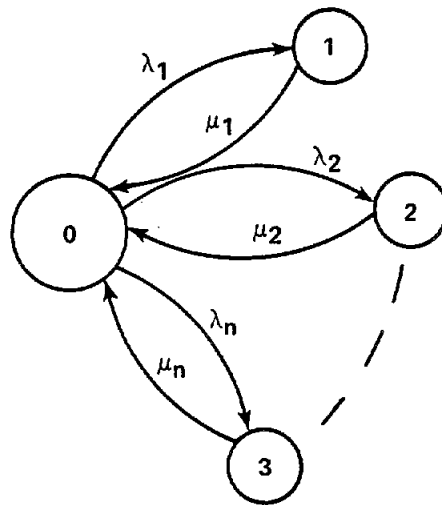


FIGURE 18. STATE SPACE MODEL FOR A SERIAL SUBSYSTEM

$$\dot{P}_0(t) = \sum_{i=1}^n \mu_i P_i(t) - \left(\sum_{i=1}^n \lambda_i \right) P_0(t)$$

$$\dot{P}_i(t) = \lambda_i P_0(t) - \mu_i P_i(t) \quad , \quad i = 1, 2, \dots, n \quad .$$

In the steady-state condition, $\dot{P}_i(t) = 0$ for all states. In particular,

$$0 = \lambda_i P_0 - \mu_i P_i \quad , \quad i = 1, 2, \dots, n$$

and

$$P_i = \frac{\lambda_i}{\mu_i} P_0 \quad , \quad i = 1, 2, \dots, n \quad .$$

Since the sum of all state probabilities must be unity,

$$P_0 + \sum_{i=1}^n \frac{\lambda_i}{\mu_i} P_0 = 1$$

and

$$P_0 \left(1 + \sum_{i=1}^n \frac{\lambda_i}{\mu_i} \right) = 1 \quad .$$

Hence, the probability the subsystem is operating is:

$$P_0 = \frac{1}{1 + \sum_{i=1}^n \frac{\lambda_i}{\mu_i}}$$

The probability the subsystem is failed is:

$$P_F = 1 - P_0 \quad .$$

The preceding two equations are used to compute the subsystem probabilities directly from the λ_i and μ_i transition rates.

One possible complication of this serial subsystem model is the existence of elements with internal parallel redundancy. Network reduction formulas can be used to represent such elements as single units. Appendix A in Volume II develops the formulas for the two basic cases.

In some PV systems, a particular function might be implemented using redundant identical elements to improve the reliability of the function. For example, two inverters could be connected in parallel. Both units operate at one-half capacity until one unit fails. The remaining unit then operates at full capacity. For this analysis, the failure rate of a unit is assumed to be constant regardless of the level at which it is operating.

A number of variations of the redundant system are possible. The variable characteristics are:

- Capacity at which each unit operates
- Whether each unit is to be repaired upon unit failure or whether repair on both units must wait until subsystem failure
- Standby or active redundancy.

The first characteristic affects the capacity of the subsystem (and hence the power production of the PV system). It will be accounted for when the subsystem reliability results are combined. The other two characteristics define four cases to be analyzed, as shown in Table 4.

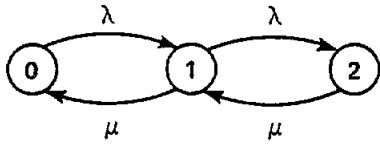
Figure 19 depicts the state transition diagrams for each of the four cases. The nodes represent subsystem states and the number in a node corresponds to the number of failed units. Transition rates between states are expressed in terms of the following parameters:

- λ = Failure rate of a single unit (failures/hour)
- μ = Repair rate of a single unit (repairs/hour).

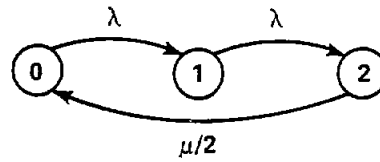
Note that the failure detection and switching functions are assumed to be perfect. Thus they are expected to have extremely low failure rates and, therefore, to have negligible influence on the model results. Their omission simplifies the computations. However, they could be included by modifying the state transition diagrams and solving the corresponding differential equations.

TABLE 4. DUAL SUBSYSTEM CASES

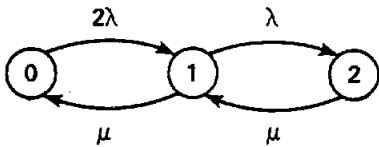
	Repair on Unit Failure	Repair on Subsystem Failure
Standby Redundancy	I	II
Active Redundancy	III	IV



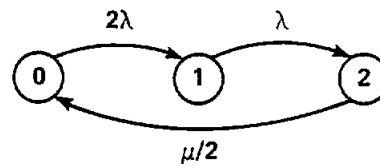
Case I



Case II



Case III



Case IV

FIGURE 19. STATE TRANSITION DIAGRAMS FOR THE DUAL SUBSYSTEM CASES

Consider Case 1. The rate of change of the probability of being in a given state (i.e., the first derivative of the state probability) is the 'rate in' minus the 'rate out'. The differential equations for Case 1 are therefore:

$$\dot{P}_0(t) = \mu P_1(t) - \lambda P_0(t)$$

$$\dot{P}_1(t) = \lambda P_0(t) + \mu P_2(t) - (\lambda + \mu)P_1(t)$$

$$\dot{P}_2(t) = \lambda P_1(t) + \mu P_2(t)$$

When the subsystem is in the steady-state condition, the 'rate in' equals the 'rate out' for each state; that is, $\dot{P}_i(t) = 0$, $i = 0, 1, 2$. Applying this simplification to the preceding equations results in:

$$P_1 = \frac{\lambda}{\mu} P_0$$

$$P_2 = \left(\frac{\lambda}{\mu}\right)^2 P_0$$

Since the sum of the state probabilities is unity,

$$P_0 + \frac{\lambda}{\mu} P_0 + \left(\frac{\lambda}{\mu}\right)^2 P_0 = 1$$

and

$$P_0 = 1 / \left(1 + \frac{\lambda}{\mu} + \left(\frac{\lambda}{\mu}\right)^2 \right)$$

The basic transition rates are used to compute P_1 and P_2 .

Solutions for the other cases are derived in a similar fashion. The results are provided in Table 5.

The solar array field subsystem presents the most difficulties for two reasons. First, a large number of states are possible because of the

TABLE 5. STEADY-STATE SOLUTIONS FOR THE DUAL SUBSYSTEM CASES

	P_0	P_1	P_2
I Standby Unit Repair	$\frac{1}{1 + \frac{\lambda}{\mu} + \left(\frac{\lambda}{\mu}\right)^2}$	$\frac{\lambda}{\mu} P_0$	$\left(\frac{\lambda}{\mu}\right)^2 P_0$
II Standby Subsystem Repair	$\frac{1}{2 + \frac{2\lambda}{\mu}}$	P_0	$\frac{2\lambda}{\mu} P_0$
III Active Unit Repair	$\frac{1}{1 + \frac{2\lambda}{\mu} + 2\left(\frac{\lambda}{\mu}\right)^2}$	$\frac{2\lambda}{\mu} P_0$	$2\left(\frac{\lambda}{\mu}\right)^2 P_0$
IV Active Subsystem Repair	$\frac{1}{3 + \frac{4\lambda}{\mu}}$	$2P_0$	$\frac{4\lambda}{\mu} P_0$

large number of components. Second, the components can be connected in a variety of series-parallel designs. Creation of a tractable state space model for an array field subsystem depends on simplifying assumptions to account for subsystem characteristics which have little impact on reliability or capacity.

The typical array field consists of a set of parallel assemblies. Each assembly consists of components such as a tracking system (sensor and motor), lens (concentrator systems), structural support, PV cells, collector surface and wiring. Basically, the state of the subsystem is defined by the numbers of operating and failed assemblies. The state of each assembly is determined using the series network reduction formulas provided in Appendix A of Volume II. These formulas allow an assembly to be expressed as a two-state element with appropriate exponential distribution parameters for failure rate, λ and repair rate, μ . Additional simplification can sometimes be achieved by eliminating subsystem states which have very small probabilities of occurrence.

The PV cells may be treated using the JPL array design methodology described earlier⁽³⁾ or as components logically connected with the remainder of the array field. The JPL technique generates a curve which describes degradation in the power output of a specified array of PV cells as a function of time. Degradation of power output is caused by PV cell failures. The impact of an individual cell failure is a function of the logical organization of the cells and the use of bypass diodes. The JPL technique does not account for degradation caused by failures of components other than PV cells. If the JPL technique is used to model cell failures, then the state space model does not include cell failures. Rather, they are represented in the power output degradation curve resulting from the JPL technique. It is combined with the state model results to predict monthly power output.

If the JPL technique is not used, then the effects of cell failures must be included in the state space model for the array field subsystem. This, of course, greatly increases the number of states to be analyzed.

In general, the state space procedure for an array field subsystem is:

- Use network reduction formulas (Appendix A, Volume II) to express each assembly as a single element.

- Define the possible subsystem states and the interstate transition rates.
- Determine the state probabilities. The last step may be performed using the differential equation procedure used for the dual subsystem. An example of this approach is included in the analysis of a generic system in a subsequent section.

Each subsystem has a certain capacity when all components are operating. Failure of a component (i.e., a transition to another state) will in general reduce the capacity of the subsystem. The magnitude of the reduction will be a function of the nature of the component failure and the logical structure of the subsystem. Let

$F_X(a)$ = Fraction of subsystem X's capacity available when subsystem X is in state a.

A value of $F_X(a)$ is associated with each state of each subsystem.

If a subsystem initially has more capacity than the system, then the subsystem may experience some degradation without degrading system performance. The capacity fraction for the degraded subsystem state would be 1.00. For example, suppose an array field is rated at 120 kW but the system is limited to 100 kW. If cell failures cause the array field to degrade to 105 kW, then the system output is unaffected. The capacity fraction for the array field remains 1.00.

Combining Subsystem Results

Application of state-space models to the subsystems provides, for each subsystem, the probability and capacity fraction for each state. Let

$P_a(i)$ = Probability subsystem "a" is in state "i"

$F_a(i)$ = Fraction of subsystem "a"'s capacity available when subsystem a is in state "i"

a = $\begin{cases} S, \text{ serial subsystem} \\ D, \text{ dual subsystem} \\ A, \text{ array field subsystem.} \end{cases}$

Each system state is a combination of subsystem states. Let (X, Y, Z) represent the system state in which the first (e.g., serial) subsystem is in state X, the second (e.g., dual) subsystem is in state Y, and the third (e.g., array field) subsystem is in state Z.

The probability of system state (X, Y, Z) is the product of the probabilities of the subsystem states:

$$P(X,Y,Z) = P_S(X) \cdot P_D(Y) \cdot P_A(Z) \quad ,$$

This equation follows from the assumption of independent subsystems.

The fractional capacity of each system state, $F(X,Y,Z)$ is a function of the fractional capacity of each subsystem state and the structure of the system. For many system states, the system fraction is the product of the subsystem fractions:

$$F(X,Y,Z) = F_S(X) \cdot F_D(Y) \cdot F_A(Z) \quad .$$

For example, suppose system state (X,Y,Z) has the serial subsystems at full capacity ($F_S(X) = 1.0$), the dual subsystem at full capacity ($F_D(Y) = 1.0$), the array field at 80 percent capacity ($F_A(Z) = 0.8$). Then

$$F(X,Y,Z) = (1.0)(1.0)(0.8) = 0.8 \quad .$$

For some system states the relationship is more complex. The system fractional capacity may be sufficiently limited by the degradation of one subsystem that the degradation of a second subsystem does not cause any further reduction in system output. Consider a system in which parallel inverters each supply one half the required capacity. Suppose the serial subsystem is at full capacity ($F_S(X) = 1.0$), one inverter is failed ($F_D(Y) = 0.5$), and the array field is at 90 percent capacity ($F_A(Z) = 0.9$). The loss of one inverter overshadows the array field degradation and the system capacity fraction is $F(X,Y,Z) = 0.5$.

As a variation of the preceding example, suppose each inverter is dedicated to one-half of the array field. Since each half of the array field provides half of the capacity, the system capacity fraction is:

$$\begin{aligned} F(X,Y,Z) &= F_S(X) \left[\left(\begin{array}{l} \text{fraction for good} \\ \text{inverter, field half} \end{array} \right) + \left(\begin{array}{l} \text{fraction for failed} \\ \text{inverter, field half} \end{array} \right) \right] \\ &= (1.0) [(1.0)(0.9/2) + (0)(0.9/2)] \\ &= 0.45 \quad . \end{aligned}$$

Combining the subsystem state data results in the probability $P(j)$ and capacity fraction $F(j)$ for each system state "j". The expected system capacity fraction is computed by:

$$\beta = \sum_j P(j) \cdot F(j)$$

where "j" is the index of the system states. The fraction, β , represents the portion of nominal system production capacity which is available after accounting for failures.

The following subsection discusses treatment of capacity degradation associated with insolation, dirt accumulation, and materials.

System Degradation Effects

The nominal system capacity is given in kilowatts for peak operating conditions (full insolation and no degradation of any other type). Actual energy production must account for the effects of various types of degradation. The capacity fraction described above accounts for the effects of failures.

Actual power output is a function of daily and monthly variations in insolation. The resulting available power can be expressed in an output duration curve in terms of equivalent hours per month as a percentage of full power.

Accumulation of dirt on PV cells and collector surfaces degrades the effectiveness of the system. This degradation is expressed in terms of percent of output per year. Cleaning of the system is assumed to eliminate all dirt-related degradation.

Suppose a given PV system degrades r percent per year because of dirt accumulation and the interval between cleanings is M months. Let n represent the number of the month since the system was implemented and m equal the number of months since the last cleaning. Then m is the remainder of n divided by M . For example, if $n = 28$ months and $M = 12$ months, then:

$$m = \text{Remainder of } (28/12) = 4 \text{ months} .$$

Energy production for month n should be modified by the multiplication factor $D(n)$, where:

$$D(n) = 1 - \left(\frac{m \cdot r}{12 \cdot 100} \right) .$$

If $r = 3\%$ per year, then the factor for the above example is $D(28) = 0.990$.

Materials used in PV systems can experience permanent degradation. Abrasion from sand and yellowing of plastics are two potential causes of material degradation. Assuming this degradation is expressed as s percent of output per year and it is linear for each annual period, a yearly multiplication factor can be developed. As before, let n equal the number of the month since the system was implemented. Then the number of year is:

$$y = \lceil [n/12] \rceil + 1$$

where $\lceil [\cdot] \rceil$ is the greatest integer function. At the beginning of the y^{th} year the degradation is:

$$1 - \frac{(y-1)s}{100}$$

and at the end of the y^{th} year it is:

$$1 - \frac{ys}{100}$$

The average of these two factors is $DP(y)$, the permanent degradation factor for year y :

$$DP = \frac{1}{2} \left(1 - \frac{(y-1)s}{100} + 1 - \frac{ys}{100} \right) = 1 - \frac{(2y-1)s}{200}$$

Energy Production Computations

The actual energy production of a PV system is estimated by combining the various degradation factors with the nominal capacity. Production in month n , $P(n)$, in kilowatt hours, is computed using the following parameters:

- W = Nominal system capacity in watts
- β = Capacity fraction for reliability (from state space model)
- n = Months since implementation of the system
- $I(n)$ = Equivalent hours of full insolation in month n
- $D(n)$ = Factor for degradation due to dirt accumulation
- $DP(y)$ = Permanent degradation factor for year y .

This formula and the expressions from the preceding subsection are used to compute $P(n)$ for each month n . Annual power production, which is input to the life cycle energy cost computations is found by summing the appropriate $P(n)$ values.

The number of computations required deserves comment. For a 30-year period, 360 computations of $P(n)$ would be required. However, this figure can usually be reduced by recognizing patterns of repetition in the factors. W and β are constant factors and may be applied on an annual basis. The $I(n)$ values, i.e., the output duration curve, repeat for every year. $DP(y)$ is fixed for each year. If the interval between cleanings is some even fraction of a year (e.g., 6 months, 12 months), then the $D(n)$ values will repeat from year to year. In this case, the annual production without permanent degradation is

$$A(y) = W \cdot \beta \cdot \sum_{n=1}^{12} I(n) \cdot D(n)$$

The actual annual production is computed by multiplying each $A(y)$ value by the associated $DP(y)$ value. This is the equivalent of 42 computations of $P(n)$.

Maintenance Costs

Maintenance costs for a PV system are estimated using expected value analysis in the state space approach to life cycle energy costs. The output of the analysis is the expected (i.e., average) annual costs for corrective and preventive maintenance. The expected value approach assumes all component failures and repairs are statistically independent. This will not always be true, but the assumption has only a small impact on total costs. Furthermore, it allows simple cost computations which are desirable in a method to be applied in early development of a PV system. All costs are expressed in constant dollars for a preselected base year. Inflation and discount rates are applied in the life cycle energy cost computations (described in the following section). The following two subsections present the computations for corrective and preventive maintenance costs.

Corrective Maintenance Costs. The expected annual costs for corrective maintenance are computed for each element of the system and then summed to obtain the total. Each element of the PV system is assumed to follow the

negative exponential distribution for the time between failures. Element i has the exponential parameter λ_i failures per hour. The reciprocal of λ_i is $MTBF_i$, the mean time between failures for element i . The expected annual number of repair actions for element i is then $(t/MTBF_i)$ where t is the annual number of hours.

Each repair action for element i may involve costs for labor, travel, and material. The latter two costs will be estimated as specific fixed costs per incident. The labor cost per repair is the product of labor hours and cost per labor hour. Labor hours may be estimated as a fixed number per repair or in terms of percentiles for the lognormal distribution. The former case is straightforward. In the latter case, assume the 50th and 90th percentile values for repair time, $Q_{.5}$ and $Q_{.9}$ respectively, have been estimated. Then the mean repair time MTTR is computed as follows:

$$MTTR = \exp\left[\mu_x + \frac{1}{2}\sigma_x^2\right]$$

where

$$\mu_x = \ln Q_{.5}$$

and

$$\sigma_x^2 = [(\ln Q_{.9} - \ln Q_{.5})/1.28]^2.$$

The cost per repair action for element i is:

$$c_i = (\text{mean repair time}) (\text{labor cost/hour}) \\ + \text{travel cost} + \text{materials cost}.$$

The total annual corrective maintenance costs, EC, can now be computed as follows:

$$EC = \sum_{\text{All } i} (c_i) \cdot (t/MTBF_i).$$

If periodic replacement of a major element is planned, then the cost of that replacement is added to EC for the year in which it occurs.

Preventive Maintenance Costs. Preventive maintenance includes activities such as cleaning, inspection, adjustment, and replacement of inverter contactors. It involves labor, materials, and travel. For preventive maintenance action of type j, data must be provided for labor hours, cost per labor

Mechanical component reliability may be represented by a hazard rate which increases as a function of time. The increase corresponds to wear-out of the part. The Weibull and normal distributions are frequently used to hour, material costs, and travel costs. The frequency, in terms of the average number of occurrences per year, must also be provided. Annual preventive maintenance costs, EP, are computed as follows:

$$EP = \sum_{\text{All } j} (\text{occurrences/year}) \cdot [(\text{labor hours})(\text{cost/labor hour}) \\ + \text{materials cost} + \text{travel cost}].$$

PV SYSTEM – EXAMPLE ANALYSES

Example System for Analysis--PV Concentrator
(Passively Cooled)--Generic Design

The original PRDA* Phase I design of the Phoenix Airport--APS/Motorola PV System, was used as the basis for a generic, passively cooled, concentrator system. Its simplified block diagram is shown in Figure 20.

The reliability and maintenance data used for this specific system are shown in Table 6. These data are estimates obtained as described earlier in this report. They provide the needed parameters for the distributions that represent the reliability and repair characteristics of the system. The first part of Table 6 provides estimates of the lognormal distribution parameters of repair time as 50th and 90th percentiles. These are subsequently converted to means and variances. Manpower costs and materials costs are also estimated. A similar set of data are provided for preventive maintenance. These include values for cleaning each of the 59 arrays. The second portion of Table 6 includes the estimated reliability data, given as mean time between failures. Degradation data are also provided, as is initial system maintenance strategy.

This array field for the generic, passively cooled concentrator system has 59 distinct units or branches, each with an independent sun-tracking system. The maximum array field output is 565 kWp. Therefore, if either the optical portion or the tracking portion of any branch fails, the system loses 565/59 or 1.7% of output capacity.

Two 250 kW capacity inverters receive the d-c output from the array field and convert it to three-phase a-c synchronized with the utility. If one inverter fails, the other can maintain operation up to 250 kW. There is an automatic as well as a manual control system. The manual control system is subject to failure only when the automatic control has failed. The other major components are the field wiring and switching monitoring panel, the distribution system, and the switching system. The failure of any one of these will cause system shutdown. System failures can also occur due to a utility outage, or unusually high winds.

* PRDA = Program Research and Development Announcement - an acronym used for a series of DOE sponsored PV power system experimental designs.

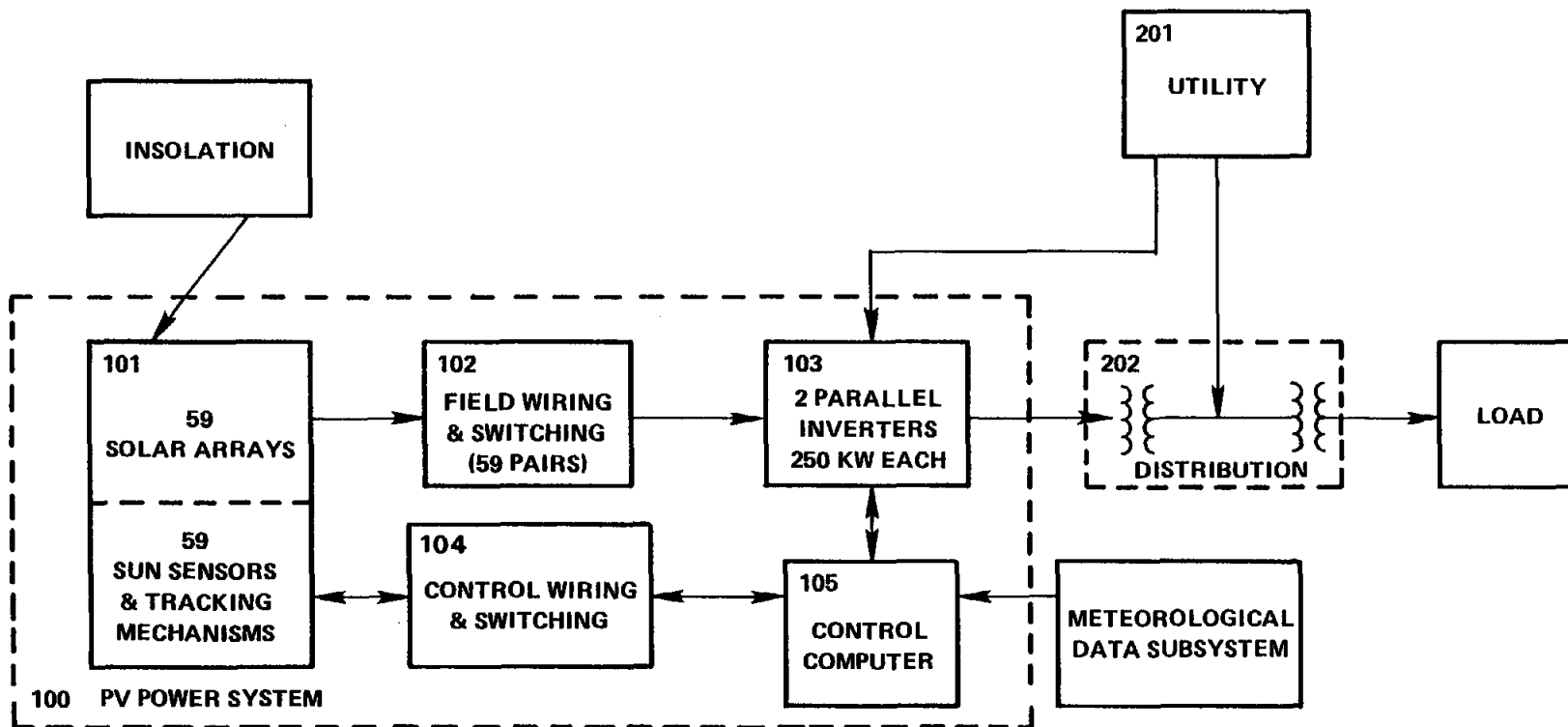


FIGURE 20. SIMPLIFIED FUNCTIONAL BLOCK DIAGRAM--GENERIC CONCENTRATOR PV POWER SYSTEM, PASSIVELY COOLED, INTERACTIVE WITH UTILITY, NO STORAGE

TABLE 6. (Continued)

Subsystem/Component	Reliability			Output Change
	MTBF Clock hr	Other Parameters	Distribution & Source	Degradation
Wiring/Switching	0.1 x 10 ⁶	--	exp. BCL est.	--
Inverter	8,760	--	" Ditto	--
Control	5,000	--	" "	--
Control (redundant)	10,000	--	" "	--
Tracking Unit	60,000	--	" Will use Weibull, later	System Maintenance Policy - Replace after 5 Tracking Unit Assembly Failures. (Also run for immediate replacement)
Array (Solar PV Collector)	120,000	--	" BCL est.	--
Lens	10 ⁶	--	" "	Dirt -3% output/year (removed by cleaning) Abrasion -3% output/year for 2 yr; -0.1%/year Bal. (Permanent). Source: BCL est.
Utility	6,257	$\lambda = 160/10^6$ hr	exp., IEEE Std 493 - 1980 p 214, Table II	--
Distr. Subsystem	8.76x10 ⁶	$\lambda = 0.1/10^2$ hr	exp., IEEE Std 493 - 1980 p 219, Table I	--
Power Switch	1.4x10 ⁶	$\lambda = 0.7/10^6$ hr	exp., IEEE Std 493 - 1980 p 123, Table 2 (Switches)	--
Weather	2,190		exp.	Shutdown due to wind, etc.

69

Preventive maintenance will be scheduled for both the optical and tracking components of the array as well as the inverters, the distribution system, and the system as a whole as shown in Table 6.

Example Application of the State Space Approach

This section describes application of the state space approach to the generic, passively cooled PV concentrator power system. The purpose of this example is to demonstrate and clarify the mechanics of the state space approach.

Figure 20, as discussed earlier, is a simplified functional block diagram of the PV system. A reliability logic diagram based on the interconnections of the components is given in Figure 21. The array field consists of 59 branches connected in parallel and has a maximum output capacity of 565 kW. Each inverter has a maximum capacity of 250 kW, thereby limiting the PV system capacity to 500 kW. Table 6 presents the basic data for the generic PV system.

Failure Rates and Repair Rates. The state space approach uses failure rates (failures/hour) and repair rates (repairs/hour). These rates are derived from the mean-time-between-failure (MTBF) data and maintenance time data in Table 6. The failure rate of each component is the reciprocal of its MTBF.

The maintenance time data for each component are in terms of percentiles. The state space method uses the exponential distribution for time to repair. In order for the results to be comparable with other techniques, the mean time to repair (MTTR) is equated to the mean of the lognormal distribution. Let Q represent the 100th percentile (i.e., the time for 100 percent of the repairs to be completed). Then:

$$MTTR = \exp \left[\mu_x + \frac{1}{2} \sigma_x^2 \right]$$

where

$$\mu_x = \ln Q_{.5}$$

and

$$\sigma_x^2 = [(\ln Q_{.9} - \ln Q_{.5}) / 1.28]^2 .$$

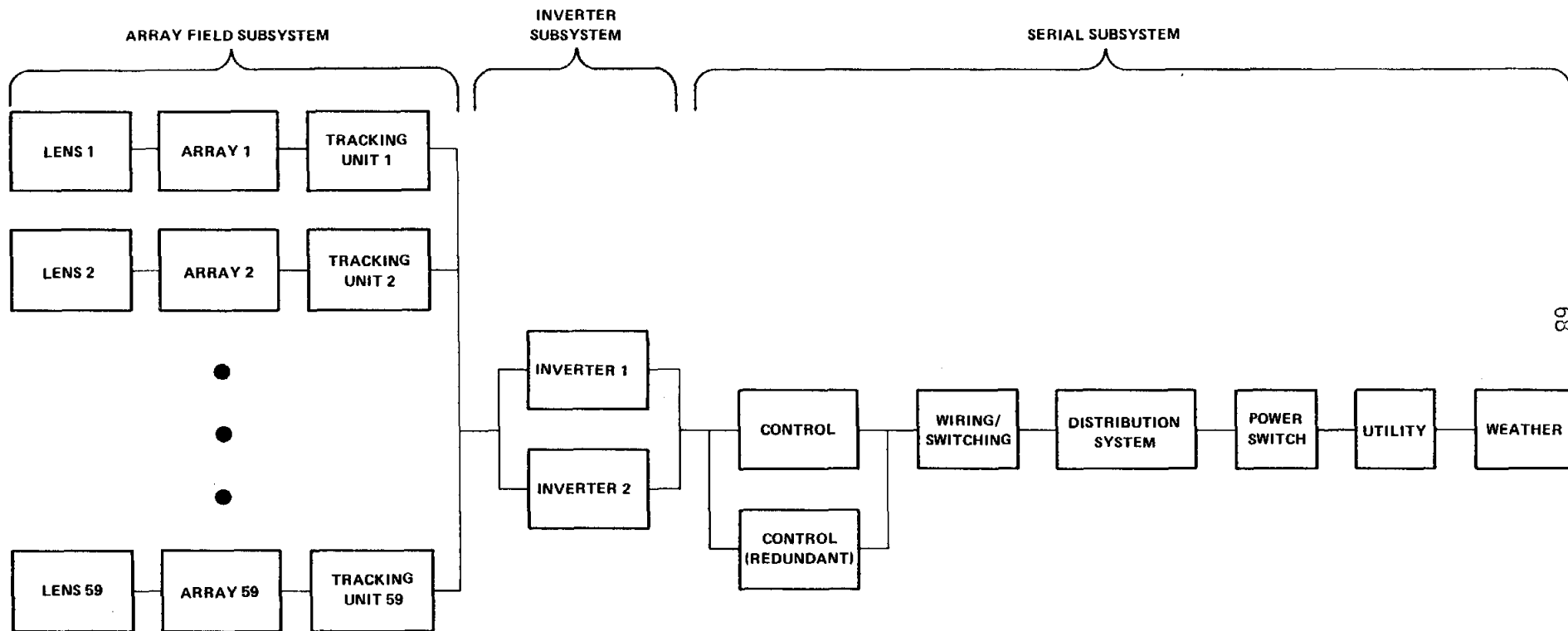


FIGURE 21. RELIABILITY LOGIC DIAGRAM FOR THE GENERIC PV SYSTEM

The repair rate for each component is then:

$$\mu = 1/\text{MTTR repairs/hour.}$$

Table 7 summarizes the failure rate and repair rate data.

State Space Model. The generic PV system is divided into three subsystems: Array Field, Power Conditioning, and Serial Elements. The following paragraphs describe the model and computations for each subsystem and the combination of subsystem results into system results.

Array Field Subsystem. The array field consists of 59 distinct branches, where each branch consists of PV cells, a tracking system, and a lens. The branches are logically in parallel since the failure of a single branch does not impact the output of any other branch. Hence, we define the states of the array field in terms of the number of failed units. The initial repair strategy for the array field is to initiate repair upon the twelfth branch failure.

Cell failures were treated directly by this early example, as seen below. More accuracy can be obtained by using the JPL array analysis technique. This technique produces a cell degradation factor which would be applied in the "Energy Production Computations". This approach is used in the three examples of Volume II.

Figure 22 depicts the Markov model for the array field. State i ($i = 0, 1, \dots, 13$) represents i branches failed. Notice that states 14 through 59 are not included. Since the repair rates are much higher than the failure rates for the components (and therefore for the branches), the probability of reaching any state beyond state 13 is negligible.

The transition rate parameters are:

λ = Failure rate of one branch

μ = Repair rate of one branch.

We will compute the steady-state probabilities of states 0 through 13 in terms of λ and μ and then compute λ and μ using component data.

For each state, the transition rate into the state equals the transition rate out. Hence:

TABLE 7. FAILURE RATE AND TIME TO REPAIR
OF MAJOR SYSTEM COMPONENTS

Subsystem/Component	Failure Rate/Hr (λ)	Repair Rate/Hr (μ)
Array - PV Collector	8.33×10^{-6}	.07199
Lens	1.0×10^{-6}	.14970
Tracking Unit	1.67×10^{-5}	.07197
Inverter	1.14×10^{-4}	.03598
Wiring	1.0×10^{-6}	.14970
Control	2.0×10^{-4}	.01404
Control, Redundant	1.0×10^{-4}	.03598
Distribution System	1.14×10^{-7}	.02991
Power Switch	7.1×10^{-7}	.25641
Utility	1.60×10^{-4}	.45045
Weather	4.56×10^{-4}	.06196

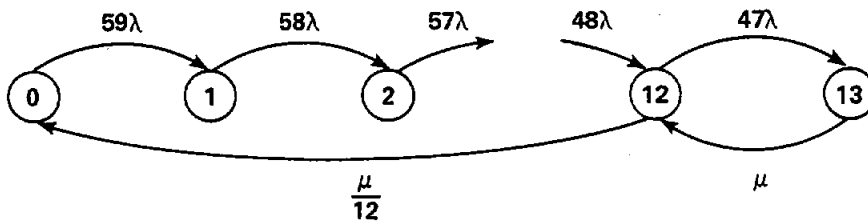


FIGURE 22. MARKOV MODEL FOR THE ARRAY FIELD

$$\begin{aligned}
(\mu/12)P_{12} &= 59\lambda P_0 \\
59\lambda P_0 &= 58\lambda P_1 \\
58\lambda P_1 &= 57\lambda P_2 \\
&\vdots \\
&\vdots \\
&\vdots \\
49\lambda P_{10} &= 48\lambda P_{11} \\
48\lambda P_{11} + P_{13} &= \mu/12 P_{12} + 47\lambda P_{12} \\
47\lambda P_{12} &= \mu P_{13}
\end{aligned}$$

Using algebraic manipulation, we can express each P_i in terms of P_0 :

$$P_i = \frac{59}{59-i} P_0, \quad i = 1, 2, \dots, 11$$

$$P_{12} = 12 \frac{59}{\mu} \lambda P_0$$

$$P_{13} = 47 \frac{12}{\mu} \frac{59}{\mu} \lambda^2 P_0$$

Next, we use the fact that $\sum_{i=0}^{13} P_i = 1$ to solve for P_0 in terms of λ and μ :

$$P_0 = \frac{1}{1 + \frac{59}{58} + \frac{59}{57} + \dots + \frac{59}{48} + 12 \frac{59}{\mu} \frac{\lambda}{\mu} + 47 \frac{12}{\mu} \frac{59}{\mu} \left(\frac{\lambda}{\mu}\right)^2}$$

Each branch consists of a PV collector, a lens, and a tracking unit. The components are logically in series. Using the network reduction formulas in Appendix A, Volume II, we have:

$$\begin{aligned}
\lambda &= \sum(\lambda\text{'s for the components}) \\
&= 26.03 \times 10^{-6} \text{ failures/hour}
\end{aligned}$$

$$P_S = \text{Pr}[\text{branch success}]$$

$$\begin{aligned}
&= \frac{1}{1 + \frac{\sum \lambda i}{\mu^i}} \\
&= .999646
\end{aligned}$$

$$\mu = \frac{\lambda P_S}{(1 - P_S)}$$

$$= .073 \text{ repairs/hour.}$$

Substituting these values of λ and μ into the preceding equations yields the P_i values. Since the nominal power rating of the array field is 565 kW, the loss of each branch circuit reduces the array field rating by:

$$\frac{1}{59} (565 \text{ kW}) = 9.58 \text{ kW.}$$

Since the system capacity is limited by the total inverter capacity to 500 kW, the failure of branch circuits will not reduce the maximum system capacity until the seventh branch failure. In particular, the capacity fraction associated with state i is:

$$F_i = \begin{cases} 1.0 & , i=0, 1, \dots, 6 \\ \frac{565 - (i/59)(565)}{500} & , i = 7, \dots, 13 \end{cases}$$

Table 8 presents the results for the array field subsystem.

Power Conditioning Subsystem. This subsystem consists of two 250 kW inverters connected in parallel. Three states are defined as follows:

State 0: Both inverters functioning (500 kW)

State 1: One inverter functioning (250 kW)

State 2: No inverters functioning (0 kW)

The probability of each state is computed directly from the availability of each inverter. For a single inverter, the availability is:

$$A = \frac{\mu}{\mu + \lambda} = .946842$$

The state probabilities are computed as follows:

$$P_0 = A^2$$

$$P_1 = 2A(1 - A)$$

$$P_2 = (1 - A)^2$$

Table 9 presents the results for the power conditioning subsystem.

TABLE 8. ARRAY FIELD SUBSYSTEM RESULTS

State, i	Probability, $P(i)$	Capacity Fraction, $F(i)$
0	.07383	1.000
1	.07511	1.000
2	.07642	1.000
3	.07779	1.000
4	.07920	1.000
5	.08067	1.000
6	.08219	1.000
7	.08377	.996
8	.08541	.977
9	.08712	.958
10	.08890	.938
11	.09075	.919
12	.01852	.900
13	.00031	.881

TABLE 9. POWER CONDITIONING SUBSYSTEM RESULTS

State, i	Probability, $P(i)$	Capacity Fraction, $F(i)$
0	.993693	1.00
1	.006297	.50
2	.000010	.00

Serial Elements Subsystem. This subsystem consists of all components not included in the previous two subsystems. With one exception, the components are logically in series since the failure of any single component causes subsystem failure. The control function has a primary unit and a standby redundant unit. The two units can be treated as a single element with an equivalent probability of success. Figure 23 presents the computations, which are based on the network reduction formulas for a standby parallel system in Appendix A, Volume II.

The next step for the serial elements subsystem is to compute the probability the subsystem is operational. The state space model for a serial subsystem (see Figure 18) provides the proper equation:

$$P_0 = \frac{1}{1 + \sum \frac{\lambda_i}{\mu_i}} = P(\text{success})$$

where λ and μ are the failure rate and repair rate respectively for the i th element in the subsystem. Substituting the appropriate values,

$$P(\text{success}) = .985829$$

and

$$P(\text{failed}) = .014171$$

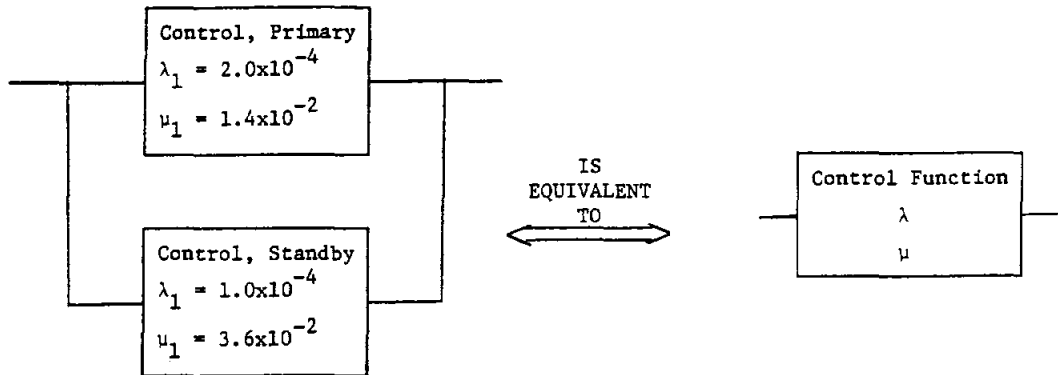
Table 10 summarizes the results for the serial subsystem.

System Reliability Results. The above analyses provide the states, state probabilities, and associated capacity fractions for each subsystem.

Use the following subscripts:

- A: Array field
- D: Power conditioning
- L: Serial elements
- S: System.

Table 11 presents the combination of subsystem states to form system states. Note that all states which result in zero output have been collapsed to two states.



$$MTTR = MTTR_1 + MTTR_2$$

$$\mu = 1 / \left(\frac{1}{\mu_1} + \frac{1}{\mu_2} \right) = .010080$$

Three states for the dual system:

State 0: Primary control functioning

$$P_0 = 1 / \left(1 + \frac{\lambda_1}{\lambda_2} + \frac{\lambda_1}{\mu} \right) = .331143$$

State 1: Primary control failed, standby control functioning

$$P_1 = \frac{\lambda_1}{\lambda_2} P_0 = .662286$$

State 2: Both controls failed

$$P_2 = \frac{\lambda_1}{\mu} P_0 = .006570$$

Two states for the single element:

$$\text{Success: } P_S = P_0 + P_1 = .993430$$

$$\text{Failure: } P_F = P_2 = .006570$$

$$\lambda = \mu(1 - P_S) / P_S = .000067$$

Hence, for the single control element:

$$\lambda = 67.0 \times 10^{-6}$$

$$\mu = 10.08 \times 10^{-3}$$

FIGURE 23. REDUCTION OF REDUNDANT CONTROLS TO A SINGLE ELEMENT

TABLE 10. SERIAL ELEMENT SUBSYSTEM RESULTS

State, i	Probability, $P(i)$	Capacity Fraction, $F(i)$
0	.985829	1.00
1	.014171	0.00

TABLE 11. SYSTEM STATES

System State, i	Subsystem States [*]			Probability, $P_S(i)$	Capacity Fraction, $F_S(i)$
	A	D	L		
1	X	X	1	.014171	0
2	X	2	0	.000010	0
3	X	1	0	.006208	.500
4	0	0	0	.072325	1.000
5	1	0	0	.073579	1.000
6	2	0	0	.074862	1.000
7	3	0	0	.076193	1.000
8	4	0	0	.077585	1.000
9	5	0	0	.079025	1.000
10	6	0	0	.080514	1.000
11	7	0	0	.082062	.996
12	8	0	0	.083669	.977
13	9	0	0	.085344	.958
14	10	0	0	.087087	.938
15	11	0	0	.088900	.919
16	12	0	0	.018142	.900
17	13	0	0	.000304	.881

* The symbol "X" indicates the subsystem may be in any of its states.

The probability of each system state, $P_S(i)$, is computed by multiplying together the probabilities of the appropriate subsystem states. Finally, the expected system capacity fraction is computed as follows:

$$\beta = \sum_{i=1}^{17} P_S(i) \cdot F_S(i)$$

$$\beta = .962 .$$

That is, system output will be limited to 0.962 of its nominal capacity because of component failures.

Energy Production Computations. The next step is to compute the system capacity fraction β , which captures the impacts of failures, with the effects of insolation, dirt accumulation, and permanent degradation.

Table 12 presents the monthly output duration curve. The total equivalent array hours at full power for month n , I_n , are computed assuming the curve is linear between data points. Each interval is 8.33 hours. The height (i.e., output fraction) associated with each interval is taken to be the average heights of the interval endpoints. For month 1, the computation is:

$$I_1 = \left(\frac{1.000 + .982}{2} \right) 8.33 + \left(\frac{.982 + .963}{2} \right) 8.33 + \dots + \left(\frac{0.15 + 0}{2} \right) 8.33$$

$$I_1 = 145.71 \text{ hours} .$$

Table 13 provides the results of performing these computations for each month.

Permanent degradation due to changes in the lens material is expressed as a fractional multiplier for each year. The assumed rate of degradation was 3.0 percent per year for the first two years and then 0.1 percent per year for all subsequent years. The factors for each three-year point are shown in Table 14. The permanent degradation factor used for year y , $DP(y)$, is the average of the factors at the three-year points which include y . For example,

TABLE 12. OUTPUT DURATION CURVE FOR GENERIC PV CONCENTRATOR
(Passively Cooled)

MONTHLY OUTPUT DURATION CURVES IN INTERVALS OF 0.33 HOURS PER MONTH																
MONTH 1	1.000	.982	.963	.945	.930	.914	.899	.871	.842	.816	.790	.769	.748	.724	.696	.647
	.607	.573	.533	.486	.438	.391	.340	.306	.239	.191	.150	.096	.050	.033	.015	0.000
	0.000	0.000	0.000	0.000	0.000	0.000	0.000	0.000	0.000	0.000	0.000	0.000	0.000	0.000	0.000	0.000
MONTH 2	1.000	.991	.981	.972	.962	.953	.940	.922	.905	.886	.864	.842	.819	.797	.760	.721
	.687	.639	.600	.560	.513	.447	.393	.332	.270	.209	.177	.136	.095	.068	.028	0.000
	0.000	0.000	0.000	0.000	0.000	0.000	0.000	0.000	0.000	0.000	0.000	0.000	0.000	0.000	0.000	0.000
MONTH 3	1.000	.992	.985	.977	.969	.962	.954	.946	.931	.916	.900	.885	.868	.852	.835	.817
	.799	.734	.716	.697	.675	.643	.612	.563	.516	.475	.423	.374	.326	.288	.249	.208
	.154	.125	.089	.048	.031	.013	0.000	0.000	0.000	0.000	0.000	0.000	0.000	0.000	0.000	0.000
MONTH 4	1.000	.993	.986	.980	.973	.966	.959	.952	.943	.926	.908	.891	.875	.859	.843	.826
	.809	.791	.769	.747	.715	.681	.663	.644	.594	.561	.541	.500	.453	.424	.380	.331
	.287	.241	.192	.143	.112	.080	.050	.029	.009	0.000	0.000	0.000	0.000	0.000	0.000	0.000
MONTH 5	1.000	.994	.987	.981	.975	.969	.962	.956	.950	.941	.930	.919	.908	.898	.879	.858
	.839	.824	.809	.793	.779	.764	.751	.735	.713	.690	.656	.626	.609	.592	.572	.545
	.518	.493	.467	.438	.406	.371	.315	.287	.255	.206	.175	.138	.086	0.000	0.000	0.000
MONTH 6	1.000	.996	.989	.982	.975	.968	.961	.954	.946	.938	.929	.920	.912	.903	.894	.876
	.858	.834	.782	.765	.748	.731	.715	.698	.680	.659	.637	.611	.584	.563	.544	.524
	.492	.464	.444	.423	.383	.345	.311	.283	.237	.192	.165	.134	.093	.025	0.000	0.000
MONTH 7	1.000	.991	.983	.974	.966	.957	.949	.938	.927	.915	.904	.891	.870	.849	.826	.803
	.783	.768	.752	.736	.720	.703	.687	.651	.620	.596	.571	.545	.519	.491	.460	.422
	.355	.320	.289	.256	.205	.159	.125	.096	.075	.053	.043	.033	.023	.014	.004	0.000
MONTH 8	1.000	.992	.985	.977	.969	.962	.954	.946	.931	.917	.902	.887	.873	.858	.844	.828
	.813	.797	.780	.761	.741	.689	.666	.646	.614	.557	.519	.493	.458	.411	.380	.343
	.299	.257	.235	.213	.171	.130	.098	.078	.059	.038	.017	0.000	0.000	0.000	0.000	0.000
MONTH 9	1.000	.993	.986	.978	.971	.964	.957	.950	.938	.924	.909	.895	.880	.864	.848	.833
	.817	.802	.781	.735	.715	.696	.666	.626	.604	.562	.525	.467	.444	.420	.350	.301
	.270	.223	.146	.105	.080	.056	.008	0.000	0.000	0.000	0.000	0.000	0.000	0.000	0.000	0.000
MONTH 10	1.000	.993	.986	.979	.973	.965	.959	.952	.942	.927	.911	.895	.879	.863	.847	.829
	.812	.794	.730	.709	.685	.637	.593	.561	.536	.548	.398	.354	.321	.235	.191	.160
	.130	.099	.065	.007	0.000	0.000	0.000	0.000	0.000	0.000	0.000	0.000	0.000	0.000	0.000	0.000
MONTH 11	1.000	.992	.984	.977	.969	.961	.953	.943	.927	.911	.895	.872	.848	.826	.805	.782
	.749	.716	.682	.644	.600	.549	.495	.412	.363	.295	.246	.198	.163	.070	.022	0.000
	0.000	0.000	0.000	0.000	0.000	0.000	0.000	0.000	0.000	0.000	0.000	0.000	0.000	0.000	0.000	0.000
MONTH 12	1.000	.980	.959	.940	.922	.905	.886	.866	.845	.805	.771	.742	.713	.685	.648	.595
	.550	.513	.478	.393	.333	.298	.269	.235	.123	.063	.039	.023	.006	0.000	0.000	0.000
	0.000	0.000	0.000	0.000	0.000	0.000	0.000	0.000	0.000	0.000	0.000	0.000	0.000	0.000	0.000	0.000

TABLE 13. MONTHLY ARRAY POWER DATA

n		Total Equivalent Array Hours at Full Power I_n
1	January	145.71
2	February	157.51
3	March	191.96
4	April	209.33
5	May	250.38
6	June	246.29
7	July	219.20
8	August	213.14
9	September	206.66
10	October	190.47
11	November	169.51
12	December	133.74

TABLE 14. PERMANENT DEGRADATION FACTORS

Year, y	DP(y)	Year, y	DP(y)
1	0.975	16	0.926
2	0.955	17	0.925
3	0.939	18	0.924
4	0.938	19	0.923
5	0.937	20	0.922
6	0.936	21	0.921
7	0.935	22	0.920
8	0.934	23	0.919
9	0.933	24	0.918
10	0.932	25	0.917
11	0.931	26	0.916
12	0.930	27	0.915
13	0.929	28	0.914
14	0.928	29	0.913
15	0.927	30	0.912

$$DP(5) = (.938 + .935)/2 = .9365$$

The JPL array methodology was not used for this example. It is demonstrated in the three examples in Volume II. If it had been used to model cell failures, then the factor $DC(y)$, the annual degradation in array capacity due to cell failures, would be included in these computations. For an example, see Section 2 of Volume II.

Degradation due to dirt accumulation is assumed to be three percent per year. Cleaning is performed every twelve months. A monthly factor, $D(n)$, is derived assuming linear degradation. Table 15 presents the dirt degradation factors.

The power production in kWh for month n of year y can be computed as follows:

$$A(n,y) = W \cdot \beta \cdot I(n) \cdot DP(y) \cdot D(n)$$

where

- W = 500 kW, nominal system capacity
- β = 0.962, capacity fraction
- $I(n)$ = Hours for month n (Table 13)
- $DP(y)$ = Permanent degradation factor for year y (Table 14)
- $D(n)$ = Dirt accumulation factor for month n (Table 15).

The annual power production in kWh for year y is then:

$$A(y) = \sum_{n=1}^{12} A(n,y) = W \cdot \beta \cdot DP(y) \cdot \sum_{n=1}^{12} I(n) \cdot D(n) .$$

Table 16 presents the results of these computations.

Maintenance Costs

Corrective Maintenance Costs. For each system component, the expected number of failures per year is multiplied by the expected cost per repair. These computations are straightforward using the data from Table 6. For example, consider the inverters. The expected annual number of failures is:

$$(\text{Failures/hr}) (\text{hrs/year})(\text{no. of units}) = (1.14 \times 10^{-4})(8760)(2) = 1.997 .$$

TABLE 15. DIRT ACCUMULATION DEGRADATION FACTORS

n	Month	D (n)
1	January	.999
2	February	.996
3	March	.994
4	April	.991
5	May	.989
6	June	.986
7	July	.984
8	August	.981
9	September	.979
10	October	.976
11	November	.974
12	December	.971

TABLE 16. ESTIMATED ANNUAL GENERIC PV SYSTEM OUTPUT
USING THE STATE SPACE APPROACH

Year	kWh ($\times 10^3$)	Year	kWh ($\times 10^3$)
1	1,104.4	16	1,038.8
2	1,070.8	17	1,037.7
3	1,053.4	18	1,036.6
4	1,052.3	19	1,035.4
5	1,051.1	20	1,034.3
6	1,050.0	21	1,033.2
7	1,048.9	22	1,032.1
8	1,047.7	23	1,030.9
9	1,046.7	24	1,029.8
10	1,045.5	25	1,028.7
11	1,044.4	26	1,027.6
12	1,043.3	27	1,026.5
13	1,042.2	28	1,025.3
14	1,041.0	29	1,024.2
15	1,039.9	30	1,023.1

The cost per failure is:

$$\begin{aligned} & (\text{Repair hours})(\text{cost/hour}) + (\text{travel and materials costs}) \\ & = \frac{1}{.03598 \text{ repairs/hour}} \$40/\text{hour} + \$300 \\ & = \$1411.60. \end{aligned}$$

Hence, the annual corrective maintenance costs for the inverters is \$2,820. Summing these costs over all components provides the expected annual corrective maintenance costs for the system.

Preventive Maintenance Costs. For each system component which receives preventive maintenance, (PM), multiply the expected number of occurrences per year by the cost per occurrence. The annual number of occurrences is computed from the PM Interval data in Table 6. The cost per occurrence is the sum of labor, travel, and materials. The latter two elements are the fixed PM costs. The labor cost is the variable PM cost times the expected time to perform the PM. Since the times in Table 6 are percentiles for the lognormal distribution, the transformation used at the beginning of this example is used here to compute the mean maintenance time. The expected annual preventive maintenance cost for this system are \$10,768.

The results of this and previously described calculations provides annual maintenance costs and power generated inputs for the life-cycle energy cost equations.

The Simulation Methodology -
The SOLREL Model

General

SOLREL is a computer model developed at Battelle-Columbus Laboratories to simulate the reliability and availability of photovoltaic systems. The model simulates the failures and subsequent repairs of all major subsystems, shuts down the system energy production as appropriate (for scheduled or unscheduled maintenance, and weather-related outages), calculates and records the cumulative energy generated, and records the cost of repair. In addition, SOLREL simulates the loss of output due to cell failures*, dirt on the array surface, and permanent degradation to the array surface. SOLREL also allows the user to test various preventative maintenance and cleaning strategies. The maintenance costs produced by SOLREL can be combined with capital and operating costs in a life cycle energy cost model (LCCOST), which will be described toward the end of this report.

The Simulation Model

SOLREL is programmed using the GASP IV simulation language supplemented by several FORTRAN subroutines. GASP IV, developed by Pritsker and Associates, consists of a collection of FORTRAN-based subroutines which allow the user to design either an event-oriented or continuous simulation. SOLREL is strictly an event-oriented simulation model since it advances through time on the occurrence of events such as failures and repair completions. Once SOLREL has been adapted to a specific system, designers can test various cost/reliability/maintenance tradeoffs by adjusting the input values on the data cards. No knowledge of either FORTRAN or GASP IV is necessary unless the

* Cell failures in the following example are treated using a failure rate for each branch circuit and establishing a strategy of repairing the array after a certain number of branch circuits have failed. However, in all three PV systems analyzed in Volume II of this report, the JPL Array Design Methodology(3), described earlier, was used.

system configuration is modified, by changing functional interconnections, or by adding or subtracting components. If such a major change is desired, the user must make some minor modifications to SOLREL codes.

The Initial Event File: Scheduling Failures. Figure 24 shows the logical flow of SOLREL. The model begins by creating an initial event file consisting of the time of first failure for each system component arranged in order of occurrence. Each of these failure times is selected at random according to an expected time between failures distribution unique for each component. Parameters of the distributions can be modified by changing the data cards. The type of distribution can be modified as well but requires changes to the SOLREL software in subroutines INTLC and REPAIR. (See Appendix B, Volume II.) For this project, all electronic components are assumed to have negative exponential failure distributions characterized by a constant hazard function. Those components which experience wear-out (or have an increasing failure rate over time), namely most mechanical components, may be modeled using a Weibull or other appropriate failure distribution.

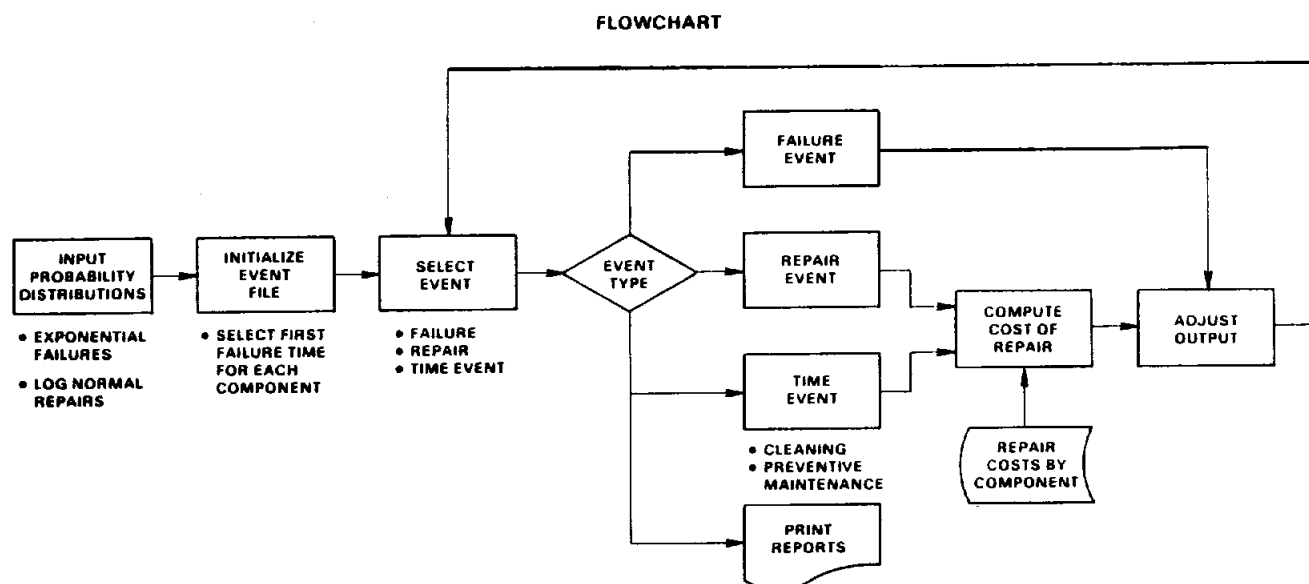


FIGURE 24. FLOWCHART FOR SIMULATION PROGRAM - SOLREL

SOLREL also schedules a time event for the first of every month, permitting the user to schedule preventive maintenance and cleaning. Preventive maintenance times and costs are input through data cards, however, those components actually receiving maintenance attention are defined within Subroutine TIMEV.

Component Failure. Once the initial event file has been created, SOLREL is ready to begin a simulated system clock which will continue throughout the system life, stopping only when events in the event file are encountered. If the first event in the event file is a failure, SOLREL will record which component failed and the time of failure. It will then compute the total kWh produced by the system from the last event (or time zero if the simulation is just beginning) to the time when the failure occurred.

Power Output Calculation Including the Effect of Degradation

To compute output (see Figure 25 which represents the Adjust Output Box of Figure 24), SOLREL begins with the system capacity (C) which has been input by the user on a data card. This capacity is then reduced by a percentage (% D) due to dirt on the array surface. This percentage reduction is defined by a time dependent curve entered on a data card and by the cleaning schedule input by the user. The capacity is reduced again by a percentage due to permanent degradation (% P). This is also defined by a time-dependent curve entered on a data card. The capacity is reduced once more by a percentage which defines the degradation over time due to cell failures (% F). For the three examples in Volume II this reduction is based on the output of the JPL technique: a time-dependent curve entered on three data cards, and by the cell repair schedule input by the user. In other words, the user can initiate total cell repair when a certain percentage of system output has been lost due to cell failure. For the example in this volume, the degradation is the percent of branch circuits which are not operating due to cell failure. Next, the capacity is reduced further due to the failure of mechanical components within strings or branch circuits which shut down only a portion of the entire system (% F). For example, a failure of a tracking drive (branch circuit) on

the generic two-axis tracking concentrator system will cause the loss of 1/59 of power. Therefore the degraded capacity will be multiplied by 58/59 to yield a final degraded capacity. Next this final degraded capacity (FDC) is applied to the output duration curve (see Figure 10) which captures the effect of changes in insolation. Twelve power output duration curves, one for each month, are stored in an external file. (See Table 19) They are produced earlier by design simulations of solar output, given historical local weather conditions and designed system efficiency. SOLREL will calculate the area under the curve and multiply that value times the degraded capacity (FDC) to yield output in kWh for the month as shown below:

$$\text{FDC} = C \cdot (1 - \% D)(1 - \% P)(1 - \% CF)(1 - \% F)$$

In some cases, the shape of the power output duration curve will be modified. For example, if a 500 kW system includes two 250 kW inverters each of which can still produce 250 kW when the other has failed, it is possible to have a power output duration curve which remains unchanged below 250 kW output but which cannot rise above 250 kW (see Figure C-1, Volume II.)

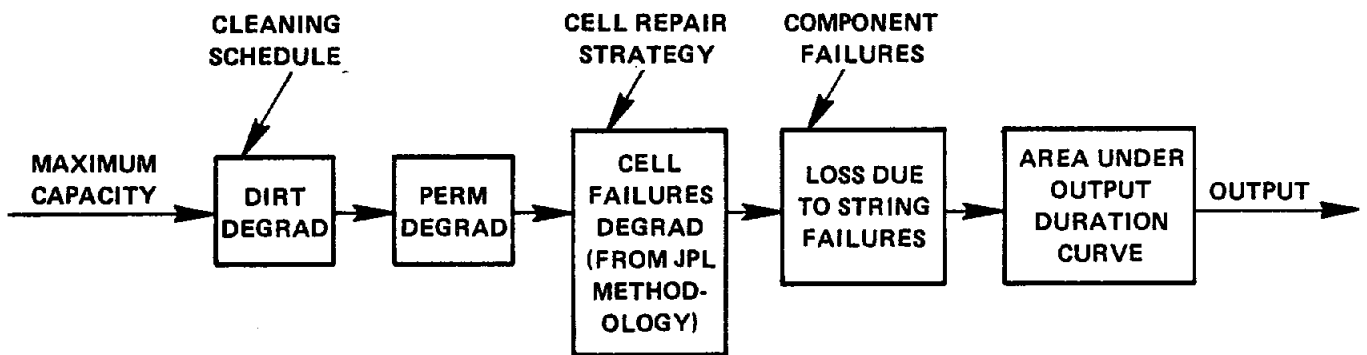


FIGURE 25. OUTPUT CALCULATION FOR EACH MONTH

Maintenance

Scheduling Repair. Once a failure has occurred and the system output to that point calculated, SOLREL schedules the repair of that component by a random selection from its repair-time probability distribution. (Note: if the system maintenance strategy so decrees, a predetermined number of components failures must occur before repair is initiated.) The repair time

distribution used in all designs simulated was lognormal, as discussed earlier. The user must specify on data cards the 50th and 90th percentile repair times for each component, and SOLREL then derives the appropriate lognormal distribution. It is important to note that the user enters repair times in terms of total man-hours. For example, suppose that 2 men spend a total of 16 man-hours to complete the repair. Each is paid at a rate of \$20 per hour. The total elapsed time on the job becomes $16/2 = 8$ working hours which, assuming an 8-hour work day converts to 24 clock hours for the array system downtime. The user should input on data cards the 50th and 90th percentile for the number of man-hours, the total dollars per working hour ($\$20 \times 2 = \40), and the number of men performing the repair (2). The repair time, which appears on the printout log and which is stored in SOLREL's event file, is the total clock hours (24 hours). Repair cost, however, is calculated from the total man-hours. If this failure caused complete shutdown, then 24 hours of output is lost. Once a time has been selected for completion of the repair, SOLREL inserts that event into the event file where it, like all other events, is stored in order of occurrence.

Maintenance Costs. When a repair event occurs, the output is calculated in the same manner as described above. A new failure time is selected at random and stored in the event file. The only additional step is to calculate the cost of repair which becomes

$$\text{Cost of Repair} = \text{fixed cost} + \frac{(\text{dollars per working hour})(\text{total man hours})}{(\text{number of men})}$$

where total dollars per working hour = (wage rate)(number of men)

and total man-hours = (number of men)(hours per man).

The fixed cost and the dollars per working hour are stored on an external file. The number of working hours is the same lognormal random variable mentioned earlier.

Preventive Maintenance and Array Cleaning. In addition to failure and repair events, SOLREL also processes time events. A time event serves two purposes. First, it allows SOLREL to accumulate monthly (and yearly) output

and cost figures and to activate a new power output duration curve each month. Second, SOLREL checks to see if any preventive maintenance/cleaning is scheduled to occur. If so, the cost is calculated in the same manner as repair cost:

$$\text{cost of PM} = \text{fixed cost} + \frac{(\text{dollars per working hour})(\text{working hours})}{(\text{number of men})}$$

The number of working hours is a random variable with lognormal distribution. To change the distribution type, SOLREL's software must be modified; however, changes in the distribution parameters can be accomplished by changing data cards. In the case of array cleaning, system output is improved to its original level after each cleaning. In other words, the clock used in conjunction with the dirt degradation curve is re-initialized (set to zero). All preventive maintenance is assumed to occur during off hours so that no system output is lost.

After each event is processed, SOLREL returns to the event file and selects the event which is scheduled to occur next. That event is then processed and the cycle repeats itself until an event indicating the end of system life is reached.

Tables and Plots. SOLREL has the capability of producing a number of summary reports including a:

- complete log of event by event system performance (Table 23)
- cost/output table (Table 24)
- system availability table (Table 25)
- component failure table (Table 26).

The event log, a portion of which is shown in Table 23, provides an event by event detailed record of the 30-year simulation. It itemizes each failure, repair, and weather-related or preventive maintenance event and provides a running summary of cumulative energy generated and maintenance dollars spent. These are both provided in current dollars and kWh as well as present value dollars and kWh.

The cost/output table shows the annual cost, output, and cents/kWh in both initial year dollars and present value dollars. The system availability table shows yearly totals for the percent of time that the system is producing

at a certain percent of system capacity. In other words, for year 1 the system may produce between 90 and 100 percent of system capacity only 10 percent of the time. The table also shows a theoretical availability which is an estimate of availability given no failures or degradation. The failure table shows the number of failures for each component by year. System MTBF may be estimated from this table by dividing the number of hours in 30 years by the number of failures in 30 years. (See Tables 24 and 25.)

SOLREL also produces plots of system costs and output over time both in initial year dollars and present value dollars (Figure 26). The plots also show levelized costs per kWh both annually and for system life (Figure 27). These plots can be produced at the end of each run or several runs can be accumulated and printed in one set of tables and plots. The decision on what plots or tables to produce is made through a data card.

Changes to Model. Table 17 lists alternative desired adjustments to the model and the changes in the programs required to achieve these adjustments. In most cases, changes to data cards or to external files are sufficient to run sensitivity analyses. In cases where the system structure (number of components or relation among components or subsystems) is affected, certain software changes are necessary.

SOLREL Analysis of Example System

To demonstrate the application of SOLREL, the generic PV concentrator system described earlier was modeled. Other systems will be modeled later in Volume II of this report to show the flexibility of the technique.

The system was modeled functionally to respond to failures as shown earlier by the block diagram of Figure 20. The input data on reliability, degradation and maintenance presented in Table 6 were used for SOLREL input data.

Random number streams are used throughout the simulation. They need to be chosen carefully so that when variations in system design are tested, the results reflect only those changes while at the same time minimizing random variations. Six independent random number streams were used, one being assigned to each of the following processes:

TABLE 17. COMPUTER PROGRAM-RELATED CHANGES
NECESSARY FOR ADJUSTMENTS TO MODEL

Type of Change	User Must Modify:		
	Data Card	External File	Software
Failure Distribution Type			x
Failure Parameters	x		
Preventive Maintenance Times	x		
P.M. Costs	x		
Components Receiving P.M.			x
System Capacity	x		
Dirt Degradation Curve	x		
Cell Failure Degradation Curve	x		
Permanent Degradation Curve	x		
Cleaning Schedule	x		
Cell Repair Initiation	x		
Output Duration Curve		x	
Effect of Failures			x
Repair Distribution Type			x
Repair Distribution Parameters	x		
Fixed and Variable Costs		x	
Financial Parameters	x		
System Configuration			x
Effect of Component Failure			x
Length of Run	x		
System Capacity	x		
Table/Plot Decision	x		

- (1) array (branch circuit) failures
- (2) array (branch circuit) repairs
- (3) non-array failures
- (4) non-array repairs
- (5) preventive maintenance
- (6) analysis of array/tracking system interaction*.

A complete listing of the components and the associated data requirements for this system appears in Table 18. This repeats Table 6 but in computer print-out form. One notable difference is the component "Branch Circuit" in Table 18, which is "Array" and "Lens" in Table 6.

Two repair/maintenance policies were tested. Array cleaning was tested for 3- and 12-month intervals. Array repair was initiated for alternative conditions of 1, 5, 8 or 12 array failures. In order to evaluate the effects of failures and repairs, maintenance costs were calculated on a levelized cost-per-kWh-produced basis. Economic parameters were thus needed. A discount rate of 15 percent, inflation rate of 8 percent, and electricity price escalation of 12 percent were assumed.

Table 19 shows 12 monthly power output duration curves. It is identical to Table 12. The numbers represent fractions of total array field capacity. They are printed in intervals of 8.33 hours. For example, in month 1, a perfectly operating system could be expected to produce more than 98.2 percent of capacity for only 8.33 hours. It would produce more than 96.3 percent of capacity for 16.66 hours (2 x 8.33).

The results of the SOLREL computer runs for the generic concentrator PV system appear in Tables 20 through 22. It can be inferred, given the input data assumptions, that cleaning this system every 12 months is a more cost-effective alternative than cleaning every 3 months. Note that the cleaning operation itself is performed during the off hours so that no output is lost.

These results indicate that failed array branch circuits should be replaced immediately. This is due to the fact that a linear cost function was

*Stream 6 is used to see if, when the optical/electrical portion of the array (branch circuit) has failed, the tracking portion of the same array has also failed. It also tests the opposite case.

TABLE 13. DESCRIPTION OF INPUT PARAMETERS
 GENERIC CONCENTRATOR SYSTEM (CLEANING AT 3-MONTH INTERVALS
 AND REPAIR AFTER 5 ARRAY FAILURES-CASE)

COMPONENT NAME	MTBF (MONTHS)	MAINT TIME (HRS)		REPAIR COST (\$)		NJM MEN	PM TIME (HOURS)			PM COST (\$)		PM INTERVAL (MONTHS)	NUM MEN
		50PCT	90PCT	FIXED	VARIABLE		50PCT	90PCT	FIXED	VARIABLE			
A BRANCH CIRCUIT	164.0	12.0	24.0	320.00	30.00	1	.5	1.0	0.00	20.00	3.0	1	
A TRACKING UNIT	92.0	12.0	24.0	320.00	30.00	1	2.0	4.0	50.00	30.00	36.0	1	
THE FIRST INVERTER	12.0	24.0	48.0	300.00	40.00	1	5.6	12.0	50.00	20.00	41.0	1	
THE SECOND INVERTER	12.0	24.0	48.0	300.00	40.00	1	5.6	12.0	50.00	20.00	41.0	1	
THE MONITORING PANEL	137.0	5.6	12.0	0.00	20.00	1							
THE CONTROL UNIT	7.0	56.8	136.0	1500.00	40.00	1							
THE MANUAL CONTROL	14.0	24.0	48.0	500.00	40.00	1							
THE DISTRIBUTION SYS	12000.0	28.0	60.0	0.00	0.00	1	8.0	18.0	0.00	40.00	12.0	1	
THE SOLID-STE SWITCH	1900.0	3.6	6.0	100.00	120.00	4							
THE UTILITY	9.0	2.0	3.6	0.00	0.00	1							
SYST DUE TO WEATHER	3.0	10.0	35.0	0.00	0.00	1							
GENERAL PREV MAINT							50.0	106.0	300.00	100.00	12.0	1	
FLAG1= 0 MEANS RESULTS FROM ALL PREVIOUS RUNS ARE BEING IGNORED													
FLAG2= 0 MEANS RESULTS FROM THIS RUN WILL NOT BE SAVED ON PERMANENT FILES													
FLAG3= 1 MEANS YEARLY SUMMARIES BUT NOT EVENT MESSAGES WILL BE PRINTED													
FLAG4= 1 MEANS TABLES FOR EACH INDIVIDUAL RUN WILL BE PRINTED													
FLAG5= 1 MEANS PLOTS FOR INDIVIDUAL RUNS ONLY WILL BE PRODUCED													
PERMANENT DEGRADATION -- 3 YEAR INTERVALS													
	1.000	.938	.935	.932	.929	.926	.923	.920	.917	.914	.911		
DEGRADATION DUE TO DIRT -- 3 YEAR INTERVALS													
	1.000	.911	.820	.730	.640	.550	.460	.370	.280	.190			
ARRAY CAPACITY IN KW.....												565.	
INVERTER DESIGN CAPACITY IN KW.....												500.	
OVERALL INFLATION RATE.....												.080	
DISCOUNT RATE.....												.150	
ELECTRICITY PRICE ESCALATION.....												.120	
LENGTH OF RUN IN MONTHS.....												360.	
UNACCEPTABLE NUMBER OF FAILED ARRAYS												5.	

TABLE 19. MONTHLY OUTPUT DURATION CURVES
FOR GENERIC CONCENTRATOR SYSTEM (INPUT DATA)

MONTHLY OUTPUT DURATION CURVES IN INTERVALS OF 8.33 HOURS PER MONTH																
MONTH 1	1.000	.982	.963	.945	.930	.914	.893	.871	.842	.816	.790	.769	.748	.724	.696	.647
	.007	.573	.533	.486	.438	.391	.343	.306	.239	.191	.150	.096	.050	.033	.015	0.000
	0.000	0.000	0.000	0.000	0.000	0.000	0.000	0.000	0.000	0.000	0.000	0.000	0.000	0.000	0.000	0.000
MONTH 2	1.000	.991	.981	.972	.962	.953	.940	.922	.905	.886	.864	.842	.819	.797	.760	.721
	.007	.639	.600	.560	.513	.447	.393	.332	.270	.209	.177	.136	.095	.068	.028	0.000
	0.000	0.000	0.000	0.000	0.000	0.000	0.000	0.000	0.000	0.000	0.000	0.000	0.000	0.000	0.000	0.000
MONTH 3	1.000	.992	.985	.977	.969	.962	.954	.946	.931	.916	.900	.885	.866	.852	.835	.817
	.799	.734	.716	.697	.675	.648	.612	.563	.516	.475	.423	.374	.326	.289	.249	.200
	.154	.125	.089	.048	.031	.013	0.000	0.000	0.000	0.000	0.000	0.000	0.000	0.000	0.000	0.000
MONTH 4	1.000	.993	.986	.980	.973	.966	.959	.952	.943	.926	.908	.891	.875	.859	.843	.826
	.808	.791	.769	.747	.715	.681	.663	.644	.594	.561	.541	.500	.453	.424	.380	.331
	.287	.241	.192	.148	.112	.080	.051	.029	.009	0.000	0.000	0.000	0.000	0.000	0.000	0.000
MONTH 5	1.000	.994	.987	.981	.975	.969	.962	.956	.950	.941	.930	.919	.906	.898	.879	.858
	.839	.824	.805	.793	.779	.764	.750	.735	.713	.690	.656	.626	.605	.592	.572	.545
	.518	.493	.467	.438	.406	.371	.315	.287	.255	.206	.175	.138	.086	0.000	0.000	0.000
MONTH 6	1.000	.996	.989	.982	.975	.966	.961	.954	.946	.938	.929	.920	.912	.903	.894	.876
	.858	.834	.782	.765	.748	.731	.715	.698	.680	.659	.637	.611	.584	.563	.544	.524
	.492	.464	.444	.423	.383	.345	.311	.283	.237	.192	.165	.134	.093	.025	0.000	0.000
MONTH 7	1.000	.991	.983	.974	.966	.957	.949	.938	.927	.915	.904	.891	.870	.849	.826	.803
	.783	.768	.752	.736	.720	.703	.687	.651	.620	.596	.571	.545	.519	.491	.460	.422
	.355	.320	.289	.256	.205	.159	.125	.096	.075	.053	.043	.033	.023	.014	.004	0.000
MONTH 8	1.000	.992	.985	.977	.969	.962	.954	.946	.931	.917	.902	.887	.873	.858	.844	.828
	.813	.797	.780	.761	.741	.688	.666	.646	.614	.557	.519	.493	.458	.411	.380	.343
	.299	.257	.235	.213	.171	.130	.098	.076	.059	.038	.017	0.000	0.000	0.000	0.000	0.000
MONTH 9	1.000	.993	.986	.978	.971	.964	.957	.950	.938	.924	.909	.895	.880	.864	.848	.833
	.817	.802	.781	.735	.715	.696	.666	.626	.604	.582	.525	.467	.444	.420	.350	.301
	.270	.223	.146	.105	.080	.056	.008	0.000	0.000	0.000	0.000	0.000	0.000	0.000	0.000	0.000
MONTH 10	1.000	.993	.986	.979	.973	.966	.959	.952	.942	.927	.911	.895	.879	.863	.847	.829
	.812	.794	.730	.706	.685	.637	.593	.561	.536	.448	.398	.354	.321	.235	.191	.160
	.130	.099	.065	.007	0.000	0.000	0.000	0.000	0.000	0.000	0.000	0.000	0.000	0.000	0.000	0.000
MONTH 11	1.000	.992	.984	.977	.969	.961	.953	.943	.927	.911	.895	.872	.848	.826	.805	.782
	.749	.716	.682	.644	.600	.549	.495	.412	.363	.295	.246	.198	.163	.070	.022	0.000
	0.000	0.000	0.000	0.000	0.000	0.000	0.000	0.000	0.000	0.000	0.000	0.000	0.000	0.000	0.000	0.000
MONTH 12	1.000	.980	.959	.940	.922	.905	.886	.866	.845	.805	.771	.742	.713	.685	.648	.595
	.550	.513	.478	.393	.333	.293	.269	.205	.123	.063	.039	.023	.006	0.000	0.000	0.000
	0.000	0.000	0.000	0.000	0.000	0.000	0.000	0.000	0.000	0.000	0.000	0.000	0.000	0.000	0.000	0.000

TABLE 20. SOLREL RESULTS: LEVELIZED COST, ¢/kWh

U.N.A.F. *	30 Year Lifetime	
	Clean Lens After:	
	3 Months	12 Months
1	1.83	1.76
5	1.87	1.80
8	1.91	1.84
12	2.06	1.98

TABLE 21. SOLREL RESULTS: LIFETIME COST, 1981 DOLLARS x 10³

U.N.A.F. *	Clean Lens After:	
	3 Months	12 Months
	1	915
5	904	858
8	897	852
12	895	850

TABLE 22. SOLREL RESULTS: LIFETIME OUTPUT, kWh x 10⁶

U.N.A.F. *	Clean Lens After:	
	3 Months	12 Months
	1	34.2
5	34.9	32.5
8	32.0	31.6
12	29.3	29.0

* Unacceptable Number of Array Failures Before Repair is Initiated.

used for array repair. In other words, repairing 12 branches simultaneously costs 12 times as much as repairing one. In actuality, there would probably be minor cost savings due to batching the repairs.

The event log, a portion of which is shown in Table 23, provides an event by event detailed record of the 30-year simulation. It itemizes each failure, repair, and weather-related or preventative maintenance event and provides a running summary of cumulative energy generated and maintenance dollars spent. These are both provided in current dollars and kWh as well as present value dollars and kWh.

Sample printouts showing the results of computer runs for the system appear in Tables 24 and 25. These outputs are useful as direct inputs to the life-cycle energy cost model and for estimating system availability.

Table 26 lists failures by year and by subsystem component. The tracking unit, branch circuit and inverters exhibited the largest number of hardware failures. The maintenance cost, cost per kWh and energy output per year are plotted in Figures 26 and 27. Annual maintenance costs can vary by as much as a factor of two.

Variability in Results. The SOLREL analysis of the case of repair on first array failure and clean every 3 months was replicated six times. The results are shown in Table 27. The mean, standard deviation, and 95 percent confidence limits on the mean are also presented. This experiment indicated tolerances of about 0.3 percent for energy output, and ± 3 percent for annual maintenance cost and number of failures.

The Computer Program for SOLREL

Appendix C in Volume II contains the details of the SOLREL computer program as run on Battelle's CDC Cyber computer. The input and the subroutines are described and a program listing is provided for each of the systems modeled.

Comparison of Results from the State Space Approach and the SOLREL Simulation Model of the Generic PV System

Three additional systems are modeled by both methods in the Volume II. A discussion of the comparative results is then given at the end of that portion of the report.

TABLE 23. LOG OF SYSTEM PERFORMANCE, MAINTENANCE COSTS AND EVENTS

		kWh	kWh
A FAILURE OF THE FIRST INVERTER HAS OCCURED ON SEPTEMBER 17, YEAR 11 THE SYSTEM OUTPUT IN KWHR FROM THE LAST EVENT TO SEPTEMBER 17, YEAR 11 WAS (ACT-PV)		14938.	11254.
A REPAIR OF THE FIRST INVERTER WAS COMPLETED IN 6 HOURS ON SEPTEMBER 17, YEAR 11 AT A COST OF \$ 4000.00 \$ 2041.10 THE SYSTEM OUTPUT IN KWHR FROM THE LAST EVENT TO SEPTEMBER 17, YEAR 11 WAS (ACT-PV)		326.	245.
THE SYSTEM OUTPUT IN KWHR FROM THE LAST EVENT TO OCTOBER 1, YEAR 11 WAS (ACT-PV)		17219.	12960.
THE SYSTEM OUTPUT IN KWHR FROM THE LAST EVENT TO NOVEMBER 1, YEAR 11 WAS (ACT-PV)		34981.	26210.
THE SYSTEM OUTPUT IN KWHR FROM THE LAST EVENT TO DECEMBER 1, YEAR 11 WAS (ACT-PV)		29828.	22352.
THE SYSTEM OUTPUT IN KWHR FROM THE LAST EVENT TO JANUARY 1, YEAR 11 WAS (ACT-PV)		32191.	24069.

TOTAL COSTS/OUTPUTS FOR YEAR 11	\$ 17000.00	524274.	
PRESENT VALUE	\$ 8956.14		397277.
LEVELLIZED CENTS PER KWH= 2.25			

THE SYSTEM WAS SHUTDOWN FOR 45 HOURS FOR CLEANING AND PM ON JANUARY 1, YEAR 12 AT A COST OF \$ 5000.00 \$ 2505.85 THE SYSTEM OUTPUT IN KWHR FROM THE LAST EVENT TO FEBRUARY 1, YEAR 12 WAS (ACT-PV)		38312.	28582.
A FAILURE OF A BRANCH CIRCUIT HAS OCCURED ON FEBRUARY 16, YEAR 12 11 ARRAY/TRACKING SYSTEM COMBINATIONS ARE NOT OPERATING THE SYSTEM OUTPUT IN KWHR FROM THE LAST EVENT TO FEBRUARY 16, YEAR 12 WAS (ACT-PV)		21591.	16089.
THE SYSTEM OUTPUT IN KWHR FROM THE LAST EVENT TO MARCH 1, YEAR 12 WAS (ACT-PV)		21142.	15739.
A FAILURE OF A BRANCH CIRCUIT HAS OCCURED ON MARCH 21, YEAR 12 12 ARRAY/TRACKING SYSTEM COMBINATIONS ARE NOT OPERATING THE SYSTEM OUTPUT IN KWHR FROM THE LAST EVENT TO MARCH 21, YEAR 12 WAS (ACT-PV)		0.	0.
A REPAIR OF A BRANCH CIRCUIT WAS COMPLETED IN 44 HOURS ON MARCH 23, YEAR 12 AT A COST OF \$ 26000.00 \$12843.98 THE SYSTEM OUTPUT IN KWHR FROM THE LAST EVENT TO MARCH 23, YEAR 12 WAS (ACT-PV)		0.	0.
THE SYSTEM OUTPUT IN KWHR FROM THE LAST EVENT TO APRIL 1, YEAR 12 WAS (ACT-PV)		15072.	11195.
THE SYSTEM OUTPUT IN KWHR FROM THE LAST EVENT TO MAY 1, YEAR 12 WAS (ACT-PV)		62556.	46362.
THE SYSTEM OUTPUT IN KWHR FROM THE LAST EVENT TO JUNE 1, YEAR 12 WAS (ACT-PV)		59995.	44367.
THE SYSTEM OUTPUT IN KWHR FROM THE LAST EVENT TO JULY 1, YEAR 12 WAS (ACT-PV)		56388.	41607.

TABLE 24. SAMPLE PRINTOUT OF ANNUAL COSTS AND OUTPUT ENERGY FROM GENERIC CONCENTRATOR SYSTEM

YEAR	CURRENT VALUE			PRESENT VALUE		
	COST (\$)	KWH	CENTS/KWH	COST (\$)	KWH	CENTS/KWH
1	21907.78	1123741.	1.95	23989.22	1109585.	1.89
2	34965.39	1135707.	3.07	32166.18	1091101.	2.95
3	33767.50	1100292.	3.07	29043.23	1029800.	2.82
4	35542.18	1133800.	3.14	23746.17	1033358.	2.78
5	24984.85	1097979.	2.28	19050.73	974567.	1.95
6	51054.98	981076.	5.20	36416.90	847724.	4.30
7	33727.50	1139420.	2.96	22643.24	959415.	2.36
8	47725.00	1069020.	4.46	30137.32	876265.	3.44
9	23769.48	1123488.	2.12	14068.74	897294.	1.57
10	32931.29	1068277.	3.08	18392.40	830651.	2.21
11	26599.30	1054855.	2.52	13859.58	796886.	1.73
12	26937.71	1146344.	2.35	13095.83	845543.	1.55
13	36333.37	1056203.	3.44	16799.52	758851.	2.21
14	26051.67	1130632.	2.30	11189.72	791301.	1.41
15	21042.05	1124377.	1.87	8490.63	766253.	1.11
16	31009.76	1151029.	2.69	11864.59	764108.	1.55
17	31844.74	1116747.	2.85	11535.70	721798.	1.60
18	31877.28	1025761.	3.11	10725.98	645700.	1.66
19	36906.40	1038574.	3.55	11721.72	637170.	1.84
20	20832.06	1075380.	1.94	6188.13	642266.	.96
21	35213.26	1035406.	3.24	3636.73	631305.	1.53
22	19301.79	1125959.	1.71	5101.25	637658.	.80
23	27586.98	1143321.	2.41	6795.61	630585.	1.05
24	14548.90	1118192.	1.30	3364.64	600811.	.56
25	36307.44	1117182.	3.25	7956.29	584403.	1.36
26	19026.80	1084534.	1.75	3854.39	552480.	.70
27	30938.58	1072748.	2.88	5852.66	532562.	1.10
28	34805.70	1066378.	3.26	6211.39	516418.	1.20
29	24160.55	1115542.	2.17	4104.65	524801.	.78
30	32413.91	1030053.	3.15	5132.37	471962.	1.09
TOTALS	903496.40	32653609.		425136.31	22704722.	1.87 (LEVELIZED)

TABLE 25. GENERIC CONCENTRATOR SYSTEM AVAILABILITY

ANNUAL SYSTEM AVAILABILITY DURING DAYLIGHT
AS A PERCENT OF SYSTEM CAPACITY

SYSTEM CAPACITY = 500.0 KW NUMBER OF DAYLIGHT HOURS PER YEAR = 3757.5

YEAR	100-90%	90-80%	80-70%	70-60%	60-50%	50-40%	40-30%	30-20%	20-10%	10-0%	TOTAL
THEORETICAL	31.61	7.03	5.99	5.40	4.40	5.23	5.59	7.21	8.78	18.76	100.00
1	32.03	9.28	8.40	6.61	6.55	5.21	5.36	5.03	5.63	15.41	100.00
2	30.55	11.32	9.18	7.00	7.28	5.49	5.30	5.12	5.52	14.16	100.00
3	25.96	12.71	9.21	7.36	9.66	5.80	5.56	5.31	6.47	11.97	100.00
4	28.04	11.83	9.08	7.54	8.21	6.03	5.46	5.53	6.12	11.29	100.00
5	24.94	13.13	10.04	7.93	8.52	5.97	5.62	5.77	6.25	11.72	100.00
6	22.40	10.74	8.44	6.50	10.60	5.52	5.05	5.27	5.50	19.90	100.00
7	27.58	12.36	9.74	7.78	8.52	6.01	5.49	5.91	6.01	10.29	100.00
8	25.92	12.57	9.52	7.62	7.26	5.71	5.40	5.41	6.17	14.32	100.00
9	24.64	14.19	10.35	8.80	8.78	6.50	5.69	6.09	6.16	8.81	100.00
10	24.80	13.42	9.99	8.17	7.01	6.15	5.46	5.30	5.89	13.21	100.00
11	24.29	12.26	9.95	7.64	9.07	5.49	5.48	5.44	5.81	15.57	100.00
12	26.27	12.65	10.37	8.01	9.89	6.33	5.35	5.64	6.46	8.54	100.00
13	24.36	12.21	9.37	7.55	6.92	5.78	5.46	5.64	5.95	14.74	100.00
14	25.43	13.89	9.72	8.66	7.61	6.26	5.54	5.75	6.18	12.65	100.00
15	23.73	13.38	10.38	7.80	10.30	6.20	5.67	5.92	6.11	10.45	100.00
16	25.78	13.48	10.39	8.24	7.45	6.22	5.49	5.59	6.24	11.12	100.00
17	22.90	13.79	11.12	9.49	9.49	6.34	5.98	5.98	6.52	9.37	100.00
18	21.43	13.11	10.10	7.98	8.80	6.06	5.40	5.52	5.94	15.66	100.00
19	22.58	11.92	9.42	7.30	8.84	5.80	5.27	5.13	5.57	18.07	100.00
20	22.04	14.38	10.38	8.44	7.61	6.23	5.50	5.85	5.89	13.67	100.00
21	22.98	14.24	10.22	8.10	8.38	6.28	5.49	5.78	6.26	12.26	100.00
22	21.26	15.33	11.32	9.14	8.19	6.70	5.79	6.21	6.32	9.75	100.00
23	25.68	13.04	10.59	8.01	8.37	6.34	5.84	5.90	6.48	9.66	100.00
24	22.75	14.67	10.62	8.03	9.10	6.53	5.36	6.20	6.32	8.85	100.00
25	25.56	13.85	10.46	8.54	8.52	6.26	5.54	5.83	6.32	8.66	100.00
26	23.03	14.13	10.83	8.14	8.04	6.02	5.65	5.67	6.36	12.13	100.00
27	22.27	13.76	10.65	8.18	8.45	6.33	5.47	5.91	5.78	13.20	100.00
28	21.12	15.57	10.17	8.71	7.87	6.36	5.41	5.89	6.13	13.26	100.00
29	25.32	14.08	10.11	8.34	8.01	6.42	5.37	5.96	6.43	9.86	100.00
30	20.53	13.57	9.54	7.87	9.43	5.90	5.36	5.46	5.93	16.39	100.00
AVERAGE	24.54	13.10	11.01	7.97	8.51	6.08	5.55	5.69	6.10	12.48	100.00

TABLE 26. GENERIC PASSIVELY COOLED CONCENTRATOR SYSTEM COMPONENT FAILURES

COMPONENT FAILURE TABLE																																	
NUMBER OF FAILURES PER COMPONENT BY YEAR																																	
COMPONENT	YEAR =	1	2	3	4	5	6	7	8	9	10	11	12	13	14	15	16	17	18	19	20	21	22	23	24	25	26	27	28	29	30	TOTAL	
A BRANCH CIRCUIT		5	4	4	5	5	4	3	9	4	6	2	6	2	2	2	2	1	4	3	4	5	0	1	2	6	4	5	7	6	3	124	
A TRACKING UNIT		9	12	5	6	14	12	7	12	10	0	5	9	5	7	6	7	4	9	7	4	8	2	7	5	0	6	6	11	6	11	228	
THE FIRST INVERTER		1	1	2	3	0	4	1	0	0	0	3	2	1	1	2	0	1	3	0	0	1	0	1	1	0	2	1	0	0	0	31	
THE SECOND INVERTER		0	1	3	2	2	1	2	2	2	0	2	3	3	0	3	1	1	0	2	1	2	0	2	2	1	0	2	1	2	3	46	
THE MONITORING PANEL		0	1	1	1	0	1	0	0	0	0	0	1	0	0	0	0	0	0	0	0	0	0	0	0	0	0	0	0	0	0	5	
THE CONTROL UNIT		2	3	1	3	1	4	2	4	0	2	1	1	2	2	2	2	1	3	3	1	5	0	3	0	0	1	3	2	1	3	58	
THE MANUAL CONTROL		0	1	0	0	0	0	0	0	0	0	0	0	0	0	0	0	0	0	0	0	0	0	0	0	0	0	0	0	0	0	1	
THE DISTRIBUTION SYS		0	0	0	0	0	0	0	0	0	0	0	0	0	0	0	0	0	0	0	0	0	0	0	0	0	0	0	0	0	0	0	
THE SOLID-STE SWITCH		0	0	0	0	0	0	0	0	0	0	0	0	0	0	0	0	0	0	0	0	0	0	0	0	0	0	0	0	0	0	0	
THE UTILITY		1	1	0	3	2	0	1	0	2	1	1	0	0	1	0	2	1	1	2	1	0	0	2	1	1	3	1	1	4	1	34	
SYST DUE TO WEATHER		3	2	3	6	3	4	2	0	4	9	7	3	3	5	2	4	2	2	2	2	5	3	4	3	6	3	5	2	6	1	7	111
TOTALS		21	19	27	18	22	21	16	17	11	19	24	19	19	20	20	26	29	30	27	26	25	18	18	22	16	14	17	21	28	28	638	

100

COST BY YEAR

SYSTEM OUTPUT BY YEAR

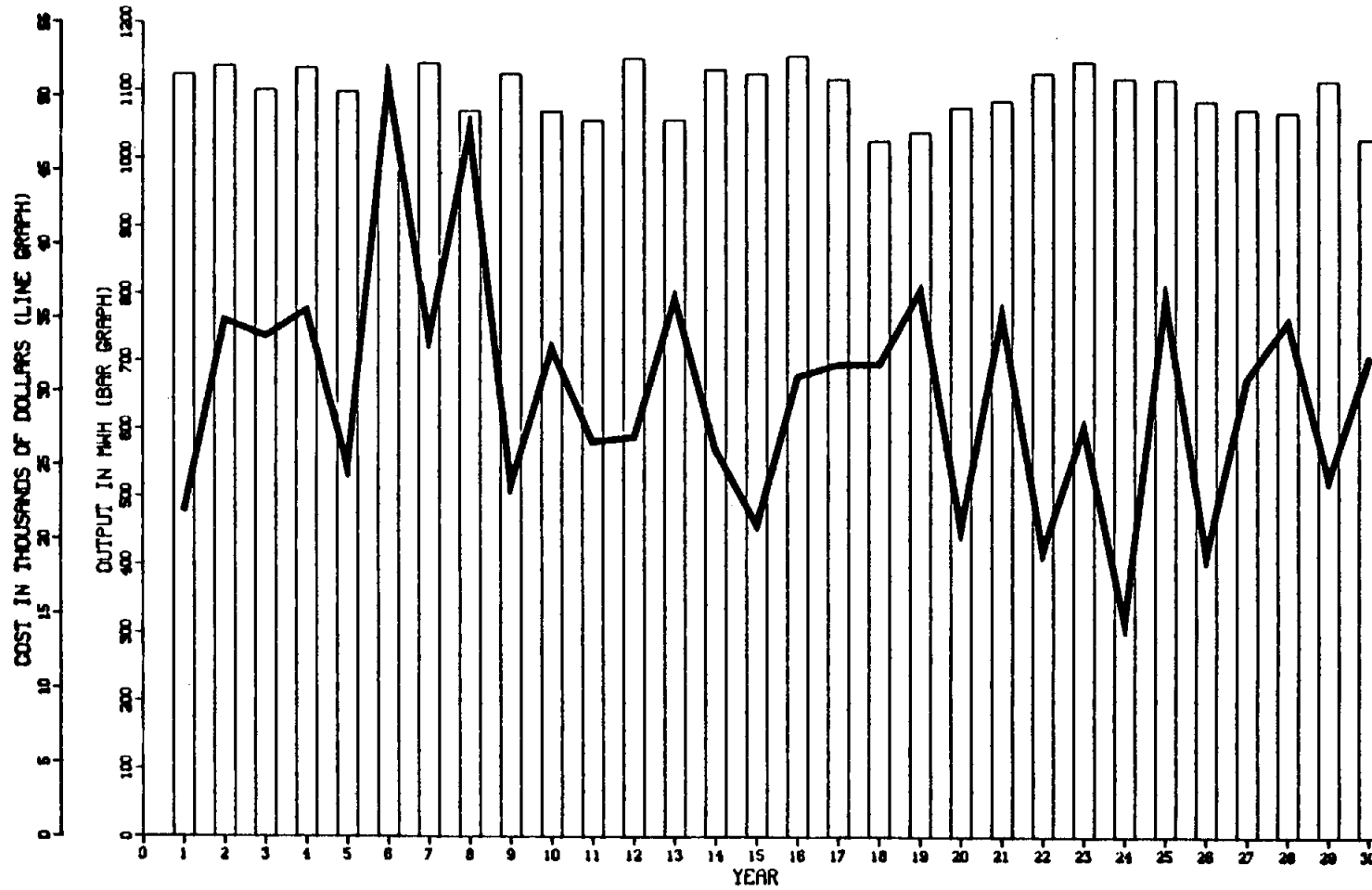


FIGURE 26. OUTPUT OF MAINTENANCE COSTS AND ENERGY FOR APS/MOTOROLA PV SYSTEM

PRESENT VALUE COST BY YEAR

LEVELIZED CENTS/KWH BY YEAR

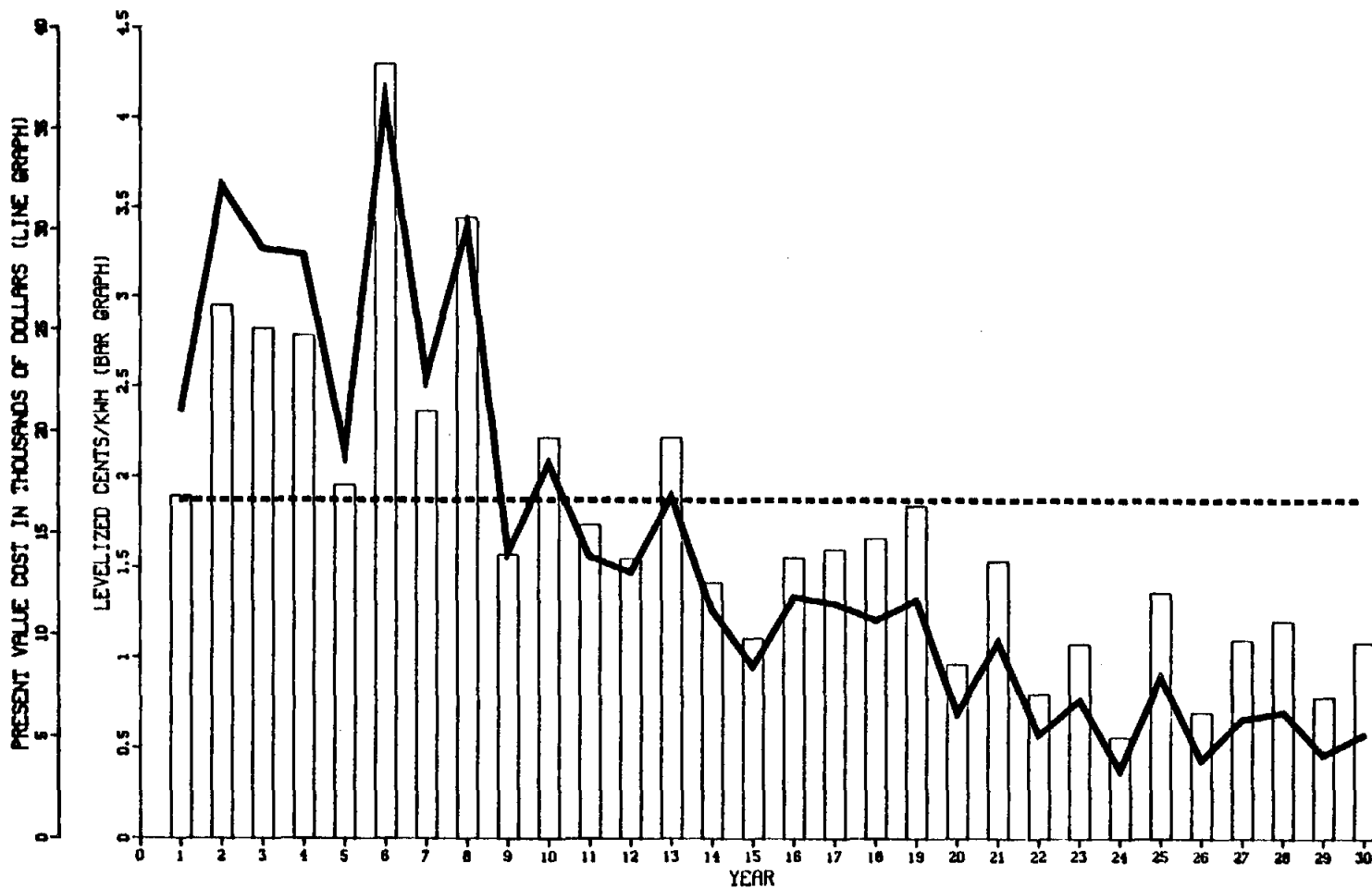


FIGURE 27. OUTPUT OF MAINTENANCE COSTS AND LEVELIZED MAINTENANCE COST PER UNIT ENERGY FOR APS/MOTOROLA PV SYSTEM

TABLE 27. ESTIMATE OF VARIANCE AMONG SOLREL RUNS--6 CASES,
REPAIR ON FIRST ARRAY FAILURE, CLEAN EVERY
3 MONTHS

	1	2	3	4	5	6	Mean	Std. Dev.	95% Conf. Int. for Mean
Number Failures	606	627	614	630	630	651	626.3	15.5	610.0-642.6
Cost (\$1000)	869	881	912	856	851	915	880.7	27.5	851.8-909.6
Output (1000 MWH)	34.2	33.9	33.9	34.0	33.9	34.2	34.0	.147	33.9-34.1

103 and 104

Confidence Interval For Means Defined As:

$$\bar{X} - t_{\alpha/2, n-1} \cdot \frac{S}{\sqrt{n}} < \mu < \bar{X} + t_{\alpha/2-1} \cdot \frac{S}{\sqrt{n}}$$

where n = number of replications

$t_{\alpha/2, n-1}$ is from t distribution at $\alpha/2$ significance level and n-1 degrees of freedom

$$s = \sqrt{\frac{\sum_i (y_i - \bar{y})^2}{n-1}}$$

$$t_{.975, 5} = 2.571$$

**LIFE-CYCLE ENERGY COST AND
SENSITIVITY ANALYSES**

LIFE-CYCLE COST ANALYSIS

Defining the Procedure

In comparing the costs of competing investments, particularly investments in electric generating equipment, it is always a major problem to properly account for the fluctuations in cost and outputs which occur over the system's useful life. For example, a 100 kW flat-panel photovoltaic system may cost close to \$1 million to build, but will then produce electricity with little operating and maintenance expense. The alternative might be to purchase electricity from the local utility which would eliminate the large initial expenditure, but result in relatively high and increasing costs in terms of cents per kWh which would continue indefinitely. The question remains, how can a decision maker make a logical choice between two competing technologies when one involves a much higher cost in year 1 but a lower cost thereafter?

Life-Cycle Costs (LCC)

The method most commonly used to assist the decision maker in making this tradeoff is life cycle costing, often referred to as present value analysis. At the very start, it is important to note that LCC is strictly an approach to analyzing the financial characteristics of a system. It in no way substitutes for such major decision making criteria as cash flow, aesthetics, environment, or political/institutional feasibility. LCC estimates the costs incurred and electricity produced by the system, year-by-year throughout its life. For each year of system life, the LCC methodology calculates the out-of-the-pocket costs which accrue to the owner, including such items as initial downpayment, interest payments, payments on principal, maintenance expense, taxes, and miscellaneous expenditures. In addition, the methodology simulates a hypothetical tax return for the system owner, carefully recording the tax credits which accrue due to interest deductions, depreciations, and operating expense deductions. Once these credits and costs are calculated for each year of system life, they may be displayed graphically as in Figure 28.

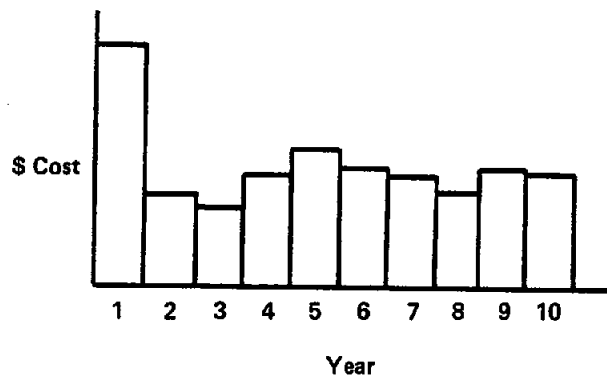


FIGURE 28. CASH FLOW OF HYPOTHETICAL INVESTMENT WITH 10-YEAR LIFE, INITIAL YEAR DOLLARS

These costs are all initial year dollars, in other words, assuming zero inflation. Inflation (at a rate of i), however, actually causes \$10 worth of goods and services at today's prices to require $\$10 \times (1+i)^n$ n years in the future.

Therefore the costs in Figure 28 must be adjusted to current year dollars so that inflation is taken into account. The results appear in Figure 29. Current dollars means the actual number of dollar bills which would change hands at the time the cost was incurred.

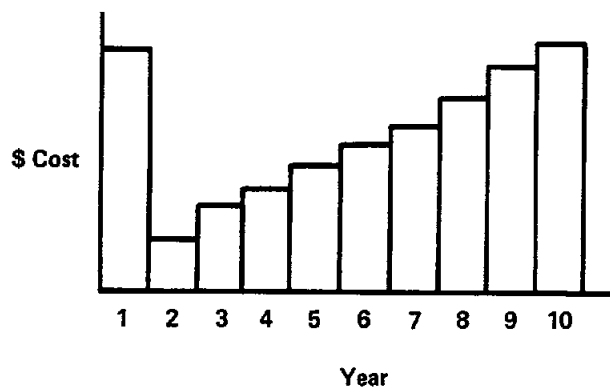


FIGURE 29. CASH FLOW OF HYPOTHETICAL INVESTMENT WITH 10-YEAR LIFE, CURRENT DOLLARS

But, businesses place a time value on money as well. Any prudent businessman would rather have a dollar in his pocket today than a promise of a dollar, even a dollar adjusted for inflation, several years in the future. The assumption is that the businessman could invest the dollar today and receive a yield greater than the rate of inflation. This yield is the businessman's discount rate. Due to this discount rate, the costs incurred in year n as shown in Figure 29 will be reduced by a factor of $(1 + d)^n$, where d is the discount rate, to calculate present value in initial year dollars. Therefore, in present value initial year dollars, the costs will be displayed as in Figure 30. Thus, at usual discount rates, expenses which occur far into the future have minimal impact on an LCC analysis.

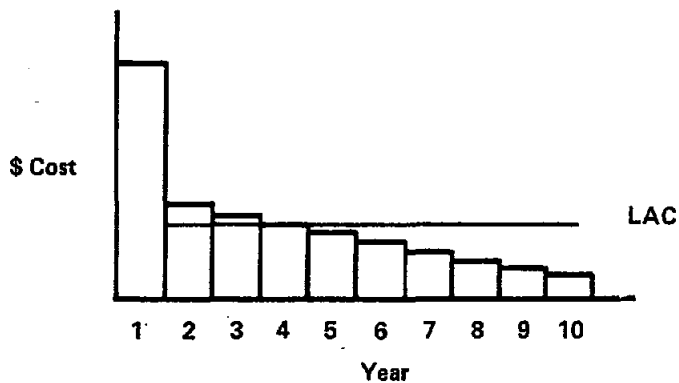


FIGURE 30. CASH FLOW OF HYPOTHETICAL INVESTMENT WITH 10-YEAR LIFE, PRESENT VALUE INITIAL YEAR DOLLARS

At this point, the present value costs for each year can be assumed to yield a single number, the LCC for the system. Note that only one LCC can result from any series of expenditures; however, an infinite number of cost streams could yield the same LCC. Therefore, this technique creates a means for comparing cost streams which have substantially different patterns of expenditures. Often the LCC is converted into a levelized annual cost (LAC) by computing the stream of equal annual costs which has a present value equal to the system life cycle cost. The LAC is shown in Figure 30 as a horizontal line.

Life-Cycle Energy Cost (LEC)

In evaluating the feasibility of a photovoltaic system, it does little good to compare costs without looking at output as well. If the competing technology is purchased energy, which is expressed in cents per kWh, then the life-cycle energy cost of the photovoltaic system must be expressed in cents per kWh. There are two methods for making this comparison.

Method 1 begins with the levelized annual cost mentioned earlier (LAC) and divides that number by the average annual system output (AAO). This yields a cost of the generated electricity in ¢/kWh expressed as LAC/AAO . At first glance, this number will normally be quite a bit higher than the current cost of electricity, often causing considerable confusion. It should not be compared to current cost of electricity but to the present value of purchased electric energy. The curve of Figure 31 shows the cost escalation of purchased energy over time. C_0 is the current cost of electricity and C_{10} , the cost of electricity (current dollars) in year 10.

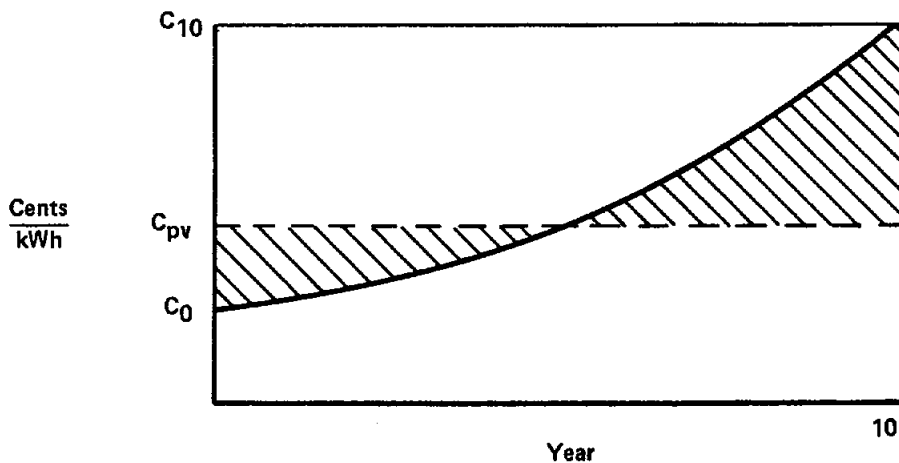


FIGURE 31. COST ESCALATION OF PURCHASED ENERGY

C_{pv} represents the present value of the cost of purchased energy. Note that the two shaded areas represent equal present values. Now by comparing C_{pv} to the PV system's cost of generated electricity (LEC), an assessment of the financial feasibility of the photovoltaic system can be made.

Method 2 computes a "present value" of the output energy which, when divided into the present value of the PV system cost, yields a cents per kWh figure comparable to the current cost of electricity. Calculating the "present value" of output involves both computational and conceptual elements. The output in kWh normally degrades over time for a photovoltaic system as shown in Figure 32.

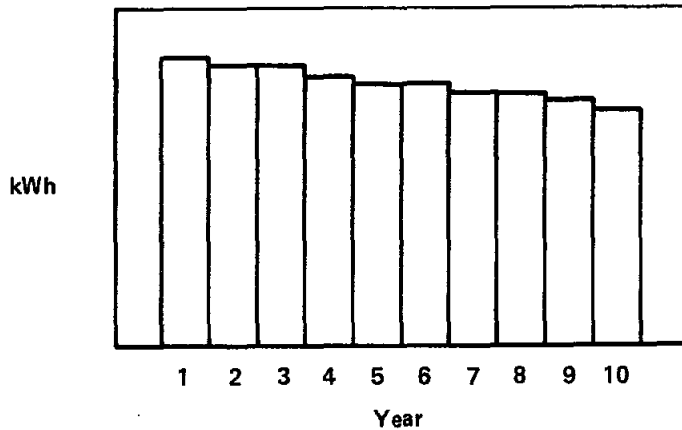


FIGURE 32. HYPOTHETICAL OUTPUT FROM PHOTOVOLTAIC SYSTEM

Next, each kWh of output is converted into its current value, in other words the current cost of electricity. The output bar chart in Figure 32 remains identical but the units on the vertical axis become dollars instead of kWh. Next the affect of the escalation rate of electricity is included (similar to method used to go from Figure 28 to Figure 29) and the results appear in Figure 33. Finally, the same discount rate used earlier is applied (same as method used to go from Figure 29 to Figure 30) to produce the present value output in dollars shown in Figure 34.

The same conversion factor used earlier to convert from kWh to dollars can then be employed again to convert the present value dollars to present value kWh. Actually the conversion was necessary in the first place only to ease the conceptual difficulty of talking of a "present value" which is not in the monetary units.

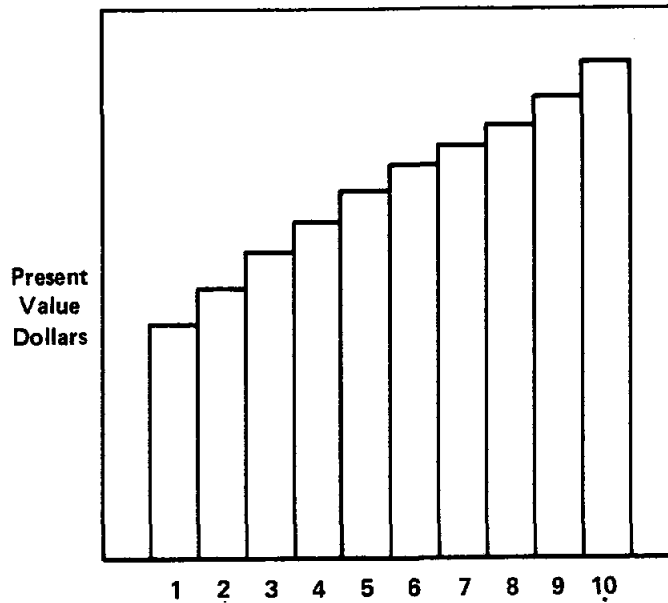


FIGURE 33. OUTPUT IN CURRENT DOLLARS EQUIVALENT

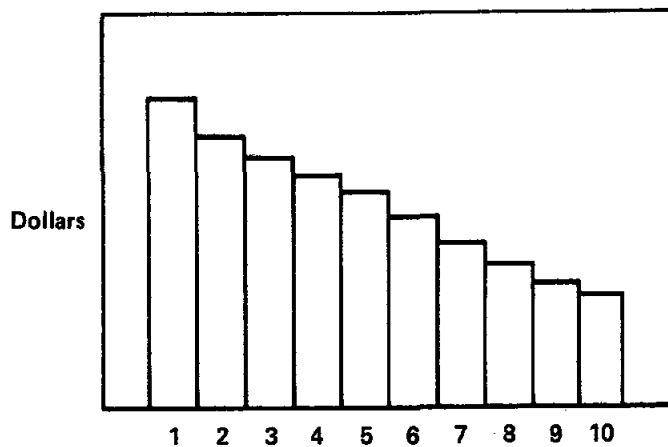


FIGURE 34. OUTPUT IN PRESENT VALUE DOLLARS

The present value cost over the system life (Figure 34) divided by the present value output over system output then yields a cents per kWh value (life-cycle energy cost) which can be compared to the current cost of purchased electrical energy to determine the financial feasibility of the photovoltaic system.

Applying the Procedure to a Specific System

Life-cycle energy cost analyses can differ in the level of detail which is used to define the various cost components. Sometimes initial cost may be divided into several components. Other times a detailed tax assessment may be needed, requiring that the attributes of the tax laws themselves be included in the model. The specific technique used by Battelle in this project is similar to the one described in "A Methodology for Determining the Economic Feasibility of Residential or Commercial Solar Energy Systems" by Audrey M. Perino⁽²²⁾. Perino divides the analysis into the following categories of present values.

- initial cost* (downpayment = D)
- salvage value (PVSV)
- investment tax credit (PVITC)
- property taxes (PVPROP)
- backup energy cost (PVENER)
- miscellaneous/maintenance cost (PVMISC)
- loan payments (PVLOAN)
- interest payments (PVINT)
- depreciation (PVDEPD).

For this project, a pessimistic discount rate of 20 percent was tested against an optimistic discount rate of 13 percent. The remaining parameters were defined as follows:

- percent downpayment = 20 percent
- general inflation rate = 8 percent
- cost of electricity escalation rate = 2 1/2 percent + inflation
- interest rate = 12 percent (optimistic case)
= 15 percent (pessimistic case)
- income tax rate = 40 percent
- price year (all costs entered in price year dollars) = 1980
- period of analysis (system life) = 30 years

*An initial cost for all PV Systems was assumed to be \$6.00 per peak Watt for these analyses.⁽⁹⁾

● borrowing period	= 30 years
● accounting period	= 7 years
● accounting method	= sum of years digit
● year of operation	= 1982
● backup energy cost	= 0
● investment tax credit	= 25 percent of initial cost
● initial system cost	= \$6.00/peak watt (\$4.80 + 25%) (1982 Cost Goal)
● property taxes	= 2.3 percent of initial cost per year
● salvage value	= 5 percent of initial cost
● maintenance	= 30 years present value total input from SOLREL

In the commercial sector, Perino assumes that miscellaneous costs, maintenance costs, property taxes, backup energy costs, depreciation, and interest payments are tax deductibles. Battelle further assumes that the photovoltaic system perfectly matches load (backup energy cost is zero) and that salvage value is zero. The total present value calculation then becomes: $TPV = PVSYS + (1 - t) (PVMISC + PVPROP) - t (PVPEPD + PVINT) - PVITC$ where $t =$ the effective rate of taxation

$$PVSYS = D \cdot IC + PVLOAN$$

IC = initial cost.

All other variables have been defined earlier.

Battelle has programmed the necessary equations to perform a photovoltaic life-cycle energy cost analysis into a computer model called LCCOST. This model can attach directly to SOLREL and can print results either in the form of tables or pie charts. Note that the bottom line levelized cents per kWh on LCCOST output tables is comparable to the current cost of electricity.

Since the cost of electricity is tax deductible in the commercial sector, the actual cost of electricity (which can be compared to the value of the table) is 1 minus the effective rate of taxation times what is actually paid to the utility. In other words, if the effective tax rate is 40 percent

and the utility charges 5 cents/kWh, then the net cost of electricity is $(1 - .40) (5¢/\text{kWh}) = 3¢/\text{kWh}$.

In addition, some sensitivity analyses have been run to test the effect of the percent downpayment and interest rates. The results are shown in Tables 28-29. Two discount rates were tested, 20 percent and 13 percent. The 20 percent discount rate is 12 percent over inflation and tends to emphasize initial expenditure over maintenance expense. Since photovoltaic systems are expensive to build and inexpensive to maintain, a high discount rate such as 20 percent represents a pessimistic scenario. A high discount rate emphasizes initial expenditures and considerably reduces the importance of expenditures a few years away. The 13 percent discount rate places more emphasis on maintenance expense relative to initial system costs and thus produces a more optimistic economic scenario for photovoltaic systems.

Two values for interest rate were tested, one being 5 percent below the discount rate and the other 1 percent below the discount rate. The interest rate is the rate applied to any loan the purchaser of the photovoltaic system must obtain to finance the initial investment. Lower interest rates are beneficial to those systems with a large loan (i.e., a large initial cost) such as PV systems. Finally, two values of percent downpayment were tested, 20 percent and 10 percent, respectively. The higher the downpayment the smaller the loan. Therefore, a high downpayment will be most beneficial for those systems with high initial investments such as a PV system. For the sensitivity analysis and for the three generic analysis of Volume II, scenario B and Scenario D were used to represent the pessimistic and optimistic financial cases, respectively.

TABLE 28. DESCRIPTION OF SCENARIOS TESTED

	<u>Discount Rate, %</u>	<u>Interest Rate, %</u>	<u>Percent Rate, %</u>
Scenario A	20	19	20
Scenario B	20	15	20
Scenario C	20	15	10
Scenario D	13	12	20
Scenario E	13	12	10

TABLE 29. COMPARISON OF LIFE-CYCLE ENERGY COSTS
In cents per kWh

	<u>SCENARIO</u>				
	<u>A</u>	<u>B</u>	<u>C</u>	<u>D</u>	<u>E</u>
Passively Cooled Concentrator Design II	11.32	8.78	10.11	6.30	7.18
Flat Panel	11.90	9.20	10.62	6.82	7.77

SENSITIVITY ANALYSISSOLRELSummary OF SOLREL Analysis

A number of simulations were run to determine parameter sensitivities such as: (1) the optimal array cleaning interval and (2) the optimal level of reliability for the inverter subsystem. These sensitivity runs used SOLREL design analyses described in Volume II for the flat-panel and passively cooled concentration systems. Table 30 shows the results of the cleaning runs. Note that since maintenance costs are tax deductible in commercial systems, the optimal interval is shorter when considering total life-cycle energy cost (with taxation versus life-cycle maintenance cost (no taxation). A discount rate of 13 percent was assumed (optimistic case as described in previous section).

TABLE 30. LEVELIZED LIFE-CYCLE ENERGY COST AS A FUNCTION OF CLEANING INTERVALS ASSUMING 13 PERCENT DISCOUNT RATE

Cleaning Interval in Months	Flat Panel LEC, ¢/kWh	Passively Cooled Concentration LEC, ¢/kWh
6	7.01 (2.66)*	6.35 (2.25)
12	6.82 (2.28)	6.30 (2.11)
18	6.87 (2.30)	6.34 (2.10)
24	6.88 (2.25)	(2.10)
30		(2.10)
36	6.94 (2.22)	

* Levelized Life-Cycle Maintenance Cost (¢/kWh) in parentheses.

The optimal cleaning interval seems to be around 12 months but would be 18 to 24 months if maintenance expenses were not tax deductible. The result is rather insensitive near the optimal point. In other words, the cleaning schedule does not have to be rigorously enforced.

Table 31 shows the results of the runs testing versus inverter cost and reliability combination in the flat-panel system. A discount rate of 20 percent was assumed.

TABLE 31. LEVELIZED LIFE-CYCLE ENERGY COST AS A FUNCTION OF INVERTER RELIABILITY AND COST

	Inverter Reliability/Cost	Flat Panel LEC, ¢/kWh
1	MTBF = 12.0 (in months) Cost \$15,500	9.33 (2.32)*
2	MTBF = 24.0 Cost \$22,689	9.19 (1.85)
3	MTBF = 32.4 Cost \$26,747	9.22 (1.73)
4	MTBF = 64.8 Cost \$39,180	9.42 (1.56)

* Levelized Life-Cycle Maintenance Cost (¢/kWh) in parentheses.

The optimal inverter (minimum LEC) reliability/cost combination seems to be the one with MTBF equal to 24 months, with a cost of \$22,689.

A more detailed analysis and discussion of the experimental design and variance reduction techniques used to arrive at the above results are discussed in the following section.

Reduction of Variation in Results

One of the primary purposes of reliability/maintainability modeling is to be able to evaluate the sensitivity of the present value and levelized cost of system-produced electricity to changes in design or maintenance strategies. The SOLREL model can produce a number of these sensitivity runs quickly and at relatively low cost. SOLREL can also be run with different random number streams to create a distribution around the estimated mean. This distribution can assist the designer in avoiding extreme cases and in understanding normal operating conditions.

In running SOLREL to test a particular design or maintenance strategy, it is essential that as much random variation as possible be either eliminated or explained. The following describes a three phase approach for using SOLREL to test alternative design and/or maintenance strategies (see Figure 35).

Phase 1 consists of a single run of SOLREL with no consideration given to the assignment of random number streams. Although this is the least costly approach, it also yields the greatest random variation.

Figure 36 shows frequency distributions which represent the random variation in maintenance costs associated with the total system as well as those associated with the components and maintenance activities. From this diagram, the random variation of the total system can be viewed as a combination of the random variations of Component A, Component B, Preventive Maintenance, and Cleaning. Each time a simulation is run, a point from each of the lower four curves (see X's) results. When these are combined they result in one point on the total system distribution. A Phase 1 run is subject to variation equal to that of the total system curve.

An example might be helpful to show why Phase 1 is often ineffective. Suppose a designer wishes to test the effect of a more reliable/more costly inverter on system effectiveness. The failure times of the inverter, however, might be linked to the same random number stream as all other failure times.

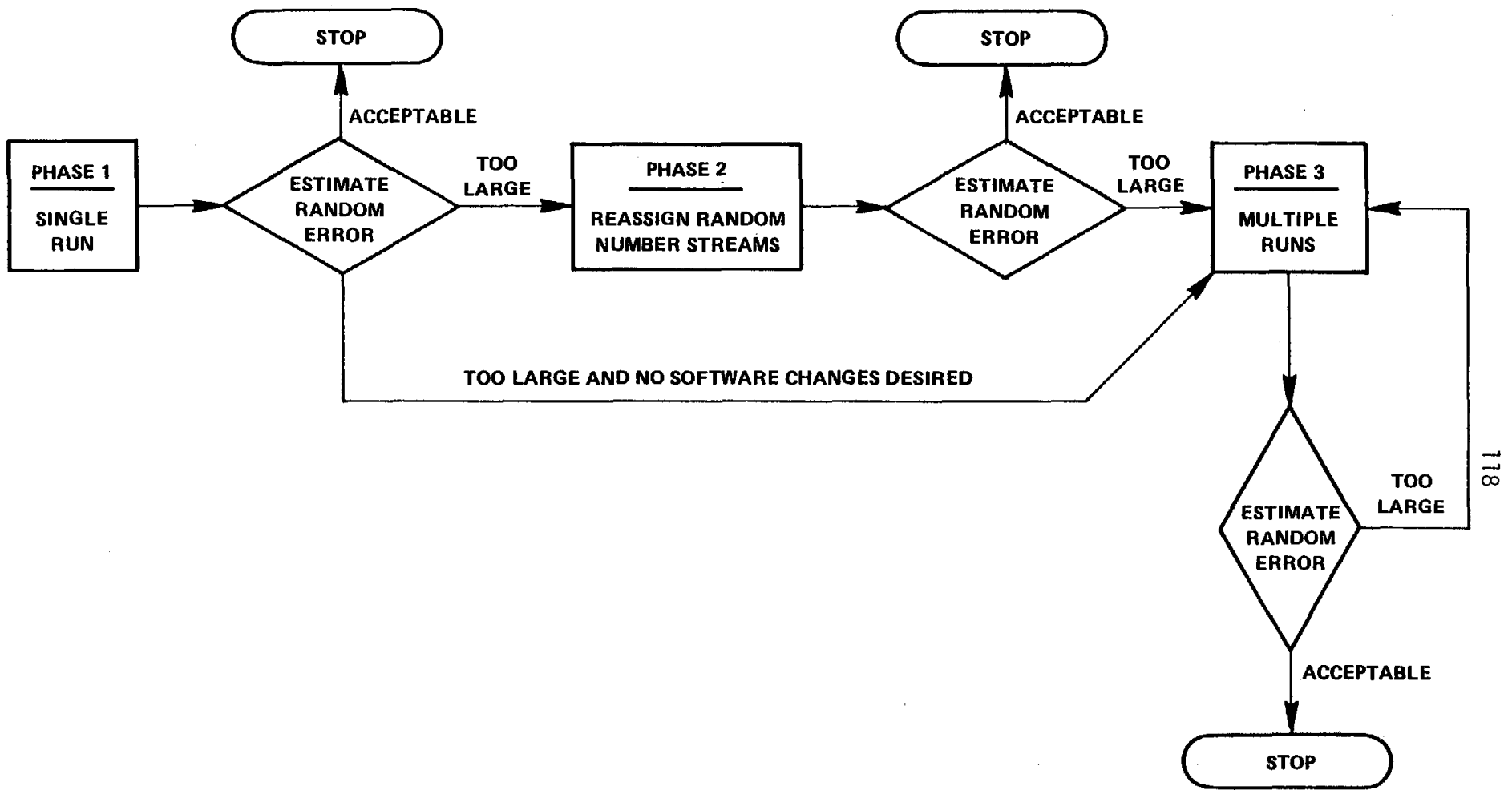


FIGURE 35. FLOW CHART FOR THREE-PHASE APPROACH TO REDUCE SOLREL OUTPUT VARIABILITY

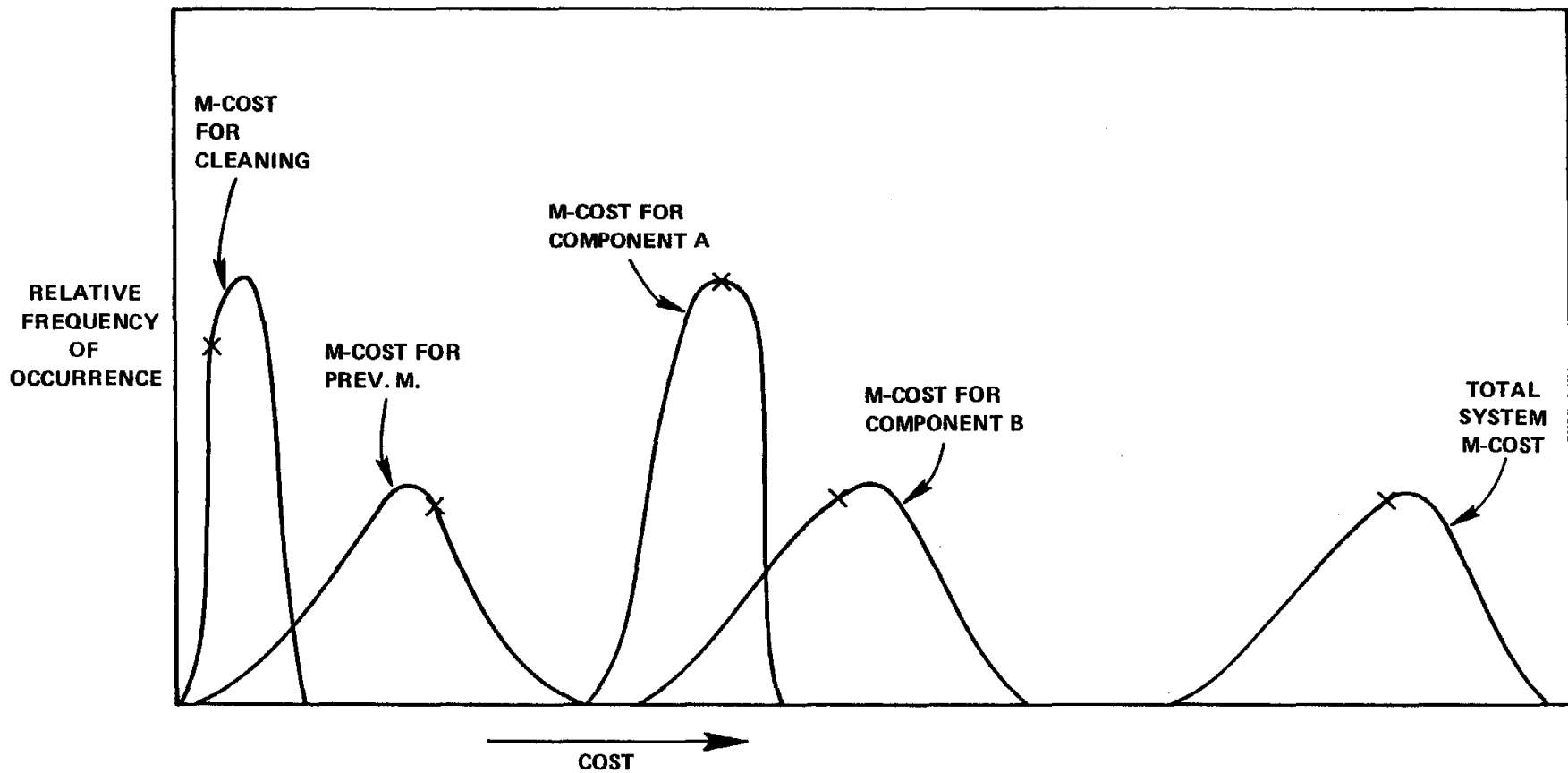


FIGURE 36. MAINTENANCE COST FREQUENCY DISTRIBUTIONS FOR COMPONENTS, GENERAL MAINTENANCE ACTIVITIES AND THE SYSTEM

If this were the case, a change in the number or timing of inverter failures in the simulation could result in changes in the number or timing of failures which occur to other components. This reduces the usefulness of the results since it is unlikely that the insertion of a more reliable inverter into a real system would affect such unrelated phenomena as failures of the control subsystem or utility outages. A single run of Phase 1 is, in some cases, sufficient to show a difference between the base case and the test case. The result, however, would be subject to the cumulative random deviation of all event types attached to the random number stream of the component being tested.

Two methods exist for reducing or explaining this random variation. The first is the reassignment of random number streams (Phase 2); and, the second is multiple runs (Phase 3). Normally it will be less expensive for a user who understands the software of SOLREL to proceed first to Phase 2 and then to Phase 3. For a user who is unfamiliar with either Fortran programming in general or the SOLREL software in particular, Phase 2 should be skipped and multiple runs performed. Figure 35 showed the decision process of selecting the proper sequence of tests. Using the previous example of a more reliable inverter, Phase 2 would involve the assignment of a single random number stream solely to generate inverter failure times and another stream solely to generate inverter repair times. With this adjustment, all other components would operate as they did previously in the base case independent of changes made to the inverter. What Phase 2 does in terms of the diagram (Figure 36) is first to run a base case where a point from each of the lower four curves results. Assume for the moment that Component A is the inverter. The points for the base case run for Component B, for Preventive Maintenance, and for Cleaning are then held fixed while tests are run on Component A. This reduces the variation to that of Component A only (see Figure 37). When comparisons are made between two simulation runs, this method limits the sources of random variation to that caused by the random number streams for inverter failure and repair. Although Phase 2 eliminates some random variation, it may not adequately describe that which still exists.

The best way to explain this remaining random error is to define the distribution of results. This can be accomplished only by employing multiple runs (Phase 3). In other words, a new set of random number streams should be

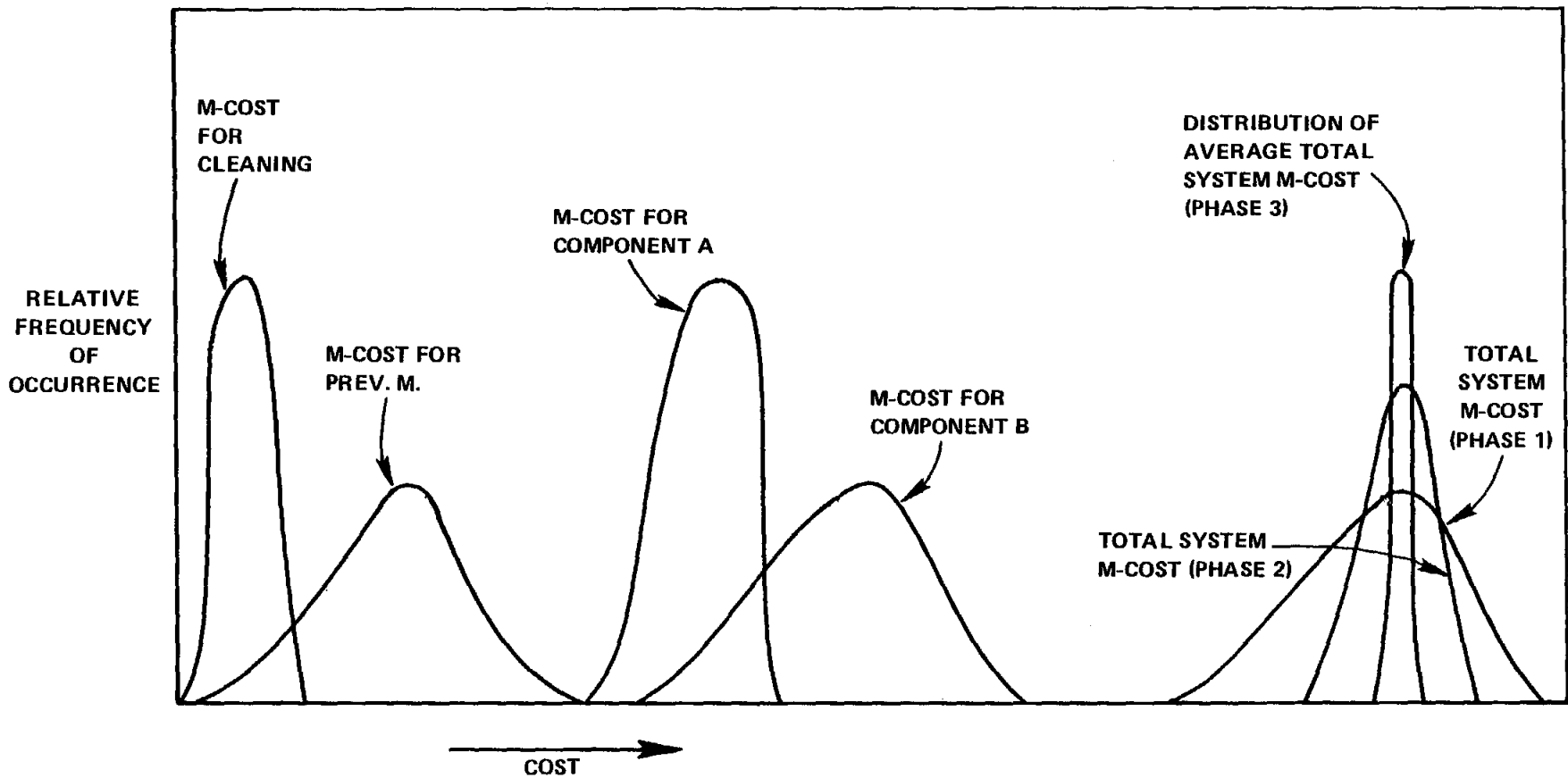


FIGURE 37. MAINTENANCE COST FREQUENCY DISTRIBUTION, SHOWING EFFECT OF MULTIPLE RUNS ON VARIABILITY OF COSTS AND THE MEAN

defined for each run by changing the GASP data card containing the random number seeds. The larger the number of runs the better defined will be the distribution of results and the more precise will be the estimate of the mean result. As the number of runs becomes large, a much tighter confidence interval around the mean can be drawn. Additional runs will also yield a better understanding of the distribution of individual results although the confidence interval for individual results could grow, shrink, or remain the same. In effect, the average total system maintenance cost curve shown in Figure 37 has been identified, allowing the designer to reduce variance in the mean to whatever extent necessary.

Flat-Panel--Test for More Reliable Inverter

The initial sensitivity analysis to consider a more reliable (and higher cost) inverter was a Phase 1 test where one random number stream was defined for all component failures and another one defined for all repair times. The optimistic case (discount rate 13 percent) was selected. The 50 kW inverter MTBF was extended from 12 to 32.4 months, and the initial inverter cost increased from \$15,500 to \$26,750, as estimated early in this report. Table 32 shows a levelized maintenance cost of 2.28 ¢/kWh for the less reliable inverter system and 1.57 ¢/kWh for the more reliable one. A relatively high random error in the cost of \$9,023 (13.8 percent) occurred. It was calculated as follows. The more reliable inverter should fail $360/32.4 = 11.1$ times in 30 years. The less reliable inverter is expected to fail 30 times in 30 years or an additional $(30 - 11.1) 18.9$ times. The expected repair cost per inverter failure is approximately $\$300 + (\$24)(\$40) = \$1,260$. Thus, the expected additional maintenance cost of the less reliable inverter would be $(1260)(18.9) = \$23,800$. Since the actual run created a maintenance cost savings of $\$98,338 - \$65,515 = \$32,823$, the estimated random error is $\$32,823 - \$23,800 = \$9,023$.

In an attempt to reduce this random error, a single random number stream was assigned to inverter failures and another to inverter repairs. This technique is most effective when the random error is caused primarily by components other than the inverter. Unfortunately, in the flat panel system, the bulk of the unscheduled maintenance cost is due to repairs of the inverter.

TABLE 32. FLAT PANEL, SUMMARY OF TESTS FOR MORE RELIABLE INVERTER
1/2 SYSTEM (51 kWp)

MTBF, months	Lifetime Maint. Cost	Initial Cost	Estimated Savings in Maint. Cost	Savings in Maint. Cost Stimulation Results	Estimated Random Error in Cost	Lifetime Output, 1000 kWh	Levelized Maint. Cost, ¢/kWh	Life-Cycle Energy Cost, ¢/kWh
<u>One Random Number Stream for All Failures and One for All Repairs (Discount Rate = 13%)</u>								
12	\$98,338	\$306,000*	-	-	-	3.021	2.28	
32.4	65,515	317,247	\$23,800	\$32,823	-\$ 9,023 -13.8%	3.036	1.57	
<u>One Random Number Stream for Inverter Failures and One For Inverter Repairs (Discount Rate = 13%)</u>								
12	108,856	306,000	-	-	-	2.997	2.58	7.04
32.4	71,673	317,247	23,800	37,183	-\$13,360 -18.6%	3.029	1.73	6.67
<u>(Discount Rate = 20%)</u>								
12	108,856	306,000	-	-	-	2.997	2.57	9.49
32.4	71,673	317,247	23,800	37,183	-\$13,360 -18.6%	3.029	1.82	9.27

123

*For a 51 kW system at \$6/W_p.

In fact (see Table 32), the estimated random error actually increased to \$13,360 under these Phase 2 conditions. Therefore, for this case, a single Phase 2 run offers no improvement over a Phase 1 run. For the Phase 2 run, the levelized life-cycle energy cost of the less reliable system was 7.04 ¢/kWh compared to 6.67 ¢/kWh (6.80 ¢/kWh when adjusted for the estimated random error) for the more reliable system. Note that a relatively large percent random variation in inverter repair costs (18.6 percent) causes a much smaller percent variation when applied to the total system lifetime cost ($\frac{6.80-6.67}{6.80} = 1.9$ percent). Based on these figures, the designer should

select the more reliable inverter. A second Phase 2 run using the same random number streams with a 20 percent discount rate (pessimistic case) also showed a preference for the more reliable system, 9.27 (9.41 adjusted for random error) ¢/kWh to 9.49 ¢/kWh.

A higher discount rate tends to emphasize the initial expenditure and deemphasize maintenance expense. Therefore, the more reliable inverter becomes a somewhat less attractive alternative. Since the decision is less certain in the 20 percent present case, and since the run produced a high random error, this case was selected for multiple runs. Table 33 shows the results of 10 additional base case runs (each with a different set of random number streams) of the less reliable inverter system (MTBF=12.0) with a 20 percent discount rate. Table 34 is the identical set of runs with the more reliable inverter (MTBF=32.4). For the system with the less reliable inverter, the average maintenance cost was \$94,109, which can be expected to vary from \$87,137 to \$101,081. Any single run, however, could vary from \$71,732 to \$116,486 (95 percent confidence). Confidence intervals are calculated in the following manner:

$$\text{Confidence interval on mean} = \bar{X} \pm t_{.975,11} \frac{S}{11}$$

where

$$t_{.975,11} = 2.201 \text{ (from standard tables).}$$

For the lifetime maintenance cost in Table 33, the average cost or \bar{X} is \$94,109 with a standard deviation of 11,417.

TABLE 33. FLAT PANEL - TEST FOR MORE RELIABLE INVERTER, MTBF = 12 MONTHS,
DISCOUNT RATE = 13 PERCENT

One random number stream for inverter repairs and one for
inverter failures

MTBF, months	Run #	Lifetime Maint. Cost	Initial Cost	Est Savings in Maint. Cost	Simulated Savings in Maint. Cost	Lifetime Output, 1000 kWh	Levelized Maint. Cost ¢/kWh	Life-Cycle Energy Cost, ¢/kWh
12	1	\$88,917	\$306,000	-	-	3.022	2.36	9.35
12	2	85,041	"	-	-	3.019	2.19	9.25
12	3	74,706	"	-	-	3.030	1.93	9.06
12	4	104,676	"	-	-	3.010	2.56	9.49
12	5	96,076	"	-	-	3.019	2.42	9.36
12	6	113,983	"	-	-	3.004	2.60	9.52
12	7	91,237	"	-	-	3.011	2.18	9.26
12	8	85,899	"	-	-	3.018	2.36	9.35
12	9	90,534	"	-	-	3.023	2.10	9.16
12	10	95,273	"	-	-	3.009	2.29	9.34
12	11*	108,856	"	-	-	3.029	2.57	9.49

\bar{x} = \$94,109

s = 11,417

\bar{x} = 3.0147

s = .0095

\bar{x} = 2.32

s = .212

\bar{x} = 9.33

s = .142

95% Conf \$71,732 - \$116,486 (normal distribution)
On obs. \$86,532 - \$101,685 (studentized t dist.)
On Mean

95% Conf 2.996 - 3.033
On Mean 3.008 - 3.021
1.90 - 2.74
2.18 - 2.46
9.05 - 9.61
9.24 - 9.42

* Run 11 was base run

TABLE 34. FLAT PANEL - TEST FOR MORE RELIABLE INVERTER, MTBF = 32.4 MONTHS,
DISCOUNT RATE = 20 PERCENT

One random number stream for inverter repairs and one for
inverter failures

MTBF, Months	Run #	Lifetime Maint. Cost	Initial Cost	Est. Savings in Maint. Cost	Simulated Savings in Maint. Cost	Estimated Random Error	Lifetime Output, 1000 kWh	Levelized Maint. Cost ¢/kWh	Life-Cycle Energy Cost, ¢/kWh
32.4	1	\$73,814	\$317,247	\$23,800	\$15,103	\$8697 11.8%	3.033	1.85	9.30
32.4	2	70,537	"	"	14,504	9296 13.1%	3.029	1.66	9.18
32.4	3	58,876	"	"	15,830	7970 13.5%	3.041	1.52	9.07
32.4	4	69,480	"	"	35,196	-11396 -16.4%	3.030	1.79	9.26
32.4	5	73,596	"	"	22,480	1320 1.8%	3.034	1.87	9.28
32.4	6	71,942	"	"	42,041	-18241 -25.4%	3.033	1.84	9.30
32.4	7	68,595	"	"	22,642	1158 1.7%	3.028	1.63	9.17
32.4	8	74,596	"	"	11,303	12497 16.8%	3.024	1.81	9.29
32.4	9	68,977	"	"	21,557	2243 3.3%	3.030	1.52	9.09
32.4	10	69,570	"	"	25,703	-1903 -2.7%	3.024	1.69	9.22
32.4	11*	71,673	"	"	37,183	-13360 -18.6%	3.029	1.82	9.27

\bar{x} = \$70,150
s = 4271

\bar{x} = 3.030
s = .0048

\bar{x} = 1.727
s = .130

\bar{x} = 9.22
s = .083

95% Conf \$61,779 - \$78,521
on obs \$67,743 - \$72,557
on Mean

95% Conf 3.021 - 3.089
Int
On obs. 1.47 - 1.98
On Mean 1.65 - 1.80
9.06 - 9.38
9.18 - 9.26

*Run 11 was base run

The 95 percent confidence interval on the mean becomes:

$$\begin{aligned} & \$94,109 \pm \frac{(2.201) (11.417)}{11} = \\ & \$94,109 \pm \$7576.6 = \\ & \$86,532 \text{ to } \$101,685. \end{aligned}$$

One would expect confidence intervals on the mean of 11 observations to be smaller than the confidence interval on any single observation which could occur. The following procedure shows how this confidence interval is calculated when a normal distribution of observations is assumed.

$$\text{Confidence interval on next observation} = \bar{X} \pm N_{.975} S$$

where

\bar{X} = average or mean of all observations

S = sample standard deviation

$N_{.975}$ = deviate from standard normal distribution = 1.96.

Again using the sample of the lifetime maintenance cost in Table 33, the confidence interval on the next observation becomes

$$\begin{aligned} & \$94,109 \pm (1.96) (11.417) \\ & = \$94,109 \pm 22,377 \\ & = \$71,732 \text{ to } \$116,486. \end{aligned}$$

The electrical output is much less variable with a mean of 3.015×10^6 MWh and a range from 3.009 to 3.020×10^6 MWh. The levelized maintenance cost averaged 2.32 ¢/kWh with a 95 percent confidence interval of 2.18 to 2.46 ¢/kWh. The average levelized life-cycle energy cost was 9.22 ¢/kWh for the more reliable inverter and 9.33 ¢/kWh for the less reliable one. Again, the confidence interval for a single run will be larger. Similar statistics are shown in Table 34 for the case of the more reliable inverter.

An additional inverter alternative was then tested to see whether an even more reliable inverter might be optimal. The first set of runs (see Table 35) was for an inverter with MTBF=64.8 months (20,000 operating hours) and cost of \$39,180. It is recognized that this high an extrapolation of MTBF and costs is theoretical only and is not likely to be practical at the present

TABLE 35. FLAT PANEL - TEST FOR MORE RELIABLE INVERTER, MTBF = 64.8 MONTHS,
DISCOUNT RATE = 20 PERCENT

One random number stream for inverter repairs

Months MTBF	Run #	Lifetime Maint. Cost	Initial Cost	Est in Maint. Cost	Sim. Results Savings in Maint. Cost	Est. Random Error Cost	Lifetime Output 10 MWH	Levelized Maint. Cost ¢/kWh	Life-Cycle Energy Cost ¢/kWh
64.8	1	\$67,347	\$329,680	\$30,800	\$21,570	\$9230 13.7%	3.039	1.65	9.48
64.8	2	64,205	"	"	20,836	9964 15.5%	3.033	1.50	9.40
64.8	3	54,919	"	"	19,787	11,013 20.0%	3.045	1.40	9.31
64.8	4	66,920	"	"	37,756	-6956 -10.4%	3.034	1.59	9.44
64.8	5	68,075	"	"	28,001	2799 4.1%	3.041	1.72	9.50
64.8	6	64,288	"	"	49,695	-18895 -29.4%	3.039	1.66	9.48
64.8	7	61,513	"	"	29,724	1076 1.7%	3.036	1.46	9.37
64.8	8	66,328	"	"	19,571	11,229 16.9%	3.030	1.54	9.43
64.8	9	60,511	"	"	30,023	777 1.3%	3.040	1.38	9.31
64.8	10	61,188	"	"	34,085	-3285 -5.3%	3.034	1.55	9.44
64.8	11	62,067	"	"	46,789	-15,989 -25.8%	3.032	1.66	9.49

128

\bar{X} = \$63,396	\bar{X} = 3.037	1.555	9.42
S = 3877.35	S = .0045	.122	.068
95% Conf on Mean = \$61,105 - \$65,687	95% Conf on Obs = 3.028 - 3.046	1.34 - 1.77	9.29 - 9.55
95% Conf on OBS = \$54,862 - \$71,930	95% Conf on Mean = 3.034 - 3.040	1.48 - 1.63	9.38 - 9.47

time. The results showed an average levelized life-cycle energy cost of 9.42 ¢/kWh, higher than for the MTBF=32.4 inverter (9.22 ¢/kWh).

Next, an inverter with MTBF=24.0 and cost = \$22,689 was tested. This resulted in the lowest levelized life-cycle energy cost of any of the four alternatives. The results appear in Table 36 and Figure 38.

Table 37 compares the four inverter alternatives in terms of levelized life cycle energy cost (LLEC). Figure 38 shows the same results graphically. The two best alternatives (MTBF=32.4 and 24.0) can be compared statistically. Their differences for all 11 runs appear in Table 37. The average difference as well as the confidence intervals on the mean and individual observation are both useful in judging whether or not the difference between the two alternatives is significant:

$$\bar{X} = .0273 \quad (\text{MTBF}=24) - (\text{MTBF}=32.4)$$

$$S = .0184.$$

95% confidence interval on mean: .0092 to .0453.

95% confidence interval on next observation: -.0090 + .0635.

These results indicate that on average the MTBF=24 inverter yields a levelized life cycle energy cost which is .0273 ¢/kWh lower than the MTBF=32.4 system. The 95 percent confidence interval on the mean indicates that for any set of 11 trials, it is highly unlikely that the MTBF=32.4 system will ever outperform the MTBF=24.0 system. The confidence interval on the next observation shows a possibility of a negative result. This indicates that for any single run, it is possible for the MTBF=32.4 system to do better than the MTBF=24.0 run. The probability of this occurring is calculated as follows:

$$P\left(\begin{array}{l} \text{LLEC} \\ 32.4 \text{ system} < 24.0 \text{ system} \end{array}\right) =$$

$$\frac{\bar{X}}{S} = N_{.5-\alpha} \text{ where } N \text{ is the standardized normal deviate}$$

$$\frac{.0273}{.0184} = 1.475 = N_{.5-\alpha}$$

From standardized normal tables $.5-\alpha = .430$. There $\alpha = .070$. In other words, there is only an 7 percent chance that for any single run the MTBF=32.4 system will outperform the MTBF=24.0 system.

TABLE 36. FLAT PANEL - TEST FOR MORE RELIABLE INVERTER, MTBF = 24 MONTHS,
DISCOUNT RATE = 20 PERCENT

One random number stream for inverter repairs.

MTBF, Months	Run #	Lifetime Maint. Cost	Initial Cost	Est Savings in Maint Cost	Simulated Savings in Maint. Cost	Est. Random Error in Cost	Lifetime Output	Levelized Maint. Cost ¢/kWh	Life-Cycle Energy Cost, ¢/kWh
24.0	1	\$77,634	\$313,189	\$18,900	\$11,283	\$7,617 9.8%	3.034	1.96	9.25
24.0	2	72,301	"	"	12,740	6,160 8.5%	3.028	1.77	9.15
24.0	3	63,324	"	"	11,382	7,518 11.9%	3.038	1.60	9.03
24.0	4	82,140	"	"	22,536	-3,636 -4.4%	3.022	1.96	9.28
24.0	5	80,768	"	"	15,308	3,592 4.4%	3.030	1.99	9.26
24.0	6	77,150	"	"	36,833	-17,933 -23.2%	3.034	1.96	9.26
24.0	7	73,511	"	"	17,726	1,174 1.6%	3.027	1.75	9.14
24.0	8	75,405	"	"	10,494	8,406 11.1%	3.026	1.95	9.27
24.0	9	76,174	"	"	14,360	4,540 6.0%	3.030	1.64	9.05
24.0	10	72,748	"	"	22,525	-3,625 -5.0%	3.025	1.80	9.19
24.0	11	74,506	"	"	34,350	-15,450 -20.7%	3.023	1.94	9.25

\bar{X} = \$75,060
 S = 4,985
 95% Conf. Int
 Mean = \$71,752 - 78,368
 Obs. = 65,290 - 84,830

\bar{X} = 3.0288
 S = .00498
 95% Conf. Int
 Mean = 3.026 - 3.032
 OBS = 3.024 - 3.034

1.85
 .1412
 1.76 - 1.93
 1.57 - 2.12

9.19
 .0898
 9.13 - 9.25
 9.02 - 9.37

TABLE 37. COMPARISON OF SYSTEM LEVELIZED LIFE-CYCLE ENERGY COST
(¢/kWh) FOR ALTERNATIVE INVERTERS

Run #	MTBF = 12 Months	MTBF = 24.0 Months	MTBF = 32.4 Months	MTBF = 64.8 Months	Difference Between Two Best Alternatives
1	9.35	9.25	9.30	9.48	+.05
2	9.25	9.15	9.18	9.40	+.03
3	9.06	9.03	9.07	9.31	+.04
4	9.49	9.28	9.26	9.44	-.02
5	9.36	9.26	9.28	9.50	+.02
6	9.52	9.26	9.30	9.48	+.04
7	9.26	9.14	9.17	9.37	+.03
8	9.35	9.27	9.29	9.43	+.02
9	9.16	9.05	9.09	9.31	+.04
10	9.34	9.19	9.22	9.44	+.03
11	9.49	9.25	9.27	9.49	+.02

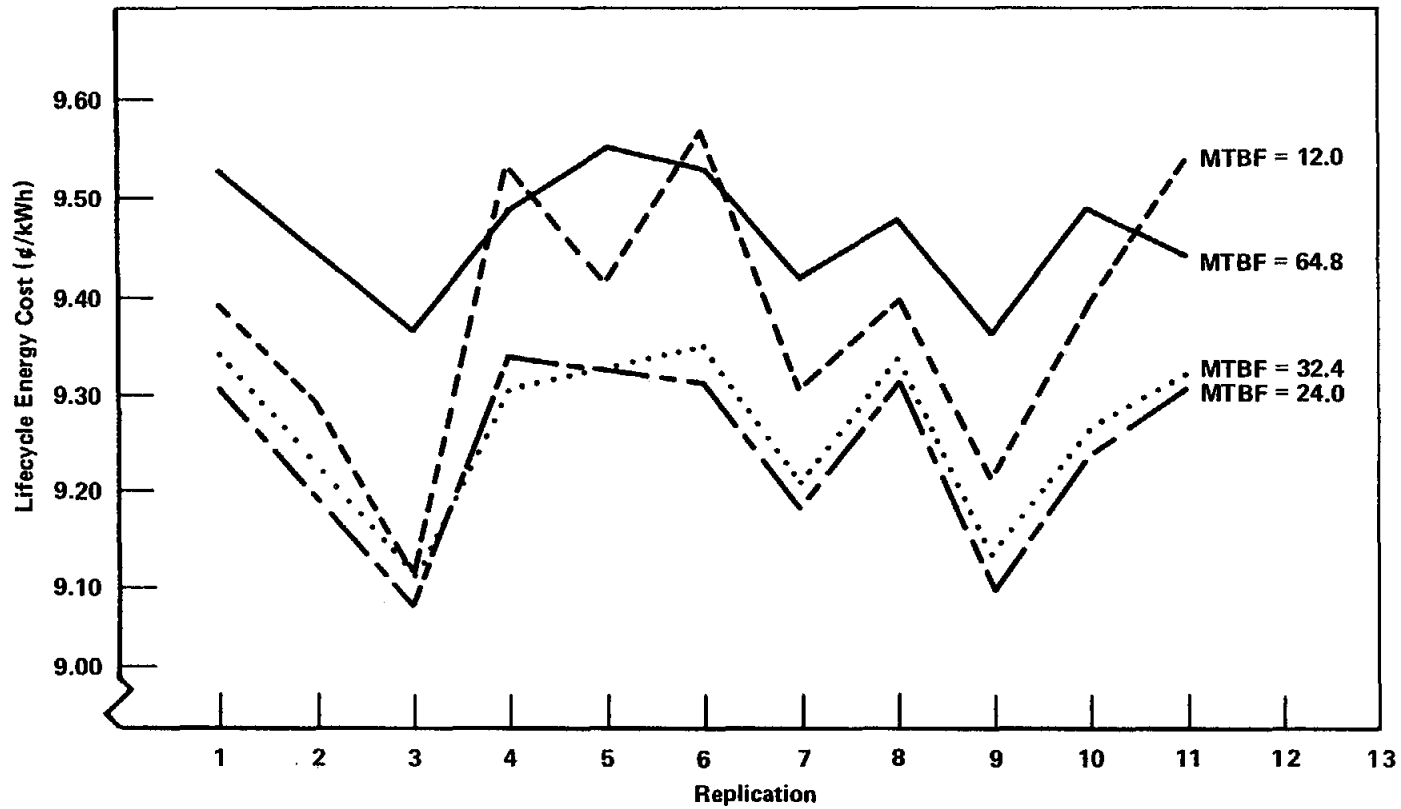


FIGURE 38. TEST FOR OPTIMUM INVERTER RELIABILITY, FLAT-PANEL SYSTEM, DISCOUNT RATE = 20 PERCENT

Flat-Panel--Test for Cleaning Intervals

Table 38 shows the results of the flat panel system being tested for array cleaning intervals of 6, 12, 18, 24, and 36 months respectively. A discount rate of 13 percent (optimistic case) was used. A random number stream was defined for all preventive maintenance times without special consideration of cleaning (Phase 1). Table 39 shows a similar set of results when the cleaning activities are assigned to a unique random number stream (Phase 2 Method). The estimated random errors have been reduced as expected. The recommended cleaning interval which minimizes maintenance cost is somewhere between 24 and 36 months (see Figure 39). Maintenance expense is tax deductible in a commercial system, however, which provides an incentive to clean the system more often. As a result, the levelized life-cycle energy cost is minimized when cleaning occurs close to every 12 months (See Table 39 and Figure 39).

Passively Cooled Concentrator-- Test for Cleaning Intervals

Both Phase 1 and 2 runs were made for cleaning intervals of 6, 9, (Phase 1 only) 12, 18, 24, and 30 (Phase 2 only) months, respectively for the passively cooled concentrator system. A discount rate of 13 percent (optimistic case) was used. The results appear in Tables 40 and 41. Again, levelized maintenance cost is minimized when cleaning occurs every 18 to 24 months (2.09 ¢/kWh see Figure 40). Due to the tax deductibility of maintenance expense, levelized life cycle energy cost is minimized when cleaning is initiated every 12 to 18 months (6.30 ¢/kWh).

Sensitivity Analysis Using the State Space Methodology

The purpose of this section is to illustrate how the state space model can be used to perform sensitivity analyses on the PV systems examined. In the state space model, the system's output, P (expressed in kW per 30 years), is expressed as a function of the following parameters:

- W, the nominal system capacity in watts

TABLE 38. FLAT PANEL - SIMULATION RUNS TO TEST FOR CLEANING INTERVAL EFFECT ON LIFE-CYCLE ENERGY COSTS, DISCOUNT RATE = 13 PERCENT
Random number stream defined for all preventive maintenance.

Cleaning Interval	Lifetime Maint	Estimated Add. Cleaning Cost @ \$320/Cleaning	Additional* Cleaning Cost Stimulation Results	Estimated Random Error in Cost	Lifetime Output (1000 kWh)	Levelized Maintenance Cost (¢/kWh)	Life-Cycle Energy Cost, (¢/kWh)
6	\$116,835	\$14,400	\$21,910	7510 6.4%	3.042	2.66 ^(2.49)	7.01 (6.94)
12	98,338	4,800	3,413	-1387 -1.4%	3.029	2.28 ^(2.31)	6.82 (6.83)**
18	92,798	1,600	-2,127	-3727 -4.0%	2.997	2.15 ^{(2.24)**}	
24 (Base Period)	94,925	-	-	- -	2.976	2.24 ^(2.24)	
36	92,883	-1,600	-2,042	-442 -0.5	2.930	2.22 ^(2.23)	

* With reference to 24 month interval. (Values in parentheses are adjusted for estimated random error.)

** Minimum.

TABLE 39. FLAT PANEL - SIMULATION RUNS TO TEST FOR CLEANING INTERVAL EFFECT ON LIFE-CYCLE ENERGY COSTS, DISCOUNT RATE = 13 PERCENT
Random number stream isolated for cleaning.

Cleaning Interval, Months	Lifetime Maint. Cost	Estimated Additional Cleaning Cost @ \$320/Cleaning	Additional Cleaning Cost Simulation Results	Estimated Random Error in Cost	Lifetime Output, 1000 mWh	Levelized Maintenance Cost ¢/kWh	Life-Cycle Energy Cost, ¢/kWh
12	\$98,338	\$6,400	\$5,455	-945 -1.0%	3.021	2.28(2.30)	6.82*(6.83)
18	98,358	3,200	5,475	+2275 +2.3%	2.997	2.30(2.25)	6.87(6.85)
24	95,666	1,600	2,783	+1183 +1.2%	2.976	2.25(2.22)	6.88(6.87)
36	92,883	-	-	- -	2.930	2.22(2.22)	6.94(6.94)

* Values in parentheses are adjusted for estimated random error.

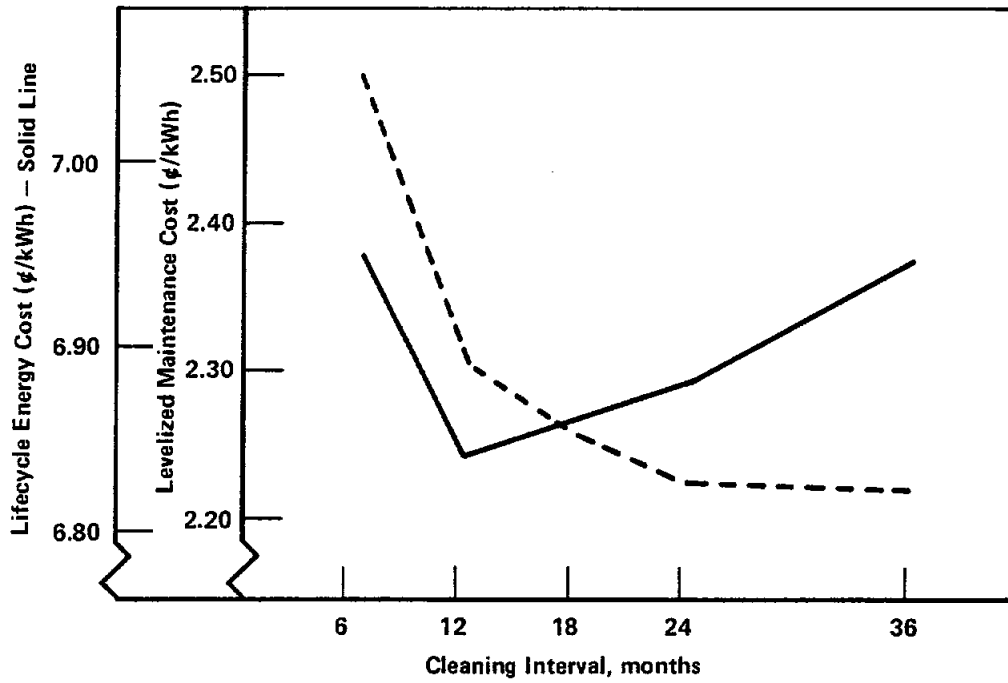


FIGURE 39. TEST FOR CLEANING INTERVALS FLAT-PANEL SYSTEM, DISCOUNT RATE = 13 PERCENT

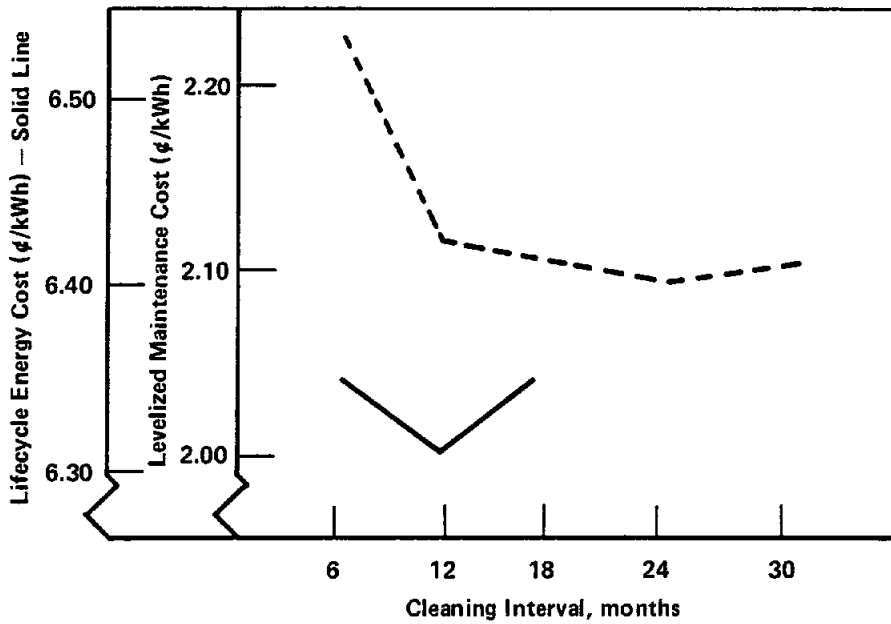


FIGURE 40. TEST FOR CLEANING INTERVALS PASSIVELY COOLED CONCENTRATOR SYSTEM, DISCOUNT RATE = 13 PERCENT

TABLE 40. PASSIVELY COOLED CONCENTRATOR-SIMULATION RUNS TO TEST FOR
CLEANING INTERVAL EFFECT ON LIFE-CYCLE ENERGY COSTS,
DISCOUNT RATE = 13 PERCENT

Random number stream defined for all preventive maintenance.

Cleaning Interval, Months	Lifetime Maint. Cost	Estimated Add. Cleaning Cost @ \$800/Cleaning	Additional Cleaning Cost Simulation Results	Estimated Random Error in Cost		Lifetime Output, 1000 kWh	Levelized Maintenance Cost, ¢/kWh	Life-Cycle Energy Cost, ¢/kWh
6	\$470,054	\$36,000	\$37,789	\$1789	0.4%	16.268	2.14(2.13)	6.29(6.29)
9	434,803	20,000	2,538	-17462	-4.0%	16.209	1.98(2.06)	
12	454,423	12,000	22,158	10158	2.2%	16.154	2.10(2.05)	6.30(6.28)
18	457,551	4,000	25,286	21286	4.7%	16.027	2.12(2.02)	
24	432,265	-	-	-	-	16.908	2.01(2.01)	

Values in parenthesis are adjusted for estimated random error.

TABLE 41. PASSIVELY COOLED CONCENTRATOR-SIMULATION RUNS TO TEST FOR CLEANING INTERVALS EFFECT ON LIFE-CYCLE ENERGY COSTS, DISCOUNT RATE = 13 PERCENT

Random number stream defined for cleaning only.

Cleaning Interval, Months	Lifetime Maint. Cost	Estimated Add. Cleaning Cost @ \$800/Cleaning	Additional Cleaning Cost Simulation Results	Estimated Random Error in Cost	Lifetime Output, 1000 mWh	Levelized Maintenance Cost, ¢/kWh	Life-Cycle Energy Cost, ¢/kWh
6	\$493,800	\$32,000	\$39,480	7480 1.5%	16.264	2.25(2.22)	6.35(6.34)
12	461,772	8,000	7,452	- 548 -0.1%	16.154	2.11(2.11)	6.30 (6.30)
18	454,320	-	-	- -	16.018	2.10(2.10)	6.34(6.34)
24	451,697	- 4,000	- 2,623	1377 0.3%	15.912	2.10 (2.09)	
30	448,140	- 6,400	- 6,180	220 -0.05%	15.776	2.10(2.10)	

Values in parentheses are adjusted for estimated random error.

- β , the expected system capacity fraction (from state space model)
- DP, the system permanent degradation factor
- I, the equivalent hours of full insolation during the given period
- D, the system degradation factor resulting from dirt accumulation.

To evaluate the effects of changes in any of these factors on the system, the state space methodology is exercised with modified factors to determine the resulting changes in the system's output and maintenance costs. The systems used were those described in detail in Volume 2.

Table 42 shows some typical changes affecting the above parameters and the required computations in the state space model.

Table 43 presents the result of the sensitivity analysis for changes in size and connection of two inverters in each of the three systems examined (in Volume 2). The alternative system designs using these inverters are as follows:

- Case 1: Both inverters are rated at 60 percent of the nominal system capacity and are operating in an active-redundancy mode.
- Case 2: Both inverters are rated at 80 percent of the nominal system capacity and are operating in an active-redundancy mode.
- Case 3: Both inverters are rated at 100 percent of the nominal system capacity, but are operating in a standby-redundancy mode.

The marginal cost/kWh given in the table (in current value dollars) is computed as the ratio of the additional maintenance costs (resulting from adding an inverter implement the described operating mode) to the increase in power production for that same operating mode. This marginal cost/kWh does not include any capital expenditure (such as the purchase of a larger or an additional inverter).

It can be seen from Table 43 that the original system is as low in maintenance cost per kWh or lower than most of the cases considered. A very slight advantage exists in all alternatives for the Lea County System. Even though this example does not recommend design changes, it does exhibit the use of the methodology in sensitivity analyses.

TABLE 42. POTENTIAL CHANGES IN SYSTEM'S INPUT DATA
AND THEIR EFFECTS ON STATE SPACE MODEL

Changes	Computation Requirements (Effects)
Components failure/repair rates	Recompute subsystem state probabilities and expected system capacity, β
Components logical configuration	Recompute subsystem state probabilities and expected system capacity, β
Change in inverter rating/other component rating	Recompute system expected capacity, β
Cleaning frequency (interval between cleaning = n months)	Recompute total annual insolation hours, given profile of degradation due to dirt (e.g., degradation rate)
Permanent degradation/degradation due to cell failures--rate or profile	Recompute annual power production
(ALL THE ABOVE CHANGES WILL REQUIRE THAT THE ANNUAL POWER PRODUCTION BE RECOMPUTED)	
Repair costs	Recompute maintenance costs
Frequency of preventive maintenance	Recompute maintenance costs

TABLE 43. RESULTS OF CHANGES IN INVERTER LOGICAL CONFIGURATION ON ALL THREE SYSTEMS

	BDM** System	Lea County System	APS** System
Original System			
β	0.964267	0.989419	0.959736
Maintenance cost, ¢/kwh (current value)	8.54***	3.24	2.63
Case 1 (Each inverter at 60%, active)			
β	0.966005	0.991280	0.961186
% change in production, 30 years	0.18	0.19	0.15
Marginal maintenance cost, ¢/kwh	882.2	0	256.2
New maintenance cost, ¢/kwh	10.11	3.23	3.01
Case 2 (Each inverter at 80%, active)			
β	0.969641	0.995011	0.964799
% change in production, 30 years	0.56	0.57	0.53
Marginal maintenance cost, ¢/kwh	285.2	0	73.4
New maintenance cost, ¢/kwh	10.7	3.22	3.00
Case 3 (Standby inverter at 100%)			
β	0.973352	0.998827	0.968486
% change in production	0.94	0.95	0.91
Marginal maintenance cost, ¢/kwh	3.4	0	0.58
New maintenance cost, ¢/kwh	8.49	3.21	2.61

*Capital costs for additional inverters are not included.

**The BDM and APS systems will require an additional inverter each, since these two systems initially have only one inverter. However, the Lea County System's inverters are each rated at 50% of nominal system capacity.

***Thermal output not included in computations for BDM.

General Discussion--Sensitivity Analyses

In this section, only two of numerous design questions have been addressed, namely the optimal cleaning internal and optional inverter design. (A summary of the types of runs performed appears in Table 44.) The SOLREL model however, can perform similar analyses on any of the components or on any of the maintenance strategies. It can also test the sensitivity of the various degradation assumptions. In fact, the sensitivity of any parameter which enters through a data card can be tested to aid the system designer in his search for the optimal system.

It is recognized, of course, that these examples are conducted on systems that are in final design and have already been optimized through various techniques. Also, the failure rates assumed are sometimes optimistic. As a result, the absolute changes in LEC are small especially in the cases of changing inverter costs and reliability. This would not be the case if the analysis started with higher inverter failure rates. These examples are done strictly to demonstrate the techniques.

The state space model is useful to quickly assess changes in system configuration, as shown.

The extent of the optimization attempted is, of course, limited by the accuracy and reality of the input cost, performance, and reliability data used.

TABLE 44. TESTS RUN USING SOLREL TO INVESTIGATE RANDOM ERRORS

Test No.	System	Discount Rate, percent	Test	Phase 1	Phase 2	Phase 3
1	Flat Panel	13	Inverter MTB = 12, 32.4 months	X	X	
2	Flat Panel	20	Inverter MTBF = 12, 24, 32.4, 64.8 months		X	X
	Flat Panel	13	Cleaning Interval = 8, 12, 18, 24, 36 months	X	X	
	Passively Cooled Concentrator	13	Cleaning Interval = 6, 9, 12, 14, 24 months	X	X	

143 and 144

CONCLUSIONS AND RECOMMENDATIONS

CONCLUSIONS AND RECOMMENDATIONS

The program provides useful procedures and models of reliability/availability to be combined with economic analyses of PV systems which will aid the PV system designer in minimizing life-cycle energy costs. Interfaces with existing design models such as PV system design simulations and the JPL Flat-Plate PV Module and Array Circuit Design Optimization Methodology are also featured. This will permit more alternative designs to be considered by evaluating the economic effect of changes in initial equipment costs to improve reliability. The economic effect of varying maintenance strategies can also be tested.

The attention given reliability during the various stages of design of a PV system should assure that proper tradeoffs, allowances, and plans are made and that the resulting system designs will be balanced from the performance/availability/cost viewpoint.

Experience gained during the program has reemphasized the fact that few reliability/maintenance cost data are available for PV components and subsystems. A vital output from the ongoing photovoltaic application experiments ("PRDA's"), once their system early-life "infant mortality" period is over, should be a wealth of data needed in these areas.

The form of the input data used in this program should provide a definition of the kind of reliability and maintainability data which should be collected from the PRDA system experiments after the performance of the systems stabilizes. The usefulness of such data in guiding future PV designs would thus be maximized.

This program was the first known to use the JPL Flat-Plate PV Module and Array Circuit Design Optimization Methodology to model concentrator systems. The curves available in the handbook for this technique were designed for flat-plate arrays. Thus, the number of cells in series-parallel connections and bypass diodes were representative of flat-plate systems. Using them to model concentrator arrays requires some interpolation. It is recommended that the JPL computer program which generated the curves used in the analyses be rerun for series-parallel cell connections and bypass diodes that are typical of concentrator systems.

The establishment of realistic reliability levels for subsystem specifications are expected to be more readily accomplished through the use of these methodologies. Iteration of subsystems reliability goals and their effect on systems can be ascertained and the most practical combination chosen.

The models, although designed in this study for intermediate-sized systems, can be altered slightly to become applicable to large utility-sized systems in one direction, and to small residential or remote systems in the other direction. For both systems, different tax-related economic considerations would apply than are used in intermediate industrial/commercial PV systems. However, the basic structure of the availability and economic computer models developed would require only minor alteration for them to be useful in evaluating these other systems.

Other activities that should be performed in the future are partially dependent on the development of appropriate field-experience data. The simulation methodology has the ability to deal with reliability data on lower (more detailed) system levels than at the subsystem levels currently demonstrated. It can also handle many more statistical distributions of part/component failures than the two used in the simulations to date (exponential and Weibull).

Additional experiments should be performed to further develop and demonstrate the methods. Activities such as "test-analyze-and-fix" should be conducted on new PV systems and subsystems. These tests, in conjunction with reliability models, can help the designer find weak reliability points in the design, which can then be modified to evolve a product that meets all reliability and life-cycle energy cost requirements.

REFERENCES

- (1) Burgess, E. L., Sandia Labs, and Walker, E. A., Special Programs Div., Dept. of Energy, "Summary of Photovoltaic Applications Experiments Designs", 10/79 (ALO-71).
- (2) Ross, R. G., "Flat-Plate Photovoltaic Array Design Optimization", 14th IEEE Photovoltaic Specialists Conference, CH 1508-1/80/000-1126\$00.75, pp. 1126-1132.
- (3) Gonzalez, C., and Weaver, R., "Circuit Design Considerations for Photovoltaic Power Systems", 14th IEEE Photovoltaic Specialists Conference, CH 1508-1/80/000-0258\$00.75, pp. 528-535.
- (4) IEEE Recommended Practice for Design of Reliable Industrial and Commercial Power Systems, IEEE Std. 493-1980, Wiley-Interscience, 1980.
- (5) Wang, P. Y., and Wolosewicz, R. M., Argonne National Laboratories, "Reliability Assessment of Solar Domestic Hot Water Systems", 1981 Operational Results Conference, Reno, Nevada.
- (6) Solar Energy Systems-Standards for Cover Plates for Flat Plat Solar Collectors, NBS Technical Note 1132.
- (7) Reliability Design Guidebook for Flat Plate Photovoltaic Modules/Arrays, DOE/JPL, Contract No. 955720-80/1.
- (8) Private Communication to authors on Acrylic Lens Degradation (10.5% transmittance loss in 20 yr), Charles Stillwell, Sandia Labs, 7/8/81.
- (9) E. L. Burgess, "Update of Photovoltaic System Cost Experience for Intermediate-Sized Applications", Proc. of the 15th Photovoltaic Specialists Conf., p. 1453 (CH 1644-4/81/0000-1453\$00.75).
- (10) Solman, F. J., "Photovoltaic Systems Performance Experience", Fifteenth PV Specialists Conference, CH 1644-4/81/0000-1146\$00.75, p. 1146.
- (11) Rigby, L. V., "Results of Eleven Separate Maintainability Demonstrations", IEEE Transactions on Reliability, Vol. R-16, No. 1, May 1967, p. 43-48.
- (12) MIL-HDBK-472 Maintainability Prediction.
- (13) a) Stember, L. H., "Reliability Considerations in the Design of Solar Photovoltaic Power Systems", SOLAR CELLS, 3(3) p. 261, 1981.
b) Stember, L. H., "Photovoltaic Systems Reliability Analysis." Fifteenth PV Specialists Conference, CH 1644-4/81/0000-1153.

- c) Noel, G. T., Stember, L. H., and Carmichael, D. C., "System Design and Reliability Considerations for an Intermediate-Size Photovoltaic Power System for a Remote Application", Fifteenth PV Specialists Conference, CH 1644-4/81/0000-0725.
- (14) Bazovsky, I., "Fault Trees, Block Diagrams and Markov Graphs", 1977 Proceedings of Annual Reliability and Maintainability Symposium, 1427-77RM-023, p. 134.
- (15) Galetto, F., "System Availability and Reliability Analysis-SARPA", 1977 Proceedings of the Annual Reliability and Maintainability Symposium, 1420-77RM-016, p. 95.
- (16) Maler, H. A., "Reliability Optimization in Telephone Switching Systems Design", IEEE Transactions on Reliability, Vol. R-26, No. 3, 8/77
- (17) Pritsker, A.A.B., "The GASP IV Simulation Language", John Wiley and Sons, NY, 1974.
- (18) "Photovoltaic System Definition and Development Project Integration Meeting" (SAND80-2374), Albuquerque, N.M., October 21-23, 1980, p. 22.
- (19) "A 150 Kilowatt Photovoltaic Flat Panel Facility for a Shopping Center Application in Lovington, NM" (DOE/ET/2305801), Lea County, Inc.
- (20) "Airport Solar Photovoltaic Concentrator Project", (DOE/CS/05317-1), Arizona Public Service/Motorola, (PRDA 35), December, 1979.
- (21) "Commercial Application of a Photovoltaic Concentrator System" (DOE/CS/05313-1), BDM Corp.
- (22) Perino, A. M., "A Methodology for Determining the Economic Feasibility of Residential or Commercial Solar Energy Systems", SAND 78-0931.

Distribution 1

DISTRIBUTION:

TID-4500-R66, UC-63a (137)

B. Annan (25)
Department of Energy
Division of PV Energy Systems
Forrestal Building
1000 Independence Ave. SW
Washington, DC 20585
Attn: M. B. Prince
V. N. Rice
A. Bulawka
A. Scolaro
A. Krantz
M. Pulscak

Department of Energy
Division of Active Heating & Cooling
Office of Solar Application for Bldgs.
Washington, DC 20585
Attn: Robert D. Jordon, Director

Department of Energy
Division of Passive & Hybrid
Office of Solar Applications
Washington, DC 20585
Attn: Michael D. Maybaum, Director

Jet Propulsion Laboratory (14)
4800 Oak Grove Drive
Pasadena, CA 91103
Attn: R. V. Powell (3)
R. Ferber
W. Callaghan
R. Ross
R. S. Sugimura
R. H. Barbieri
S. Krauthamer
A. Lawson
A. Pearson
J. Smith
E. Royal
J. Evans

Jet Propulsion Laboratory
Solar Data Center
MS 502-414
4800 Oak Grove Drive
Pasadena, CA 91103

Solar Energy Research Institute (6)
1536 Cole Boulevard
Golden, CO 80401
Attn: E. Witt
R. Koontz (3)
D. Ritchie
R. DeBlasio

SERI, Library (2)
1536 Cole Boulevard, Bldg. #4
Golden, CO 80401

NASA Lewis Research Center
21000 Brookpark Laboratory
Cleveland, OH 44135

Florida Solar Energy Center
300 State Road 401
Cape Canaveral, FL 32920
Attn: S. Chandra

EPRI (3)
P. O. Box 10412
Palo Alto, CA 94303
Attn: Frank Goodman
Edgar Demeo
Roger Taylor

House Science and Technology
Committee
Room 374-B
Rayburn Building
Washington, DC 20515
Attn: Don Teague

Office of Technology Assessment
U. S. Congress
Washington, DC 20510

New Mexico Solar Energy Inst. (3)
New Mexico State University
Box 3SOL
Las Cruces, NM 88003
Attn: John Schaeffer

Distribution 2

Aerospace Corporation (2)
Attn: S. Leonard
Ed Simburger
P. O. Box 902957
Los Angeles, CA 90009

Reliability Technology Associates
Attn: R. T. Anderson
13947 Arapaho Lane
Lockport, IL 60441

California Energy Commission
Attn: Arthur J. Soinski
1111 Howe Avenue
Sacramento, CA 95825

General Electric Co.
Attn: E. M. Mehalick
Advanced Energy Programs
P. O. Box 8661
Philadelphia, PA 19101

Arizona Public Service
Attn: J. McGuirk
P. O. Box 21666
Phoenix, AZ 85036

BDM Corporation
Attn: W. R. Kauffman
1801 Randolph Rd. SE
Albuquerque, NM 87106

Lea County Electric Coop
Attn: P. Felfe
P. O. Drawer 1447
Lovington, NM 88260

Battelle Columbus Labs (15)
Attn: L. Stember
505 King Avenue
Columbus, OH 43201

Sandia National Laboratories:
2525 R. P. Clark
3141 L. J. Erickson (5)
9700 E. H. Beckner
9720 D. G. Schueler
9721 J. Banas
9723 E. L. Burgess
9723 H. H. Baxter, Jr.
9723 K. L. Biringer
9723 D. Chu
9723 G. J. Jones
9723 T. S. Key
9723 H. N. Post
9723 C. B. Rogers
9723 M. G. Thomas
9724 E. C. Boes
9724 D. E. Arvizu
9724 C. J. Chiang
9724 M. W. Edenburn
9724 D. L. King
9724 A. B. Maish
9724 M. Rios (25)
9724 C. B. Stillwell
3151 W. L. Garner (3)
8214 M. A. Pound

Distribution 3

DISTRIBUTION:

TID-4500-R66, UC-63a (137)

B. Annan (25)
Department of Energy
Division of PV Energy Systems
Forrestal Building
1000 Independence Ave. SW
Washington, DC 20585
Attn: M. B. Prince
V. N. Rice
A. Bulawka
A. Scolaro
A. Krantz
M. Pulscak

Department of Energy
Division of Active Heating & Cooling
Office of Solar Application for Bldgs.
Washington, DC 20585
Attn: Robert D. Jordon, Director

Department of Energy
Division of Passive & Hybrid
Office of Solar Applications
Washington, DC 20585
Attn: Michael D. Maybaum, Director

Jet Propulsion Laboratory (14)
4800 Oak Grove Drive
Pasadena, CA 91103
Attn: R. V. Powell (3)
R. Ferber
W. Callaghan
R. Ross
R. S. Sugimura
R. H. Barbieri
S. Krauthamer
A. Lawson
A. Pearson
J. Smith
E. Royal
J. Evans

Jet Propulsion Laboratory
Solar Data Center
MS 502-414
4800 Oak Grove Drive
Pasadena, CA 91103

Solar Energy Research Institute (6)
1536 Cole Boulevard
Golden, CO 80401
Attn: E. Witt
R. Koontz (3)
D. Ritchie
R. DeBlasio

SERI, Library (2)
1536 Cole Boulevard, Bldg. #4
Golden, CO 80401

NASA Lewis Research Center
21000 Brookpark Laboratory
Cleveland, OH 44135

Florida Solar Energy Center
300 State Road 401
Cape Canaveral, FL 32920
Attn: S. Chandra

EPRI (3)
P. O. Box 10412
Palo Alto, CA 94303
Attn: Frank Goodman
Edgar Demeo
Roger Taylor

House Science and Technology
Committee
Room 374-B
Rayburn Building
Washington, DC 20515
Attn: Don Teague

Office of Technology Assessment
U. S. Congress
Washington, DC 20510

New Mexico Solar Energy Inst. (3)
New Mexico State University
Box 3SOL
Las Cruces, NM 88003
Attn: John Schaeffer

Distribution 4

Aerospace Corporation (2)
Attn: S. Leonard
Ed Simburger
P. O. Box 902957
Los Angeles, CA 90009

Reliability Technology Associates
Attn: R. T. Anderson
13947 Arapaho Lane
Lockport, IL 60441

California Energy Commission
Attn: Arthur J. Soinski
1111 Howe Avenue
Sacramento, CA 95825

General Electric Co.
Attn: E. M. Mehalick
Advanced Energy Programs
P. O. Box 8661
Philadelphia, PA 19101

Arizona Public Service
Attn: J. McGuirk
P. O. Box 21666
Phoenix, AZ 85036

BDM Corporation
Attn: W. R. Kauffman
1801 Randolph Rd. SE
Albuquerque, NM 87106

Lea County Electric Coop
Attn: P. Felfe
P. O. Drawer 1447
Lovington, NM 88260

Battelle Columbus Labs (15)
Attn: L. Stember
505 King Avenue
Columbus, OH 43201

Sandia National Laboratories:
2525 R. P. Clark
3141 L. J. Erickson (5)
9700 E. H. Beckner
9720 D. G. Schueler
9721 J. Banas
9723 E. L. Burgess
9723 H. H. Baxter, Jr.
9723 K. L. Biringer
9723 D. Chu
9723 G. J. Jones
9723 T. S. Key
9723 H. N. Post
9723 C. B. Rogers
9723 M. G. Thomas
9724 E. C. Boes
9724 D. E. Arvizu
9724 C. J. Chiang
9724 M. W. Edenburn
9724 D. L. King
9724 A. B. Maish
9724 M. Rios (25)
9724 C. B. Stillwell
3151 W. L. Garner (3)
8214 M. A. Pound